Journal of Medicinal Chemistry

Subscriber access provided by UNIVERSITY OF ADELAIDE LIBRARIES

Article

Discovery of Clinical Candidate *N*-((1*S*)-1-(3-Fluoro-4-(trifluoromethoxy)phenyl)-2-methoxyethyl)-7-methoxy-2-oxo-2,3-dihydropyrido[2,3-*b*]pyrazine-4(1*H*)-carboxamide (TAK-915): A Highly Potent, Selective, and Brain-Penetrating Phosphodiesterase 2A Inhibitor for the Treatment of Cognitive Disorders

Satoshi Mikami, Shinji Nakamura, Tomoko Ashizawa, Izumi Nomura, Masanori Kawasaki, Shigekazu Sasaki, Hideyuki Oki, Hironori Kokubo, Isaac D. Hoffman, Hua Zou, Noriko Uchiyama, Kosuke Nakashima, Naomi Kamiguchi, Haruka Imada, Noriko Suzuki, Hiroki Iwashita, and Takahiko Taniguchi

J. Med. Chem., **Just Accepted Manuscript** • DOI: 10.1021/acs.jmedchem.7b00807 • Publication Date (Web): 10 Aug 2017

Downloaded from http://pubs.acs.org on August 10, 2017

Just Accepted

"Just Accepted" manuscripts have been peer-reviewed and accepted for publication. They are posted online prior to technical editing, formatting for publication and author proofing. The American Chemical Society provides "Just Accepted" as a free service to the research community to expedite the dissemination of scientific material as soon as possible after acceptance. "Just Accepted" manuscripts appear in full in PDF format accompanied by an HTML abstract. "Just Accepted" manuscripts have been fully peer reviewed, but should not be considered the official version of record. They are accessible to all readers and citable by the Digital Object Identifier (DOI®). "Just Accepted" is an optional service offered to authors. Therefore, the "Just Accepted" Web site may not include all articles that will be published in the journal. After a manuscript is technically edited and formatted, it will be removed from the "Just Accepted" Web site and published as an ASAP article. Note that technical editing may introduce minor changes to the manuscript text and/or graphics which could affect content, and all legal disclaimers and ethical guidelines that apply to the journal pertain. ACS cannot be held responsible for errors or consequences arising from the use of information contained in these "Just Accepted" manuscripts.

ACS Publications

Journal of Medicinal Chemistry is published by the American Chemical Society. 1155 Sixteenth Street N.W., Washington, DC 20036

Published by American Chemical Society. Copyright © American Chemical Society. However, no copyright claim is made to original U.S. Government works, or works produced by employees of any Commonwealth realm Crown government in the course of their duties.

Discovery of Clinical Candidate *N*-((1*S*)-1-(3-Fluoro-4-(trifluoromethoxy)phenyl)-2-methoxyethyl)-7-methoxy-2-oxo-2,3-dihydropyrido[2,3-*b*]pyrazine-4(1*H*)-carboxamide (TAK-915): A Highly Potent, Selective, and Brain-Penetrating Phosphodiesterase 2A Inhibitor for the Treatment of Cognitive Disorders

Satoshi Mikami,[*,†] *Shinji Nakamura,*[†] *Tomoko Ashizawa,*[†] *Izumi Nomura,*[†] *Masanori Kawasaki,*[†] *Shigekazu Sasaki,*[†] *Hideyuki Oki,*[†] *Hironori Kokubo,*[†] *Isaac D. Hoffman,*[‡] *Hua Zou,*[‡] *Noriko Uchiyama,*[†] *Kosuke Nakashima,*[†] *Naomi Kamiguchi,*[†] *Haruka Imada,*[†] *Noriko Suzuki,*[†] *Hiroki Iwashita,*[†] *and Takahiko Taniguchi*[†]

AUTHOR AFFILIATIONS:

[†]Pharmaceutical Research Division, Takeda Pharmaceutical Company Limited, 26-1, Muraoka-Higashi 2-chome, Fujisawa, Kanagawa 251-8555, Japan

‡Takeda California, Inc., 10410 Science Center Drive, San Diego, California 92121, United States

ABSTRACT

Phosphodiesterase (PDE) 2A inhibitors have emerged as a novel mechanism with potential therapeutic option to ameliorate cognitive dysfunction in schizophrenia or Alzheimer's disease through upregulation of cyclic nucleotides in the brain, and thereby achieve potentiation of cyclic nucleotide signaling pathways. This article details the expedited optimization of our recently disclosed pyrazolo[1,5-*a*]pyrimidine lead compound **4b**, leading to the discovery of clinical candidate **36** (TAK-915), which demonstrates an appropriate combination of potency, PDE selectivity, and favorable pharmacokinetic (PK) properties, including brain penetration. Successful identification of **36** was realized through application of structure-based drug design (SBDD) to further improve potency and PDE selectivity, coupled with prospective design focused on physicochemical properties to deliver brain penetration. Oral administration of **36** demonstrated significant elevation of 3',5'-cyclic guanosine monophosphate (cGMP) levels in mouse brains, and improved cognitive performance in a novel object recognition task in rats. Consequently, compound **36** was advanced into human clinical trials.

INTRODUCTION

Phosphodiesterases (PDEs) are a superfamily of enzymes that catalyze the hydrolysis of the second messengers, 3',5'-cyclic adenosine monophosphate (cAMP) and/or 3',5'-cyclic guanosine monophosphate (cGMP) into inactive 5'-AMP and/or 5'-GMP,[1] thereby regulating the cellular levels of these cyclic nucleotides, their downstream signaling cascades, and, as a result, a diverse array of biological responses.[2–4] PDEs are encoded by 21 separate genes that are categorized into 11 different PDE families (PDE1–11) on the basis of amino acid sequence similarity, substrate specificity, and mode of regulation.[1,5]

PDE2A, which is a dual-substrate enzyme capable of accommodating and degrading both cAMP and cGMP, has the highest expression in regions of the brain associated with cognitive processes, such as the cortex, hippocampus, and striatum.[6–11] In the central nervous system (CNS), both cAMP and cGMP play important roles in modulating intracellular signal transduction pathways related to long-term potentiation (LTP), a surrogate measure of synaptic plasticity,[12–16] which is considered a key element of the neurobiological foundations of cognitive function.[17]

On the basis of these features, it has been hypothesized that PDE2A inhibition would be beneficial for the treatment of cognitive dysfunction associated with schizophrenia or dementia in Alzheimer's disease, by suppressing the degradation of intracellular cAMP and/or cGMP levels in brain areas critical for cognitive function and memory. Thus, the search for potent and selective PDE2A inhibitors has attracted considerable attention in the pharmaceutical industry.[18–36] As shown in Figure 1, Bayer reported a highly potent PDE2A inhibitor BAY 60-7550 (**1**)[18] possessing the imidazo[5,1-*f*][1,2,4]triazin-4(3*H*)-one motif as a core, which augmented cognition and memory in animal behavioral models.[37,38] Although this compound has been frequently used preclinically as a key pharmacological tool in this research field, poor CNS

penetration has limited its clinical use.[39] Meanwhile, Pfizer recently disclosed a highly potent and selective PDE2A inhibitor PF-05180999 (**2**) with oral bioavailability and CNS-penetrant attributes, which was advanced to human clinical trials.[26,27]

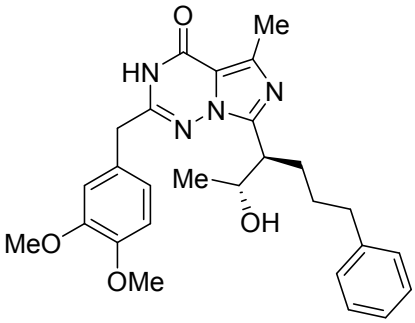

1 (BAY 60-7550, Bayer)
PDE2A IC_{50}: 4.7 nM
PDE selectivity: 50x (vs. PDE1C)

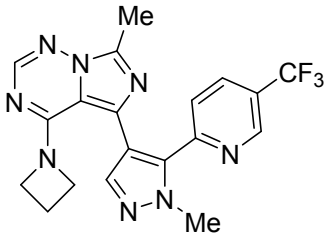

2 (PF-05180999, Pfizer)
PDE2A IC_{50}: 1 nM
PDE selectivity: 2000x (vs. PDE10A)

Figure 1. Structures and profiles of representative PDE2A inhibitors.

In the preceding publication,[40] we described our lead-generation approach that began with high-throughput screening hit **3** from our in-house compound library and led to the identification of lead compound **4b**, which possessed a reasonable balance of potency, PDE selectivity, and PK properties including brain penetration (Figure 2). Reflecting these favorable attributes, oral dosing of **4b** significantly elevated cGMP levels in mouse brains, but its high systemic exposure at effective dosage in vivo and selectivity profile against all other PDE families (180-fold vs. PDE3A) were insufficient for consideration as a clinical candidate. As PDEs are expressed in a variety of tissues,[10] inhibition of off-target PDEs could induce undesired side effects. Potential side effects include vasodilation and tachycardia, which are attributed to inhibition of PDE1 and PDE3,[41,42] or visual disturbances, which are attributed to inhibition of

PDE6.[43–45] Therefore, achieving high selectivity is crucial for the development of a clinically beneficial PDE inhibitor with minimized safety concerns. Hence, our medicinal chemistry efforts were focused on moving beyond delivery of an in vivo tool compound into identification of a clinical candidate with the following attributes: (i) PDE2A IC_{50} < 5 nM, (ii) >1000-fold selectivity over all other PDEs, and (iii) reasonable brain penetration. To this end, we applied SBDD utilizing a PDE2A co-crystal structure of **4b**.[40] Simultaneously, we tracked topological polar surface area (TPSA), hydrogen bond donor (HBD) count, and multidrug resistance protein 1 (MDR1) efflux ratio to maximize the probability of preserving the excellent brain exposure characteristics of **4b**.

Herein, we disclose a new series of PDE2A inhibitors derived from **4b** and the subsequent optimization efforts employing SBDD, which culminated in the discovery of *N*-((1*S*)-1-(3-fluoro-4-(trifluoromethoxy)phenyl)-2-methoxyethyl)-7-methoxy-2-oxo-2,3-dihydropyrido[2,3-*b*]pyrazine-4(1*H*)-carboxamide **36** (TAK-915,[29] Figure 3), a compound with fully aligned drug attributes. Furthermore, we describe the binding mode of **36** in the human PDE2A catalytic domain, which accounts for its potent inhibitory activity and high PDE selectivity. We also report on the pharmacological profile of **36**, which helps demonstrate the promise of PDE2A inhibition as a potential therapeutic approach in the treatment of cognitive impairment for a range of neuropsychiatric and neurodegenerative disorders.

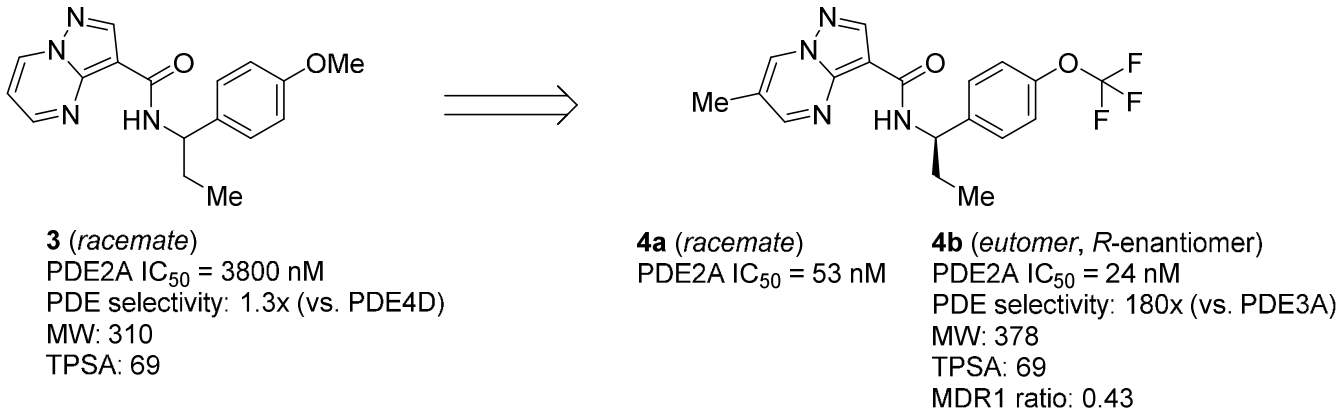

Figure 2. Transition from high-throughput screening hit **3** to lead compounds **4a** and **4b**.[40]

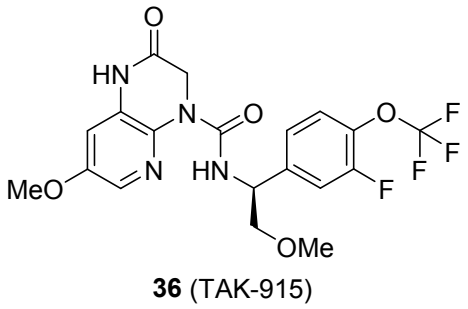

Figure 3. Structure of **36**.

RESULTS AND DISCUSSION

Drug Design Strategies. The program leading to discovery of **36** began with examination of a co-crystal structure of **4b** (Figure 4). As reported previously,[40] the characteristic interactions are as follows: (i) the C7 hydrogen of the pyrazolo[1,5-*a*]pyrimidine core most likely forms a weak C–H hydrogen bond[46] with the carbonyl group of Gln859, a conserved amino acid in all PDEs that is key to cyclic nucleotide binding, (ii) the core sits within a hydrophobic clamp formed by Phe862 on the top and Ile826 on the bottom, and is stabilized by π–π and CH–π interactions, (iii) the amide carbonyl group is engaged in two hydrogen bonding interactions with water molecules, one of which provides a bridging interaction with Tyr655, and (iv) the right-hand side (RHS)

phenyl group fits into the hydrophobic pocket newly created by ligand-binding. In addition, the amide N–H forms an intramolecular hydrogen bond with the N4 nitrogen atom of the core. In good agreement with our previous findings about the structure–activity relationships (SARs), this internal hydrogen bond plays a critical role in potency via stabilization of the bound conformation. Through this analysis of the binding mode of **4b**, we envisioned that the identification of additional interactions with the protein as well as access to pockets unique to the PDE2A in the PDE family would be key for realizing our potency and selectivity goals. To this end, we devised four drug design strategies, as shown in Figure 5. Strategy 1 involves replacement of the pyrazolo[1,5-*a*]pyrimidine core to enable an unambiguous hydrogen bond interaction with Gln859. This strategy also expands the structural diversity around the core ring, and consequently increases the probability of finding a high-quality clinical candidate. Strategy 2 involves optimization of the RHS phenyl group to fill the PDE2A-specific hydrophobic pocket optimally, which might enhance both potency and selectivity. Strategy 3 involves incorporation of a polar functionality into the branched ethyl group. As this portion is close to the solvent accessible region and is surrounded by protein-bound metal ions containing a highly ordered water network and hydrophilic amino acid residues, such as His656 and Gly826, addition of a polar functionality may enhance potency while also improving physicochemical properties by decreasing the overall molecular lipophilicity. Strategy 4 involves introduction of substituents into the core to fill the surrounding space efficiently. This strategy is supported by the previous finding that substitution on the pyrazolo[1,5-*a*]pyrimidine core contributes significantly to potency and PDE selectivity,[40] and is, therefore, expected to improve both inhibitory activity and selectivity.

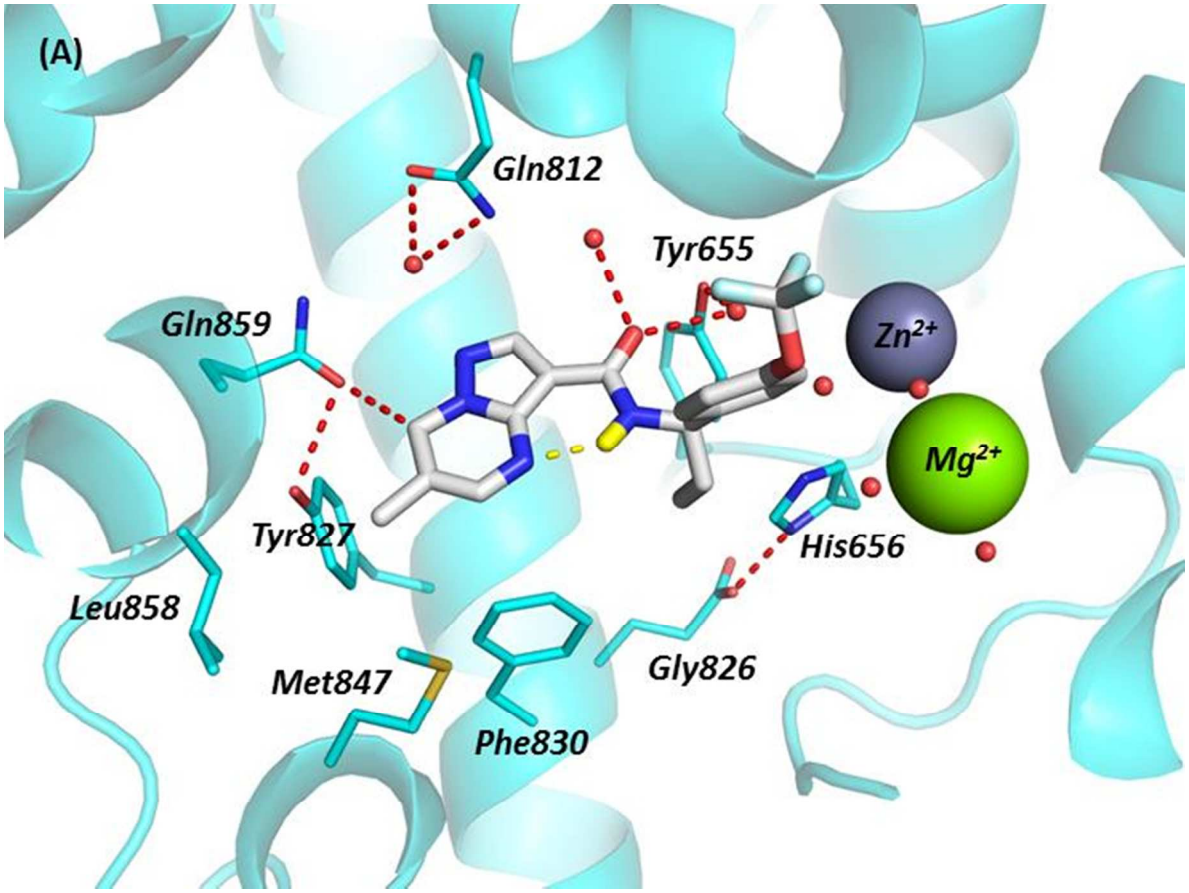
(A)
Gln812
Tyr655
Gln859
Zn2+
Mg2+
Tyr827
His656
Leu858
Met847
Gly826
Phe830

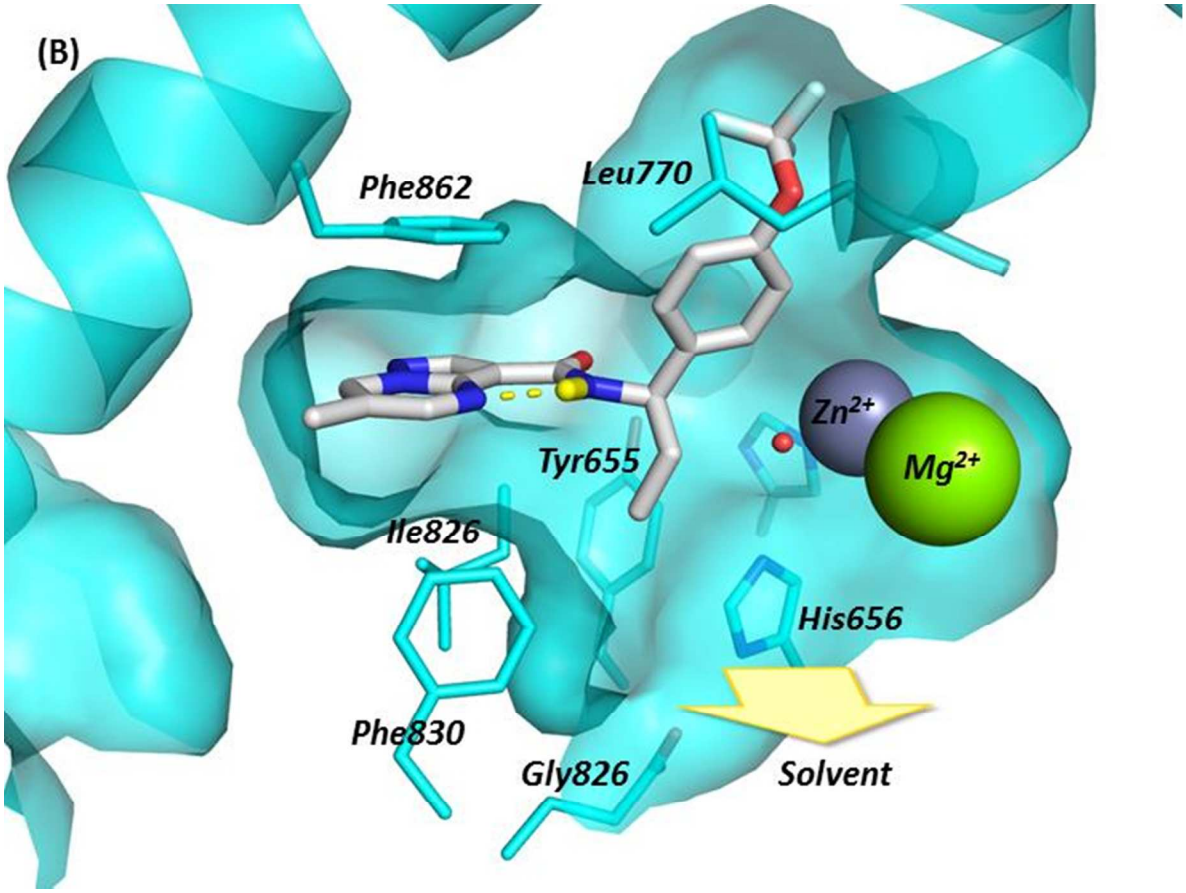

Figure 4. X-ray crystal structure of **4b** bound in the PDE2A catalytic site (PDB 5XKM) viewed from the top (A) and the entrance of the catalytic site (B). The key hydrogen bonding interactions of **4b** with PDE2A and the intramolecular hydrogen bond in **4b** are indicated by red and yellow dotted lines, respectively.

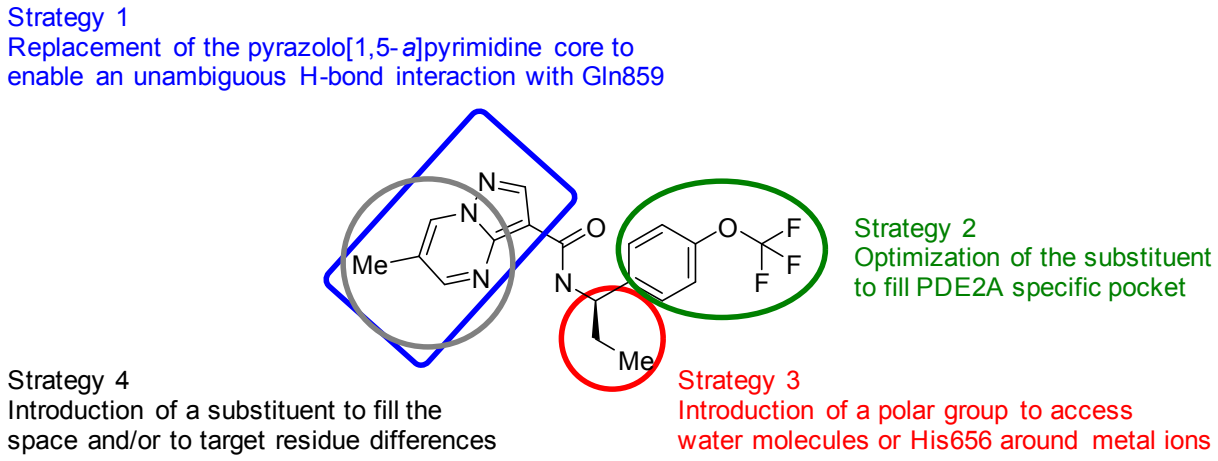

Figure 5. Drug design strategies to improve PDE2A inhibitory activity and PDE selectivity.

Strategy 1: Exploration of New Alternative Cores. We focused initially on replacement of the pyrazolo[1,5-*a*]pyrimidine core. As the C–H hydrogen bond (C–H···O) observed between the core and Gln859 is generally weaker than a classic hydrogen bond, we hypothesized that establishing an unambiguous hydrogen bond interaction with either or both the carbonyl and –NH_2 groups of Gln859 would further increase potency. Notably, one proposed molecular mechanism for the dual cAMP/cGMP specificity of PDEs like PDE2A involves rotation of the side chain of invariant glutamine (Gln859 in PDE2A) to recognize both cAMP and cGMP (Figure 6). This is commonly referred to as the "glutamine switch".[47,48] With this design hypothesis and glutamine switch mechanism in hand, we designed novel alternative core structures that could create a classic hydrogen bond with Gln859 in a binding mode similar to that for cAMP or cGMP (Figure 7). Considering the importance of the intramolecular hydrogen bond observed in pyrazolo[1,5-*a*]pyrimidine analogs, a nitrogen atom that could serve as a hydrogen bond acceptor (HBA) was also incorporated into the newly designed core to ensure a critical internal hydrogen bond network with the neighboring amide N–H, and thereby adopt a similar conformation to the RHS benzylamine moiety of **4b**. At this design stage, physicochemical properties, such as TPSA and the number of HBD, were also considered to optimize the MDR1 efflux ratio, and thus obtain a compound with favorable brain penetration. To minimize P-glycoprotein (P-gp) efflux, TPSA should be maintained below 90 $Å^2$, and the HBD count should be kept below 2.[49,50] Within this chemotype series, in which the amide NH interacts with the nitrogen atom of the core scaffold, the TPSA and HBD count would be affected by the strength of the intramolecular hydrogen bond; assuming that these polar functionalities are completely masked, the apparent TPSA and HBD count would decrease by approximately 20 $Å^2$ and 1, respectively.[51] On the basis of these considerations, we targeted

TPSA values below 110 Å^2 and HBD counts of less than 3. Additionally, an MDR1 efflux ratio of less than 2.0 was considered as our target range.

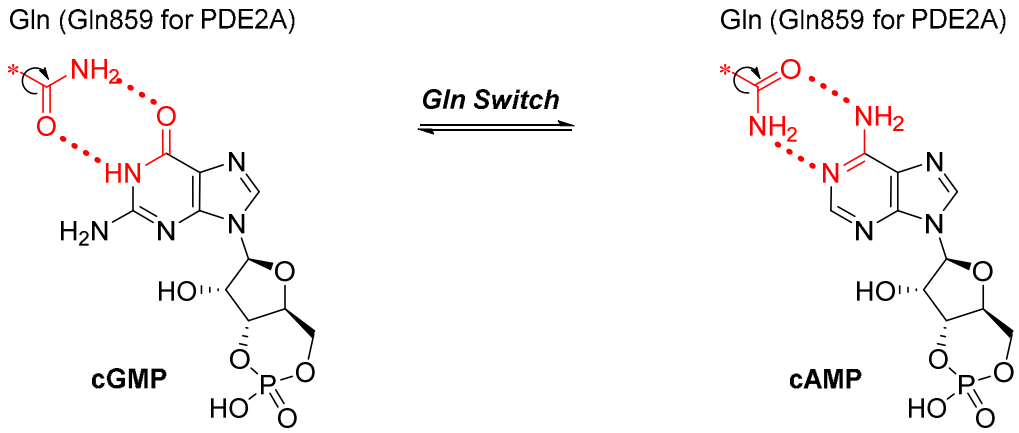

Figure 6. Glutamine switch mechanism proposed to explain the accommodation of both cyclic nucleotide substrates in dual-substrate PDEs.[47,48]

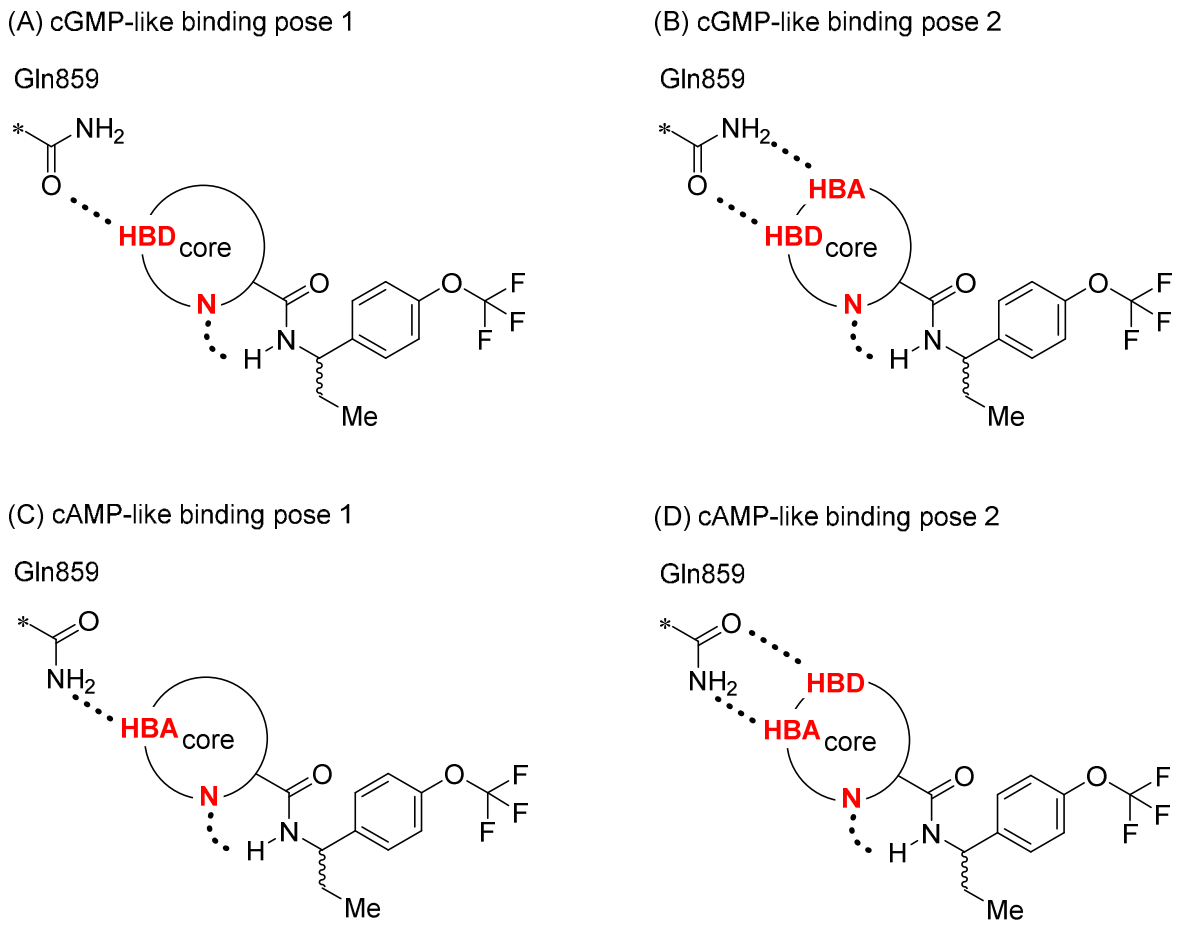

Figure 7. Drug design concepts (A)–(D) to identify new alternatives to the pyrazolo[1,5-*a*]pyrimidine core.

Representative results from our exploration of new core scaffolds are summarized in Table 1. All compounds synthesized possessed TPSA values within our target range. For comparison, pyrazolo[1,5-*a*]pyrimidine derivatives **4a** and **5** are also included in the table. Notably, **4a** is 9-fold more potent than **5**, which highlights the significant contribution of the methyl group at the 6-position of **4a** to potency enhancement.[40] Compound **6**, which contains a lactam moiety seemingly capable of achieving a more effective hydrogen bond with Gln859, exhibited greater PDE2A inhibitory activity when compared with **5**, revealing the superiority of

the 3,4-dihydropyrido[2,3-*b*]pyrazin-2(1*H*)-one core over the pyrazolo[1,5-*a*]pyrimidine core. However, the interaction energy gained between the lactam moiety and Gln859 may be partially offset by attenuation of the π–π and CH–π interactions with Phe862 and Ile826, respectively, owing to the decreased π-electron density of the core. To confirm this speculation, the PDE2A inhibitory activity of **7**, which possesses a lactam moiety and a similar aromaticity to **5**, was characterized. Compound **7** demonstrated improved potency (PDE2A IC_{50} = 21 nM) in comparison with **6**, which suggests that interactions with both Gln859 and Phe862/Ile826 may contribute to the potency enhancement. On the other hand, **8**, designed to form a hydrogen bond between the core and the $–NH_2$ group of Gln859 in a cAMP-like binding mode, exhibited significantly decreased potency compared with **4a**. Moreover, a similar trend was observed with **9**, a reversed lactam counterpart of **7**. Although we cannot exclude the possibility of this representing suboptimal placement of the HBA and/or HBD, we postulated that the loss in potency was associated with the side chain of Gln859 being unlikely to freely rotate to accommodate the cores of **8** and **9**. From the X-ray crystal structure of **4b**, the side chain of Gln859 forms a hydrogen bond with neighboring Tyr827, and the energetic penalty of disrupting this preexisting hydrogen bonding network was likely not overcome by the interaction energy gained between each core and Gln859. Meanwhile, to confirm the role of the pyridine nitrogen atom in the core in **6**, this atom was replaced by a CH group to afford **10**. Compound **10** exhibited a pronounced loss of inhibitory activity, reinforcing the importance of the intramolecular hydrogen bond on the potency in this core series, as was the case with pyrazolo[1,5-*a*]pyrimidine core derivatives. Thus, the examination of various cores targeting the interaction with Gln859 identified two promising novel cores in **6** and **7**. Unfortunately, further profiling revealed that **7** had significant in vitro phototoxicity, presumably inherent in the 1,5-

naphthyridin-2(1*H*)-one core, and also exhibited decreased CNS penetration, likely associated with the more acidic nature of the N–H proton relative to that of the core in **6** (data not shown). Consequently, the 3,4-dihydropyrido[2,3-*b*]pyrazin-2(1*H*)-one motif in **6** was chosen as a core for further investigation.

Table 1. In Vitro Activities of Derivatives Possessing Various Fused Bicyclic Cores

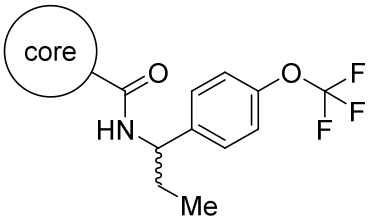

compd	core	anticipated binding mode[a]	PDE2A IC_{50} (nM)[b]	TPSA (Å^2)
4a	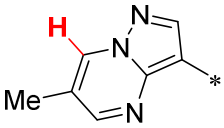	(A)	53 (47–59)	69
5	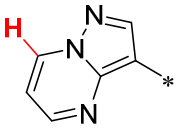	(A)	480 (350–650)	69
6	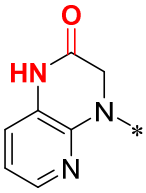	(A) or (B)	78 (61–98)	84
7	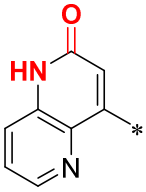	(A) or (B)	21 (18–26)	84
8	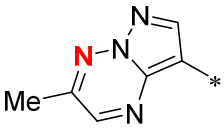	(C)	6500 (4200–9800)	81
9	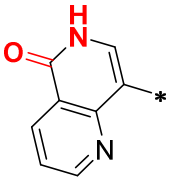	(C) or (D)	19000 (15000–24000)	84

10	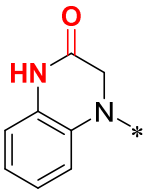	(A) or (B)	70000 (40000–120000)	71

[a] Refer to Figure 7. [b] IC_{50} values (95% confidence intervals given in parentheses) were calculated from percent inhibition data (duplicate, $n = 1$). All values are rounded to two significant digits.

As **6** showed attractive in vitro activity, chiral separation was performed. Upon HPLC separation of the two enantiomers, we observed that the activity of the racemic **6** resided predominantly in the **6a**, which displayed a PDE2A IC_{50} of 66 nM (Table 2). Furthermore, eutomer **6a** exhibited moderate PDE selectivity, with a minimum 30-fold selectivity over PDE1A. Notably, the PDE selectivity profile of eutomer **6a** almost tracked that of racemic **6**, suggesting that distomer **6b** is also inactive toward other PDEs.

Table 2. In Vitro Activity Profiles of **6** and Its Enantiomers **6a** and **6b**

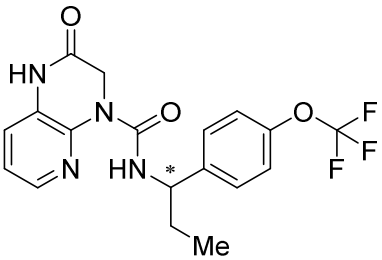

compd	stereo	PDE2A IC_{50} (nM)[a]
6	*rac*	78 (61–98)
6a	*eutomer*	66 (46–93)
6b	*distomer*	>100000

	6		**6a**	
PDE subtypes	IC_{50} (nM)[a]	Selectivity ratio[b]	IC_{50} (nM)[a]	Selectivity ratio[b]
PDE1A	3200	41	2000	30
PDE2A3	78	–	66	–
PDE3A	8100	100	4200	64

PDE4D2	>10000	>130	>10000	>150
PDE5A1	9800	130	>10000	>150
PDE6AB	>10000	>130	>10000	>150
PDE7B	>10000	>130	>10000	>150
PDE8A1	>10000	>130	>10000	>150
PDE9A2	>10000	>130	>10000	>150
PDE10A2	>10000	>130	>10000	>150
PDE11A4	>10000	>130	>10000	>150

[a] IC_{50} values were calculated from percent inhibition data (duplicate, $n = 1$). All values are rounded to two significant digits. [b] Selectivity ratio (rounded to two significant digits) = PDE"X" IC_{50}/PDE2A IC_{50}.

Strategy 2: Optimization of the RHS Phenyl Group. Given the hydrophobic nature and limited space of the binding pocket around the RHS phenyl group (Figure 4), we replaced the trifluoromethoxy group with less lipophilic and compact substituents (**11**–**14**) (Table 3). Consistent with our previous SARs for the pyrazolo[1,5-*a*]pyrimidine analogs represented by **4a**, replacing the trifluoromethoxy group with a methoxy group (**11**) resulted in an approximately 8-fold decrease in potency. The potency decrease may be attributed to the following two factors: (i) differences in conformational preferences, as the O–CF_3 bond prefers an orthogonal orientation to the phenyl plane, whereas the O–CH_3 bond favors an in-plane conformation;[52] and (ii) decreased hydrophobic contacts between the methoxy group and the surrounding hydrophobic residues in the binding pocket, as evidenced by the significant change in the LogD values (ΔLogD = 0.83). Trifluoromethyl and cyclopropyl analogs **12** and **13**, with different three-dimensional conformations of the trifluoromethoxy group, exhibited comparable inhibitory activity to **6**, but reduced PDE selectivity. These results indicate that the geometry of the substituent at this position affects PDE selectivity rather than potency. In particular, trifluoromethyl analog **12** had a slightly reduced LogD value relative to **6**. Furthermore, larger groups, such as an azetidine ring (**14**), significantly decreased the PDE2A inhibitory activity, indicative of the limited space around this position. To examine the effects of other substitution

patterns, *meta*- and *ortho*-trifluoromethoxy derivatives **15** and **16** were synthesized; however, both compounds showed considerable losses in potency. This is likely due to the more restricted pocket size around positions other than the *para*-position and/or an unfavorable conformational change brought about by introduction of an *ortho*-substituent. We next expanded the scope of our investigations to explore disubstituted analogs by keeping the trifluoromethoxy group at the *para*-position and, simultaneously, introducing minimally sized hydrophobic groups, such as a fluorine atom into the *meta*- or *ortho*-positions. Incorporation of a fluorine atom into the *meta*-position (**17**) led to a 2-fold gain in inhibitory activity, whereas substitution of a fluorine atom at the *ortho*-position (**18**) was detrimental to the potency relative to **6**. Taken together, the exploration of various substituents on the RHS phenyl group yielded some promising substituted phenyl groups, as typified by **6**, **12**, and **17**.

Table 3. SAR of the RHS Phenyl Group

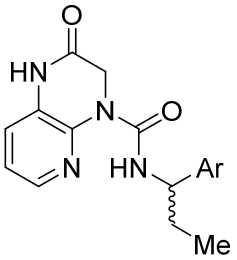

compd	Ar	PDE2A IC_{50} (nM)[a]	PDE selectivity[b]	LogD[c]
6	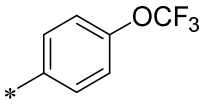	78 (61–98)	41-fold (PDE1A)	3.61
11	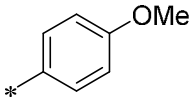	610 (480–780)	NT	2.78

12	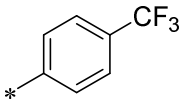	72 (46–110)	4.2-fold (PDE1A)	3.45
13	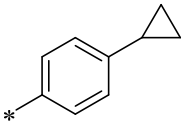	80 (64–100)	4.4-fold (PDE1A)	3.75
14	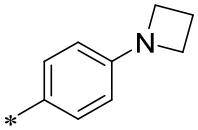	500 (410–590)	NT	3.13
15	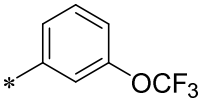	4100 (3400–4900)	NT	NT
16	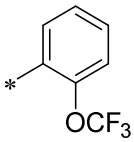	8100 (5500–18000)	NT	3.52
17	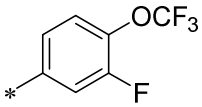	42 (33–52)	15-fold (PDE1A)	3.67
18	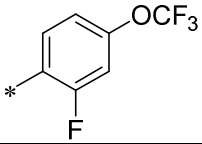	210 (160–290)	28-fold (PDE1A)	3.83

[a] IC_{50} values (95% confidence intervals given in parentheses) were calculated from percent inhibition data (duplicate, n = 1). All values are rounded to two significant digits. [b] Minimum selectivity (rounded to two significant digits) over other PDEs. The least selective PDE was given in parenthesis. [c] LogD values at pH 7.4.

Strategy 3: Conversion of the Branched Ethyl Group. We next focused on varying the branched ethyl group in **6** (Table 4). On the basis of our above-described hypothesis, polar functionalities containing HBA or HBD were introduced to exploit new interactions with adjacent water molecules or polar amino acid residues such as His656 and Gly826, around metal ions (Figure 4). Compound **19**, possessing a methoxymethyl group, exhibited a 4-fold increase in potency and significant improvement in PDE selectivity. This modification also significantly decreased the LogD value by nearly 1 unit. Elongation of the side chain by one carbon atom (**20**)

did not affect the potency in comparison with **6**. Moreover, replacement of the oxygen atom of **19** with a methylene group (**21**) decreased the potency by an order of magnitude. These results indicate that the ether oxygen atom in **19** is likely engaged in an additional interaction. Encouraged by this result, we pursued other polar functionalities. The primary alcohol in **22** was tolerated, but had no significant impact on either potency or PDE selectivity compared with **6**, whereas the corresponding tertiary alcohol in **23** increased potency and PDE selectivity, suggesting that the *gem*-dimethyl group may assist in suitably positioning the alcohol moiety by restricting bond rotation. Moreover, **24**, possessing a sulfone group, displayed a similar potency enhancement to **23**, demonstrating that a range of HBAs or HBDs could contribute to potency enhancement. Thus, the installation of polar functionalities not only enhanced potency and PDE selectivity, but also of reduced LogD values; however, these advantageous changes were accompanied by increased TPSA values and, in some cases, HBD counts outside the range of our aforementioned criteria (i.e., TPSA < 110 Å^2, HBD count < 3), resulting in unacceptable MDR1 efflux ratios, as evidenced by **22**–**24**. On the basis of improved PDE2A inhibitory activity and PDE selectivity in conjunction with a significant reduction in lipophilicity and no sign of P-gp efflux, the methoxymethyl branched group in **19** was selected for further optimization.

Table 4. SAR of the Branched Group at the Benzylic Position of the RHS Amine Moiety

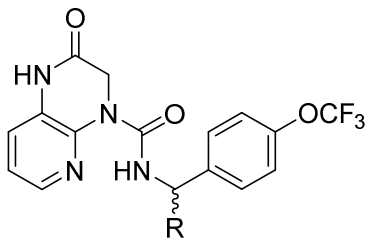

compd	R	PDE2A IC_{50} (nM)[a]	PDE selectivity[b]	LogD[c]	TPSA (Å^2)	MDR1[d]
6	–Et	78 (61–98)	41-fold (PDE1A)	3.61	84	0.53

19	$–CH_2OMe$	19 (15–24)	310-fold (PDE1A)	2.95	93	0.68
20	$–CH_2CH_2OMe$	62 (37–100)	14-fold (PDE5)	3.09	93	0.77
21	–*n*-Pr	250 (190–330)	NT	4.05	84	0.59
22	$–CH_2OH$	65 (35–120)	54-fold (PDE1A)	2.16	104	2.8
23	$–C(Me)_2OH$	24 (18–33)	150-fold (PDE1A)	2.54	104	2.8
24	$–CH_2SO_2Me$	29 (22–38)	220-fold (PDE1A)	1.91	118	26

[a] IC_{50} values (95% confidence intervals given in parentheses) were calculated from percent inhibition data (duplicate, n = 1). All values are rounded to two significant digits. [b] Minimum selectivity (rounded to two significant digits) over other PDEs. The least selective PDE was given in parenthesis. [c] LogD values at pH 7.4. [d] MDR1 efflux ratios in P-gp overexpressing cells.

Strategy 4: Introduction of Substituents into the Core. A comparison of the aligned sequences of all PDEs, particularly around the core (i.e., Tyr827, Leu858, and Met847 for PDE2A), revealed some variation of amino acid residues across the PDE family.[53,54] Such residue variation provides each member of the PDE family with various degrees of differences in the shape, size, and polarity of the binding pocket. In support of this finding, introduction of a substituent into the pyrazolo[1,5-*a*]pyrimidine core significantly affected both potency and PDE selectivity.[40] Therefore, targeting such residue differences around the core could be expected to improve both inhibitory activity and selectivity. Thus, we explored substitutions on the 3,4-dihydropyrido[2,3-*b*]pyrazin-2(1*H*)-one core of **19**, while maintaining the methoxymethyl branched linker, as summarized in Table 5. Introduction of a methyl group into the 6-position (**25**) or 8-position (**27**) decreased inhibitory activity, whereas methyl substitution at the 7-position in **26** resulted in a 2-fold boost in potency with the requisite selectivity of 1100-fold over other PDEs. Armed with these promising results, our focus was directed toward varying the substituent at the 7-position. The more lipophilic and bulkier cyclopropyl group in **28** further increased the potency concomitant with an improvement of PDE selectivity. On the other hand, the electron-withdrawing chloro group in **29** was detrimental to both potency and PDE selectivity. Based on these results, we presumed that incorporation of an electron-donating

substituent, such as an alkyl group, at this position may positively affect the potency in two ways: (i) space filling around the 7-position increases interactions with the surrounding amino acid residues and (ii) increased electron density of the core results in enhanced π–π and CH–π interactions with Phe862 and Ile826. Although 7-alkyl analogs provided notable advantages with respect to PDE2A inhibitory activity and PDE selectivity, they suffered from high lipophilicity as evidenced by higher LogD values. Therefore, we introduced other less lipophilic substituents at the 7-position. The methoxy group in **30** produced a minimal increase in lipophilicity with comparable potency to and improved selectivity over cyclopropyl analog **28**. On the other hand, larger substituents, such as an isopropoxy group (**31**), were not well tolerated, suggesting limited space in the binding pocket around the 7-position. It is also worth noting that **30** possessed a TPSA value within our target range, and consequently, an acceptable MDR1 efflux ratio, despite the incorporation of the additional methoxy group, thus validating our initial criteria for TPSA values (TPSA < 110 Å^2) of taking into account the expected effect of an intramolecular hydrogen bond.

Table 5. SAR of Substitutions at the 3,4-Dihydropyrido[2,3-*b*]pyrazin-2(1*H*)-one Core

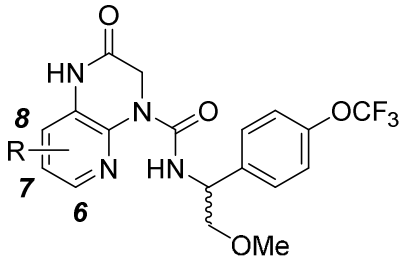

compd	R	PDE2A IC_{50} (nM)[a]	PDE selectivity[b]	LogD[c]	TPSA (Å^2)	MDR1[d]
19	H	19 (15–24)	310-fold (PDE1A)	2.95	93	0.68
25	6-Me	40 (31–52)	50-fold (PDE1A)	3.38	93	0.63
26	7-Me	8.7 (7.6–10)	1100-fold (PDE5)	3.35	93	1.0

27	8-Me	85 (67–110)	NT	3.16	93	0.74
28	7-*c*-Pr	3.5 (3.0–4.1)	1300-fold (PDE3A)	3.85	93	1.0
29	7-Cl	33 (30–36)	210-fold (PDE5)	3.74	93	0.58
30	7-MeO	2.8 (2.6–3.1)	2700-fold (PDE5)	3.20	102	1.3
31	7-*i*PrO	77 (66–90)	NT	3.94	102	1.1

[a] IC_{50} values (95% confidence intervals given in parentheses) were calculated from percent inhibition data (duplicate, n = 1). All values are rounded to two significant digits. [b] Minimum selectivity (rounded to two significant digits) over other PDEs. The least selective PDE was given in parenthesis. [c] LogD values at pH 7.4. [d] MDR1 efflux ratios in P-gp overexpressing cells.

Profiling Enantiomers of 30 and Its Close Analogs. Having identified **30** as a promising racemic compound that met our initial objectives of potency and PDE selectivity, the compound was subjected to chiral separation and in vitro profiles were obtained for both enantiomers. In addition, the RHS phenyl portion of **30** was replaced with other promising counterparts, exemplified by **12** and **17** (Table 4), to afford eutomers **34** and **36**, respectively, after chiral separation (Table 6). Compound **32** displayed potent inhibitory activity and excellent selectivity against other PDEs, whereas **34** was less potent and selective than expected. Of the synthesized analogs, **36** was the best with respect to potency (IC_{50} = 0.61 nM) and PDE selectivity (4100-fold vs. PDE1A; for a more detailed selectivity profile, refer to Table 7). In addition, **36** showed a favorable MDR1 efflux ratio with a TPSA value in the range of our criteria. On the basis of it possessing the best combination of potency, PDE selectivity and MDR1 efflux ratio, **36** was selected for further in vitro and in vivo profiling.

Table 6. In Vitro Profiles and Physicochemical Properties of Analogs **32**–**37**[a]

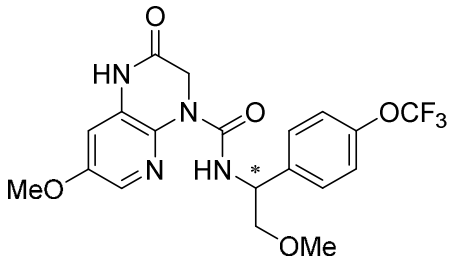

32 or **33**

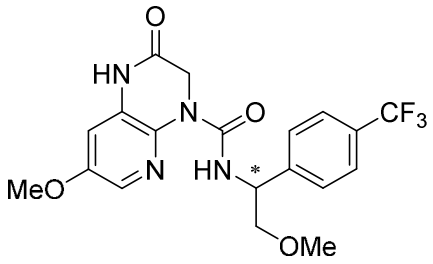

34 or **35**

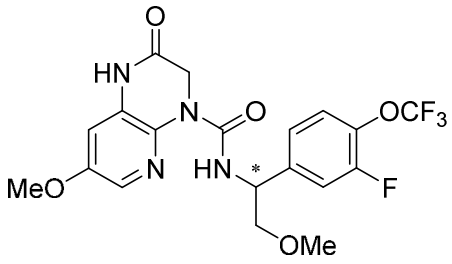

36 or **37**

compd	stereo	PDE2A IC_{50} (nM)[b]	PDE selectivity[c]	LogD[d]	TPSA (Å^2)	MDR1[e]
32	*R*	1.6 (1.4–1.9)	3300-fold (PDE1A)	3.19	102	1.5
33	*S*	39000 (28000–54000)	–	–	–	–
34	ND[f]	7.2 (6.4–8.0)	83-fold (PDE1A)	3.03	93	0.79
35	ND[f]	21000 (10000–42000)	–	–	–	–
36	*R*	0.61 (0.53–0.70)	4100-fold (PDE1A)	3.32	102	0.87
37	*S*	910 (720–1200)	–	–	–	–

[a] Racemic compounds were chirally separated and each enantiomer was profiled. The absolute configurations of **33** and **36** were determined as *S* and *R*, respectively, via single crystal X-ray analysis of the corresponding RHS benzylamine precursors (see the Supporting Information). [b] IC_{50} values (95% confidence intervals given in parentheses) were calculated from percent inhibition data (duplicate, n = 1). All values are rounded to two significant digits. [c] Minimum selectivity (rounded to two significant digits) over other PDEs. The least selective PDE was given in parenthesis. [d] LogD values at pH 7.4. [e] MDR1 efflux ratios in P-gp overexpressing cells. [f] Not determined.

Table 7. PDE Selectivity Profile of **36**

PDE subtypes	IC_{50} (nM)[a]	selectivity ratio[b]
PDE1A	2497	4100
PDE2A3	0.61	–
PDE3A	>30000	>49000
PDE4D2	14882	24000
PDE5A1	>30000	>49000
PDE6AB	>30000	>49000
PDE7B	>30000	>49000
PDE8A1	>30000	>49000
PDE9A2	>30000	>49000
PDE10A2	>30000	>49000
PDE11A4	>30000	>49000

[a] IC_{50} values were calculated from percent inhibition data (duplicate, n = 1). All values are rounded to two significant digits. [b] Selectivity ratio (rounded to two significant digits) = PDE"X" IC_{50}/PDE2A IC_{50}.

As shown in Table 8, **36** exhibited relatively high, but acceptable, rat and mouse liver microsomal clearance, and demonstrated increased metabolic stability in human liver microsomes. PK evaluations of **36** in rats and mice were favorable with excellent oral bioavailability in both species, and moderate (rat) to low (mouse) systemic clearances. Moreover, **36** demonstrated excellent brain permeability with a brain-to-plasma ratio of 1.01 in rats and 0.91 in mice. These PK results, together with improved human in vitro microsomal stability relative to rat and mouse counterparts, indicated the potential of **36** for good oral absorption in humans.

Table 8. PK Parameters and K_p Values of **36** in Rat and Mouse[a]

	rat	mouse	human
Metabolic stability[b] (μL/min/mg)	84	73	33
CL_{total}[c] (mL/min/kg)	39.3	8.6	–
Vd_{ss}[d] (mL/kg)	3429	1602	–
C_{max}[e] (ng/mL)	64.2	201.0	–
T_{max}[f] (h)	1.7	1.7	–
$AUC_{0–8h}$[g] (ng·h/mL)	242.5	1076.8	–
F[h] (%)	56.7	55.6	–
K_p[i]	1.01	0.91	–

[a] Cassette dosing at 0.1 mg/kg, iv and 1 mg/kg, po (non-fasted). Average of three rats or mice. [b] Metabolic stability was determined by incubation with liver microsomes. [c] Total clearance. [d] Volume of distribution at steady state. [e] Maximum plasma concentration. [f] Time of maximum concentration. [g] Area under the plasma concentration vs time curve (0–8 h). [h] Oral bioavailability. [i] Brain-to-plasma ratio at 2 h after oral administration of **36** at a dose of 10 mg/kg.

X-ray Crystal Structure of 36 Bound in the PDE2A Catalytic Domain. To rationalize the structural basis for the potent PDE2A inhibitory activity and excellent PDE selectivity of **36**, its X-ray co-crystal structure in complex with PDE2A was determined (Figure 8A and 8B). Close inspection of the obtained crystal structure revealed that **36** binds to PDE2A in a manner similar to the binding mode of **4b**, and that the *R* configuration is the active form. As expected, the

lactam moiety of the 3,4-dihydropyrido[2,3-*b*]pyrazin-2(1*H*)-one core forms a hydrogen bonding interaction with the conserved Gln859 residue as in cGMP-like binding pose 1 (Figure 6A), whereas the core is sandwiched between Phe862 and Phe830/Ile826 and stabilized by π–π and CH–π interactions. The methoxy group at the 7-position of the core serves two purposes with respect to potency and PDE selectivity. First, its electron-donating properties enhance the π–π and CH–π interactions of the bicyclic core with Phe862 and Phe830/Ile826, which accounts for the potency increase over the non-substituted analog. Second, it efficiently occupies the small hydrophobic cavity consisting of the side chains of Tyr827, Leu858, and Met847, which is likely one of the key factor for enhanced potency. Utilization of this pocket also improved selectivity over PDE1A, as PDE2A possesses a more hydrophobic binding environment in this pocket owing to the presence of Leu858 in contrast to the more polar Ser416 in PDE1A. We, therefore, reasoned that such distinctions in interactions with PDE2A vs PDE1A may improve selectivity over PDE1A. Further, the carbonyl group of the urea portion interacts with the OH group of Tyr655 via a bridging water molecule. The branched methoxymethyl group is oriented toward the solvent accessible region, most likely leading to a partial gain in solvation energy, although no explicit interactions with water molecules were observed. In addition to the expected intramolecular hydrogen bond between the urea NH and the N5 nitrogen atom of the core scaffold, the oxygen atom in the branched methoxymethyl group forms another key intramolecular hydrogen bond with the urea NH. These two separate internal hydrogen bonds would assist additively in locking the RHS phenyl moiety into an optimal conformation for effectively occupying the binding-induced hydrophobic pocket.

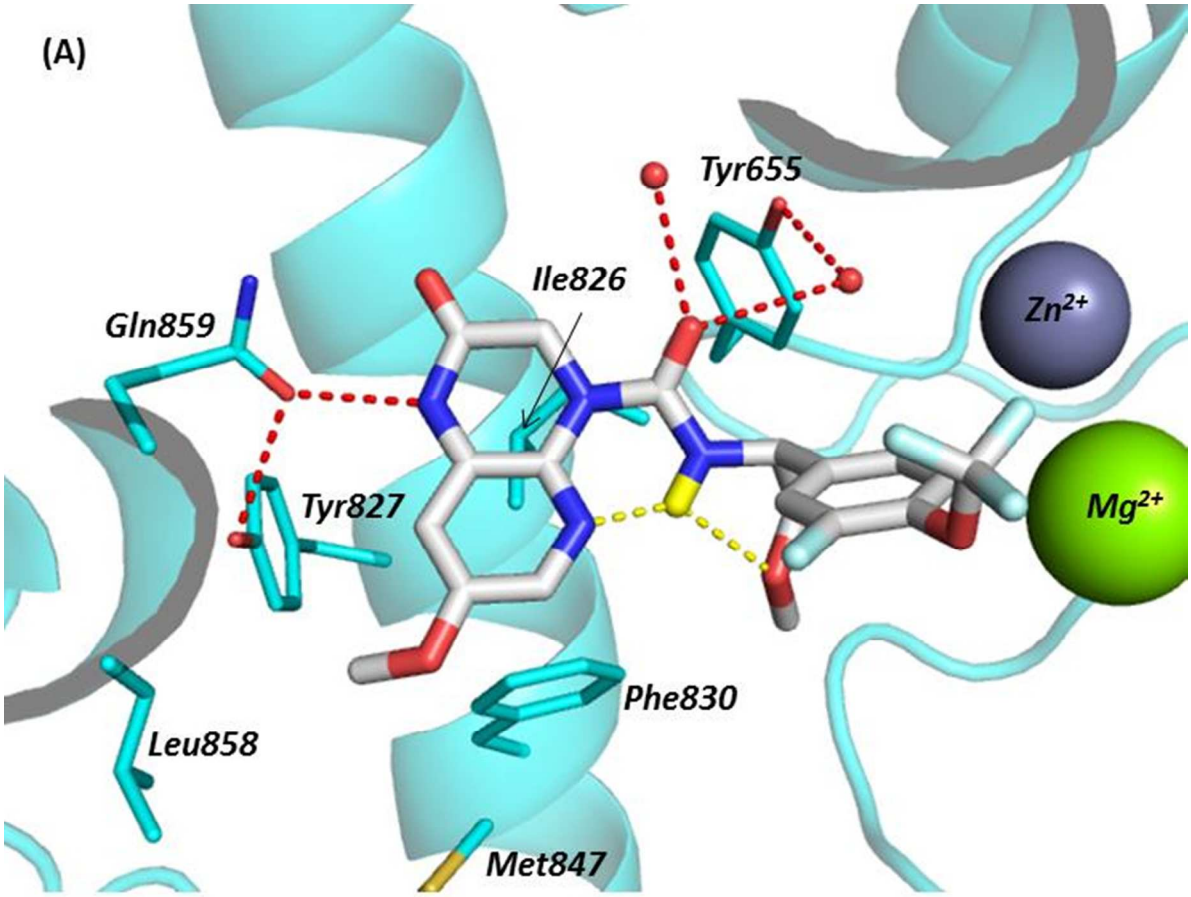
(A)
Tyr655
Ile826
Gln859
Zn2+
Mg2+
Tyr827
Phe830
Leu858
Met847

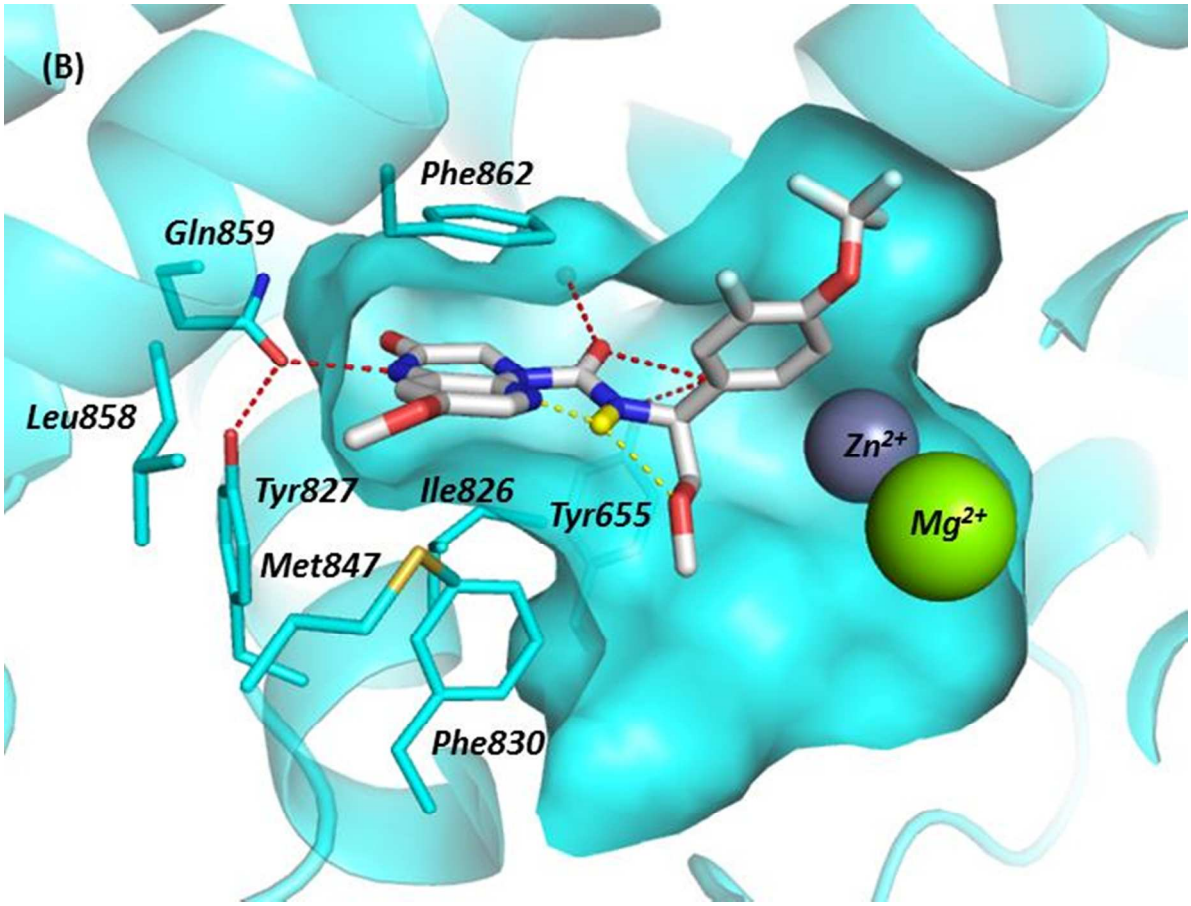

Figure 8. X-ray crystal structure of **36** bound in the PDE2A catalytic site (PDB 5VP0) viewed from the top (A) and the entrance of the catalytic site (B). The key hydrogen bonding interactions of **36** with PDE2A and the intramolecular hydrogen bond in **36** are indicated by red and yellow dotted lines, respectively.

In Vivo Pharmacology of 36. Compound **36** was assessed for its ability to increase the levels of cyclic nucleotides in the hippocampus, one of the brain regions where PDE2A is particularly localized (Figure 9).[6–11] Oral dosing of **36** (3 or 10 mg/kg) in mice produced a dose-dependent increase in cGMP levels, with significant cGMP increases observed at a dose of 10 mg/kg. However, **36** did not have an appreciable impact on cAMP (data not shown). These results are in good agreement with and further validate previous observations using our lead compound **4b** or other reported compounds,[23,37,40,55] in which PDE2A inhibitors predominantly contribute to the

elevation of cGMP under physiological conditions. We next examined the effect of **36** on cognitive performance in a novel object recognition (NOR) task in rats,[56] predictive of potential pro-cognitive activity of drugs. The test was designed to take advantage of the instinctive preference of rats to explore novel objects rather than familiar objects. In this study, **36** was orally administered 2 h prior to the acquisition trial and the exploration time for two identical objects was recorded (Figure 10A). After 48 h of the acquisition trial, one of the familiar objects was replaced with a novel object, the time spent investigating each of the objects was recorded (Figure 10B), and the novelty discrimination index (NDI) was calculated as the percentage of novel object interaction time relative to total interaction time in the retention trial (Figure 10C). As shown in Figure 10A, oral administration of **36** (0.01–1 mg/kg) did not significantly affect the total exploration time in the acquisition trial. On the other hand, during the retention trial (Figure 10B), rats treated with 0.1 and 1 mg/kg of **36** explored the novel object for a greater time, indicative of preserved memory for the familiar object presented during the acquisition trial, whereas rats in vehicle conditions or dosed with 0.01 mg/kg of **36** did not exhibit statistically meaningful differences between exploration times for familiar and novel objects, indicating deterioration or loss of memory for the familiar object. In addition, a 1 mg/kg oral dose of **36** significantly increased the NDI, as shown in Figure 10C. These results suggest that **36** enhanced recognition memory in a NOR task in rats. In-depth studies of the efficacy of **36** in various behavioral animal models relevant to schizophrenia will be reported in due course.

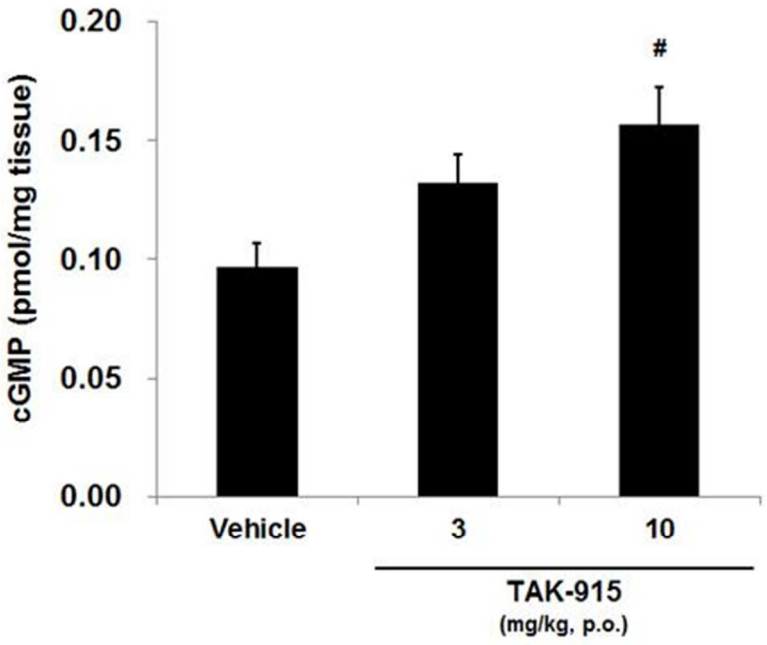

Figure 9. Effect of **36** on cGMP contents in mouse hippocampi. Male C57BL/6J mice were sacrificed by focused microwave irradiation of the brain 60 min after administration of **36**. Values are expressed as pmol/mg tissue weight (mean ± S.E.M., n = 12 per each group). The statistical significance was determined by a one-tailed Williams' test with significance set at #p ≤ 0.025 (vs vehicle group).

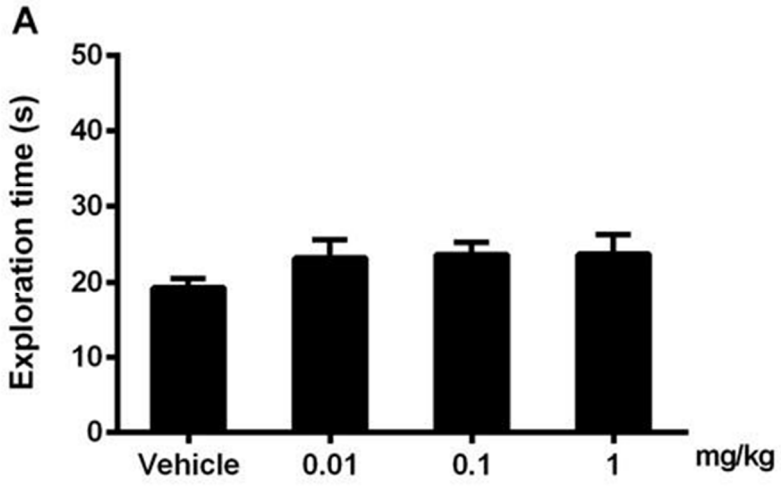

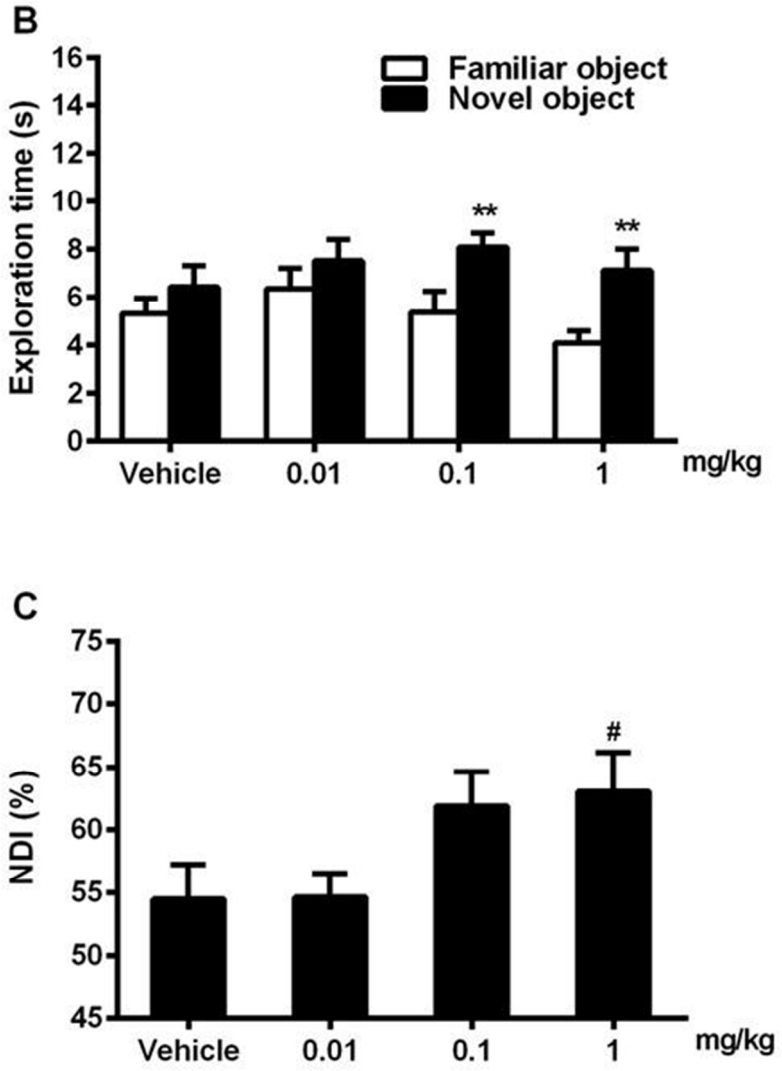

Figure 10. Effects of **36** on a novel object recognition task in rats. Vehicle or **36** (0.01, 0.1, and 1 mg/kg) was orally administered 2 h prior to the acquisition trials. Exploration times in the acquisition trial (A) and the retention trial (performed 48 h after the acquisition trial) (B) were scored. Novelty discrimination index (NDI) (C) in the retention trial was calculated as: novel object interaction time/total interaction time × 100 (%). Data are presented as the mean ± S.E.M., $n = 9$ for 1 mg/kg, $n = 10$ for the other groups; **$p \leq 0.01$ vs familiar object by paired t-test, #$p \leq 0.025$ vs vehicle by one-tailed Williams' test.

CHEMISTRY

The synthesis of 2-oxo-1,2-dihydro-1,5-naphthyridine-4-carboxylic acid, the core leading to **7** is depicted in Scheme 1. Aromatic nucleophilic substitution (S_NAr) of 2-chloropyridine **38**

with the potassium salt of *tert*-butyl ethyl malonate afforded di-ester adduct **39**, which was then subjected to TFA-mediated hydrolysis of the *tert*-butyl ester and subsequent decarboxylation to give ethyl ester **40**. Reduction of the nitro group was carried out under hydrogen in the presence of palladium on charcoal, and the resulting amino group was coupled with 2,2-diethoxylacetic acid, which was readily prepared by basic hydrolysis of the corresponding ester, to afford **42** in 53% yield over four steps from starting material **38**. Elaboration of the additional ring was accomplished via a one-pot three-step process involving hydrolysis of the diethyl acetal under acidic conditions, followed by cyclization and subsequent dehydration. Ethyl ester **43** was hydrolyzed to carboxylic acid **44**, which was finally coupled with RHS benzyl amine **45**,[40] using HATU in the presence of Hünig's base in DMF to provide final product **7**.

Scheme 1. Synthesis of 2-Oxo-1,2-dihydro-1,5-naphthyridine Derivative **7**[a]

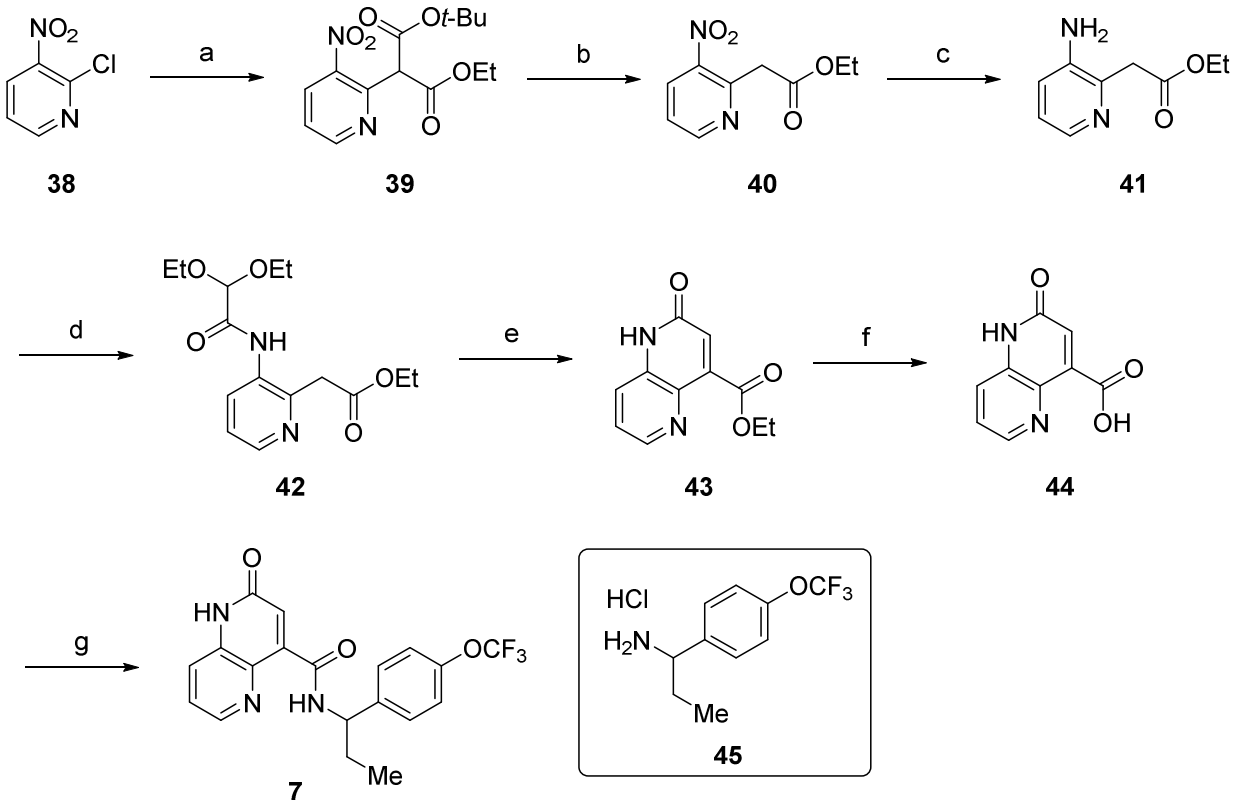

[a] Reagents and conditions: (a) *tert*-butyl ethyl malonate, KO*t*-Bu, THF, 60 °C to reflux, 3 h, (taken on crude); (b) TFA, CH_2Cl_2, rt, overnight, (taken on crude); (c) H_2, 10% Pd/C, EtOH, 50 psi, rt, overnight, (taken on crude); (d) 2,2-diethoxylacetic acid, HATU, DIEA, DMF, rt, overnight, 53% (4 steps from **38**); (e) TFA, H_2O, cat. I_2, 50 °C, overnight, then piperidine, toluene, reflux, 6 h, 26%; (f) 2 M NaOH aq., EtOH, rt, 2 h, 87%; (g) **45**, HATU, DIEA, DMF, rt, 2.5 h, 46%.

The preparation of **8**, outlined in Scheme 2, began with N-amination of 3-aminopyrazole (**46**) using hydroxylamine-*O*-sulfonic acid (HOSA) to afford a mixture of regioisomers **47** and **48** with no regioselective preference. The condensation of **47** with 2-oxo-propionaldehyde under acidic conditions provided pyrazolo[1,5-*b*][1,2,4]triazine **49**. Installation of the carboxylic acid group at the desired position was achieved via a two-step sequence consisting of Vilsmeier formylation and subsequent Pinnick oxidation. The resulting carboxylic acid **51** was finally subjected to amidation with benzylamine **45**[40] to afford **8**.

Scheme 2. Synthesis of 3-Methylpyrazolo[1,5-*b*][1,2,4]triazine Derivative **8**[a]

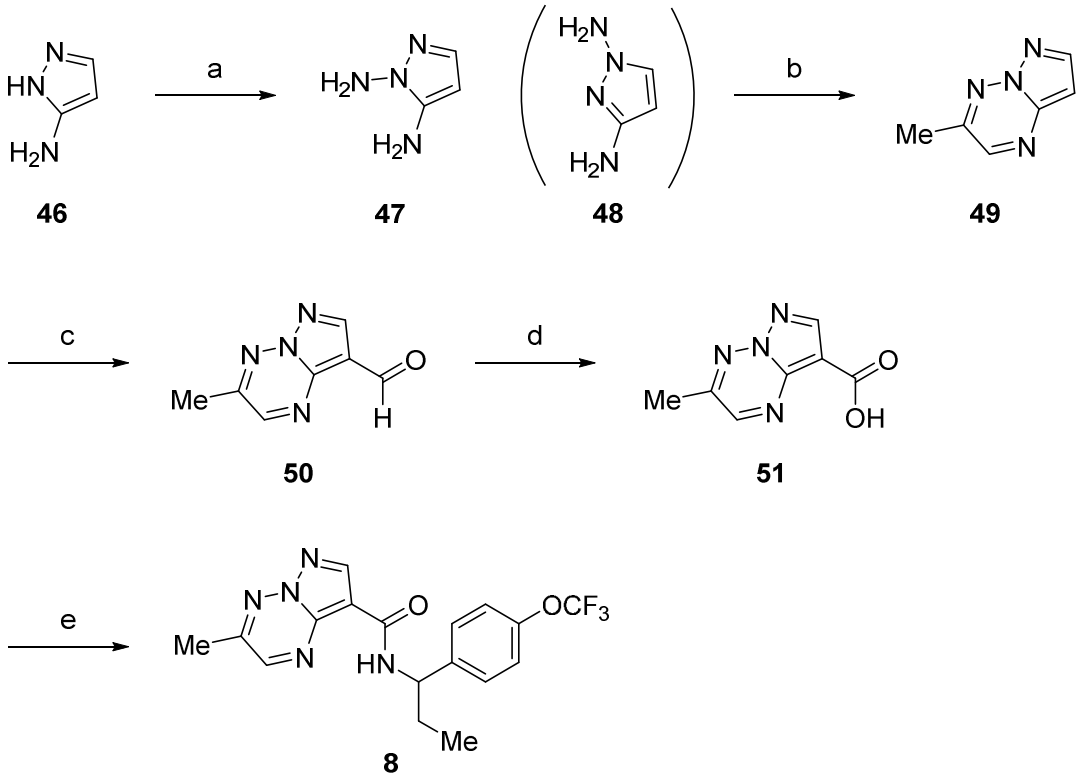

[a] Reagents and conditions: (a) HOSA, KOH, DMF, 0 °C to 15 °C, 2 h, 17%; (b) 2-oxo-propionaldehyde, concd HCl, H_2O, 60 °C to reflux, 1 h, 37%; (c) $POCl_3$, DMF, 0 °C to 40 °C, 16 h, 28%; (d) $NaClO_2$, NaH_2PO_4, 2-methyl-2-butene, *t*-BuOH, H_2O, 30 °C, 16 h, (taken on crude); (e) **45**, EDCI, HOBt, Et_3N, DMF, 10–15 °C, 16 h, 3% (2 steps from **50**).

The synthetic routes utilized to prepare 3,4-dihydropyrido[2,3-*b*]pyrazin-2(1*H*)-one derivatives are shown in Schemes 3 and 4. Derivatives **6**, **10**–**27**, and **29** were prepared as illustrated in Scheme 3. Treatment of 2-chloro-3-nitropyridines **52a**–**f** with methyl glycinate in the presence of triethylamine afforded 2-substituted aminopyridines **53a**–**f**. 5-Bromopyridine **53f** was exposed to copper(I) chloride under microwave irradiation to give the corresponding chloropyridine **53g**. Reduction of the nitro groups in **53a**–**e** and **53g** by catalytic hydrogenation over palladium or platinum on carbon, followed by heating in ethanol, induced intramolecular ring closure to furnish 3,4-dihydropyrido[2,3-*b*]pyrazin-2(1*H*)-one cores **54a**–**e** and **54g**. Finally, the desired compounds **6**, **10**–**23**, **25**–**27**, and **29** were obtained by treatment of **54**, including

commercially available **54h**, with either 4-nitrophenyl chloroformate or triphosgene, followed by reaction with RHS benzylamine **45**, **S23**, **S24**, or **S32** (experimental details for RHS benzylamines **S23**, **S24** and **S32** are provided in the Supporting Information) in the presence of Et_3N. Additionally, sulfone derivative **24** was prepared via *m*-chloroperoxybenzoic acid (*m*-CPBA)-mediated oxidation of sulfide **56**.

Scheme 3. Synthesis of 3,4-Dihydropyrido[2,3-*b*]pyrazin-2(1*H*)-one Derivatives **6**, **10–27**, and **29**[a]

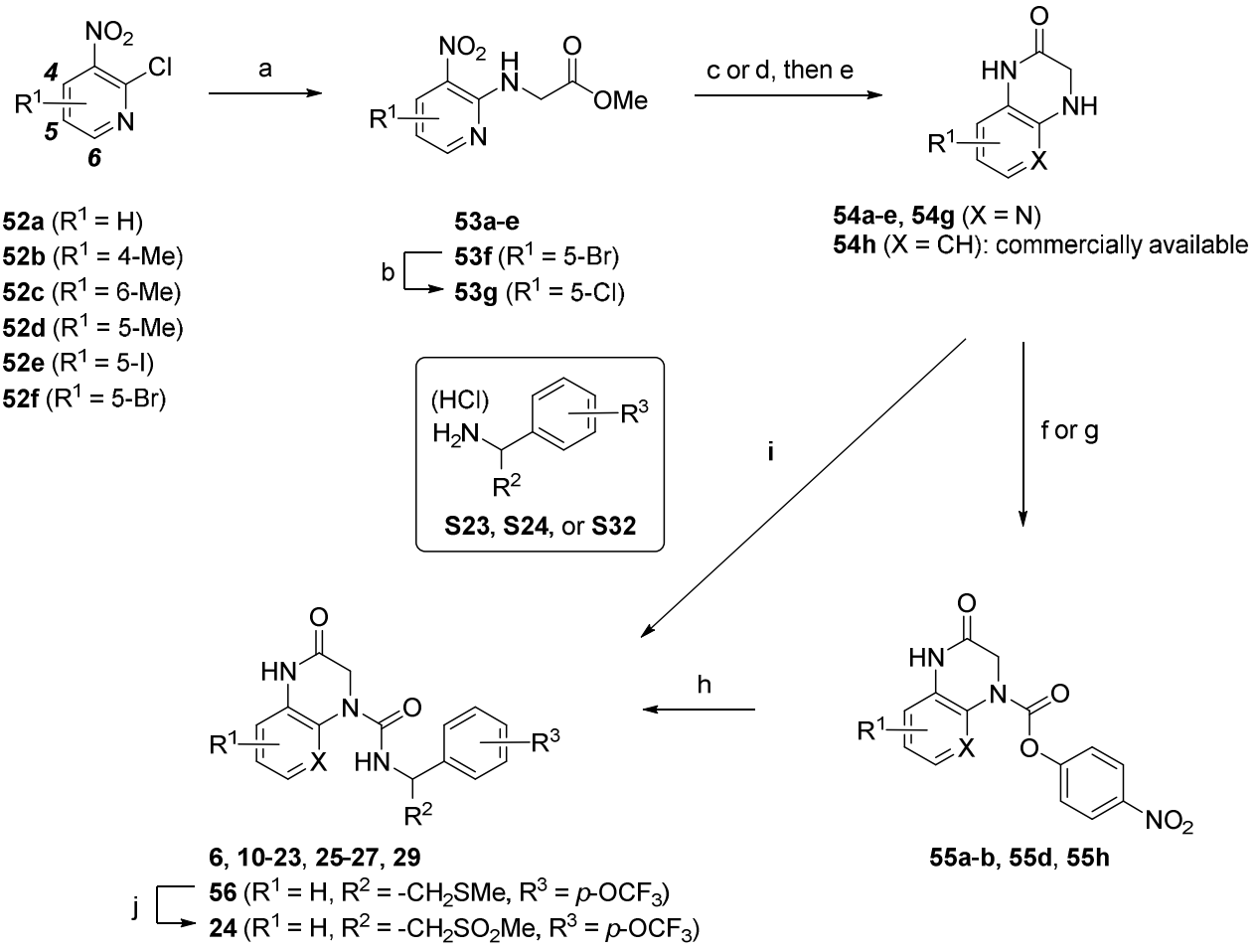

[a] Reagents and conditions: (a) methyl glycinate hydrochloride, Et_3N, DMF or EtOH, rt–90 °C, 3–16 h, 31%–quant.; (b) CuCl, NMP, 150 °C (microwave), 2.5 h, 64%; (c) H_2 (balloon pressure), 10% Pd/C, EtOH, rt, 16 h or overnight, (taken on crude) (for **54a–d**); (d) H_2 (balloon pressure), 5% Pt/C, THF, rt, 2–16 h, (taken on crude) (for **54e** and **54g**); (e) EtOH, reflux, 5–16 h, 58–99%;

(f) 4-nitrophenyl chloroformate, pyridine, DMA, rt–80 °C, 16–24 h, 70–81% (for **55a**, **55d**, and **55h**); (g) 4-nitrophenyl chloroformate, DIEA, THF, 0 °C to rt, 1 h, 51% (for **55b**); (h) RHS benzylamine **45**, **S23**, **S24**, or **S32**, Et_3N, DMF, rt–80 °C, 1–16 h, 23–96%; (i) triphosgene, THF, 40 °C, 1–5 h, then RHS benzylamine **S25** or **S26**, Et_3N, THF, rt–60 °C, 16 h–overnight, 3–95%; (j) *m*-CPBA, EtOAc, rt, overnight, 66%.

To allow for late-stage variations of the R^2 substituent, an alternative synthetic route to that outlined in Scheme 3 was developed (Scheme 4). The synthesis of derivatives **28** and **30**–**37** commenced with N–H protection of lactam **54e** as the (2-(trimethylsilyl)ethoxy)methyl (SEM) acetal. SEM-protected core **57** was then reacted with triphosgene, followed by reaction with RHS benzylamine **S23** or **S24** in the presence of Et_3N to produce ureas **58**–**60**. Modifications of the 7-substituent on the core to obtain **61**–**65** were accomplished using two different approaches. First, iodide **58** was subjected to a palladium-catalyzed Suzuki–Miyaura cross-coupling reaction to give 7-cyclopropyl analog **61** in good yield. Second, iodides **58**–**60** underwent palladium-catalyzed boronic pinacol ester formation, followed by oxidative cleavage with alkaline hydrogen peroxide to afford phenolic intermediates, which were subsequently treated with alkyl iodides in the presence of potassium carbonate (K_2CO_3) to provide 7-alkoxyl analogs **62**–**65**. SEM-protected analogs **61**–**65** were exposed to trifluoroacetic acid (TFA), which, in all cases, gave a mixture of the desired product and partially deprotected intermediate **66** containing a hydroxymethyl moiety. To facilitate hydrolysis of the remaining hemiaminal functionality, the mixture was treated with ammonia in methanol to give completely deprotected products **28**, **30**, **31**, **67**, and **68**. Finally, chiral HPLC separation of racemic compounds **30**, **67**, and **68** afforded corresponding enantiomer pairs **32**–**37**.

Scheme 4. Synthesis of 3,4-Dihydropyrido[2,3-*b*]pyrazin-2(1*H*)-one Derivatives **28** and **30**–**37**[a]

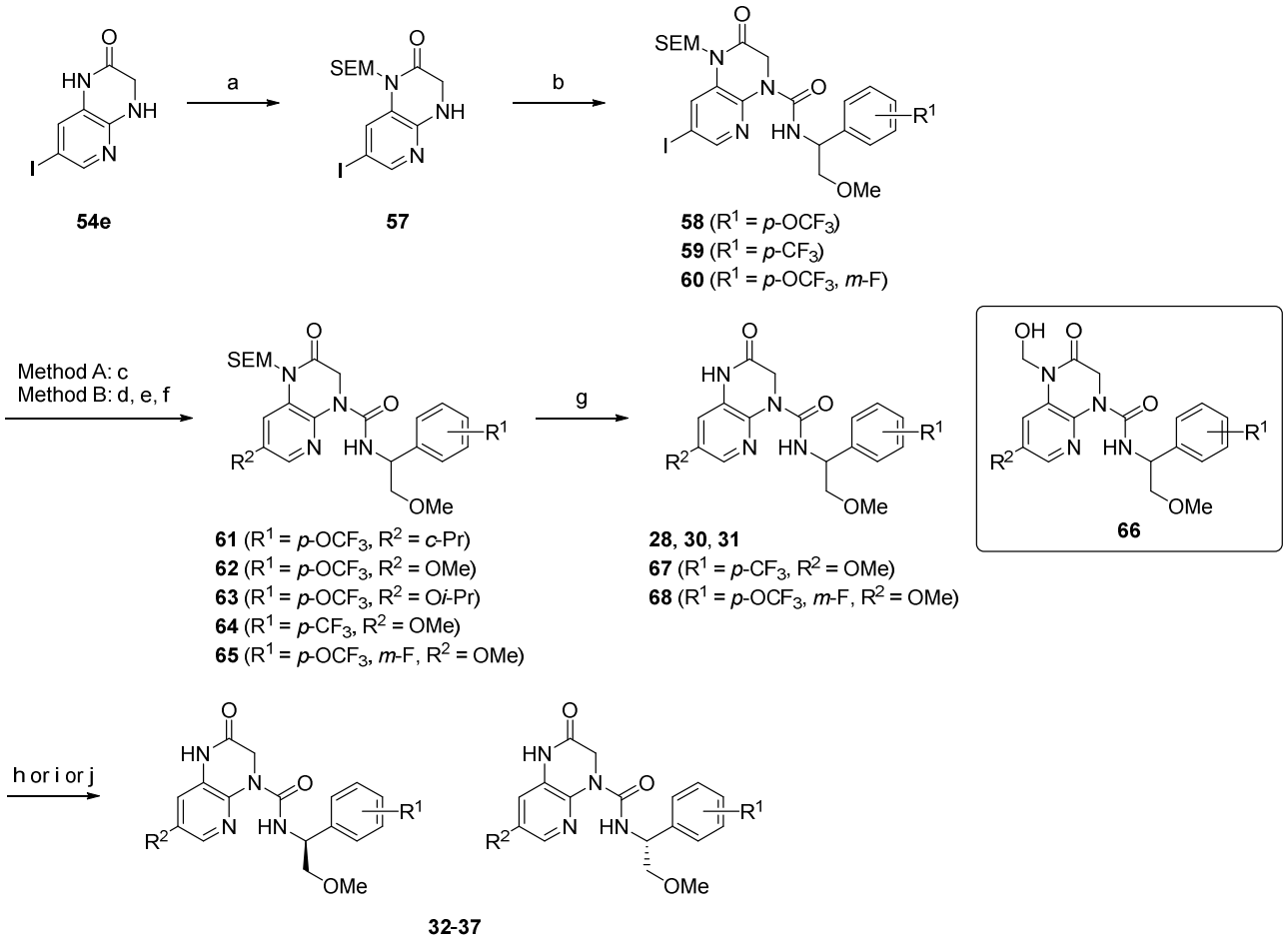

[a] Reagents and conditions: (a) KHMDS, DMF, DMSO, 0 °C, 20 min, then SEMCl, rt, 3 h, 38%.; (b) triphosgene, THF, 40 °C, 1–5 h, then RHS benzylamines **S23** or **S24**, Et_3N, THF, rt–60 °C, 16 h–overnight, 64–95%.; (c) cyclopropylboronic acid, $Pd(OAc)_2$, Cy_3P, K_3PO_4, toluene, 100 °C, overnight, 73%; (d) B_2pin_2, $PdCl_2$(dppf), KOAc, DMF, 80 °C, overnight, (taken on crude); (e) 2 M NaOH aq., THF, 0 °C, 30 min, then 35–36% H_2O_2 aq., rt, 1.5–2 h, 80–97% (2 steps from **58**–**60**); (f) R^2I, K_2CO_3, DMF, rt–70 °C, overnight, 60–82%; (g) TFA, H_2O, rt, 1–3.5 h, then NH_3, MeOH, rt, 10 min–2 h, 67–93%; (h) Chiralpak IA, CO_2/MeOH = 860:140 (for **32** and **33**); (i) Chiralpak AD, hexane/EtOH = 600:400 (for **34** and **35**); (j) Chiralpak AD, hexane/EtOH = 860:140 (for **36** and **37**).

CONCLUSION

Capitalizing on an X-ray crystal structure of PDE2A in complex with pyrazolo[1,5-*a*]pyrimidine analog **4b** as the initial lead structure, we developed a multipronged drug design strategy to further improve the PDE2A inhibitory activity and PDE selectivity of **4b**.

Simultaneously, to increase the probability of obtaining CNS-penetrant compounds, we set target values for two physicochemical properties (TPSA < 110 $Å^2$, HBD count < 3) that play a critical role in CNS exposure, by taking into consideration the masking effect of HBA and HBD through intramolecular hydrogen bonding. Our medicinal chemistry optimization effort identified **36** to have the best balance of potency, PDE selectivity, and brain penetration. In subsequent animal studies, **36** showed a dose-dependent increase in cGMP levels in the brain and improved cognitive performance in a rat NOR test. Improved potency of **36** ultimately led to a lower systemic exposure at effective dosage in vivo compared with the lead compound **4b**. Reflecting this attribute coupled with its excellent PDE selectivity, **36** exhibited a favorable profile in preclinical safety studies. Based on these results, **36** was selected as a clinical candidate and has progressed into clinical trials.

EXPERIMENTAL SECTION

General Chemistry Information. All solvents and reagents were obtained from commercial sources and were used as received. Microwave-assisted reactions were carried out in a single-mode reactor, Biotage Initiator 2.0 or 2.5 microwave synthesizer. Yields were not optimized. All reactions were monitored by thin layer chromatography (TLC) analysis on Merck Kieselgel 60 F254 plates or Fuji Silysia NH plates, or LC–MS (liquid chromatography–mass spectrometry) analysis. LC–MS analysis was performed on a Shimadzu liquid chromatography–mass spectrometer system operating in APCI (+ or −) or ESI (+ or −) ionization mode. Analytes were eluted using a linear gradient with a mobile phase of water/acetonitrile containing 0.05% TFA or 5 mM ammonium acetate and detected at 220 nm. Column chromatography was carried out on silica gel ((Merck Kieselgel 60, 70–230 mesh, Merck) or (Chromatorex NH-DM 1020, 100–200

mesh, Fuji Silysia Chemical, Ltd.)), or on prepacked Purif-Pack columns (SI or NH, particle size: 60 μm, Fuji Silysia Chemical, Ltd.). Analytical HPLC was performed using a Corona Charged Aerosol Detector or photo diode array detector with a Capcell Pak C18AQ (3.0 mm ID × 50 mm L, Shiseido, Japan) or L-column2 ODS (2.0 mm ID × 30 mm L, CERI, Japan) column at a temperature of 50 °C and a flow rate of 0.5 mL/min. Mobile phases A and B under neutral conditions were a mixture of 50 mmol/L ammonium acetate, water, and acetonitrile (1:8:1, v/v/v) and a mixture of 50 mmol/L ammonium acetate and acetonitrile (1:9, v/v), respectively. The ratio of mobile phase B was increased linearly from 5% to 95% over 3 min, and then maintained at 95% over the next 1 min. Mobile phases A and B under acidic conditions were a mixture of 0.2% formic acid in 10 mmol/L ammonium formate and 0.2% formic acid in acetonitrile, respectively. The ratio of mobile phase B was increased linearly from 14% to 86% over 3 min, and then maintained at 86% over the next 1 min. All final test compounds were purified to >95% chemical purity as measured by analytical HPLC. Elemental analyses were carried out by Takeda Analytical Laboratories, and all results were within ±0.4% of the theoretical values. Melting points were determined on a BÜCHI B-545 melting point apparatus or a DSC1 system (Mettler-Toledo International Inc., Greifensee, Switzerland). Proton nuclear magnetic resonance (^{1}H NMR) spectra were recorded on a Varian Mercury-300 (300 MHz), Varian (400 MHz), Bruker DPX300 (300 MHz), or Bruker Avance III (400 MHz) instrument. All ^{1}H NMR spectra were consistent with the proposed structures. All proton shifts are given in parts per million (ppm) downfield from tetramethysilane (δ) as the internal standard in deuterated solvent, and coupling constants (*J*) are in hertz (Hz). NMR data are reported as follows: chemical shift, integration, multiplicity (s, singlet; d, doublet; t, triplet; q, quartet; quint, quintet; m, multiplet; dd, doublet of doublets; td, triplet of doublets; ddd, doublet of doublet of doublets; and brs, broad singlet), and

coupling constants. Very broad peaks for protons of, for example, hydroxyl and amino groups are not always indicated.

2-Oxo-N-(1-(4-(trifluoromethoxy)phenyl)propyl)-2,3-dihydropyrido[2,3-b]pyrazine-4(1H)-carboxamide (6). To a solution of **55a** (904 mg, 2.62 mmol) in DMF (15 mL) were added 1-(4-(trifluoromethoxy)phenyl)propan-1-amine hydrochloride (**45**) (736 mg, 2.88 mmol) and Et_3N (1.10 mL, 7.85 mmol). The mixture was stirred at rt for 1 h and then poured into $NaHCO_3$ aqueous solution. The mixture was extracted with EtOAc, washed with 1 M HCl aqueous solution and saturated aqueous NaCl, dried over anhydrous Na_2SO_4 and concentrated in vacuo. The residue was purified by column chromatography (silica gel, hexane/ethyl acetate, 9:1 to 0:100) to afford **6** (910.6 mg, 2.31 mmol, 88%) as a white solid. ^{1}H NMR (300 MHz, $CDCl_3$) δ 0.96 (3H, t, *J* = 7.4 Hz), 1.76–1.96 (2H, m), 4.67 (2H, s), 4.90 (1H, q, *J* = 7.2 Hz), 6.99 (1H, dd, *J* = 7.6, 4.9 Hz), 7.12–7.25 (3H, m), 7.30–7.42 (2H, m), 7.99 (1H, dd, *J* = 5.1, 1.7 Hz), 9.91 (1H, s), 10.46 (1H, d, *J* =7.2 Hz). MS (ESI/APCI) mass calculated for $[M + H]^+$ ($C_{18}H_{18}F_3N_4O_3$) requires *m/z* 395.1, found *m/z* 395.2. HPLC purity: 98.9%. mp 185 °C.

2-Oxo-N-((1R or 1S)-1-(4-(trifluoromethoxy)phenyl)propyl)-2,3-dihydropyrido[2,3-b]pyrazine-4(1H)-carboxamide (6a). Resolution of the enantiomers of **6** was carried out chromatographically using a Chiralpak IC 50 mm ID × 500 mm L column (hexane/ethanol, 400:600) at 60 mL/min. Resolution of **6** (907 mg, 2.30 mmol) provided 439 mg of **6a** as the first eluting enantiomer, which was triturated with hexane/ethyl acetate (5:1) to afford **6a** (416.9 mg, 1.03 mmol, 45%, 89% theoretical) as a pale yellow solid. Analytical HPLC analysis carried out on a 4.6 mm ID × 250 mm L Chiralpak IC column with the same eluent as above at a flow rate of 0.5 mL/min indicated that **6a** was of 99.7% ee. ^{1}H NMR (300 MHz, DMSO-d_6) δ 0.88 (3H, t, *J* = 7.3 Hz), 1.70–1.89 (2H, m), 4.41 (2H, s), 4.81 (1H, q, *J* = 6.9 Hz), 7.10 (1H, dd, *J* = 7.7, 5.1

Hz), 7.25–7.37 (3H, m), 7.38–7.51 (2H, m), 8.02 (1H, dd, *J* = 5.1, 1.7 Hz), 10.34 (1H, d, *J* = 7.5 Hz), 10.82 (1H, brs). MS (ESI/APCI) mass calculated for $[M + H]^+$ ($C_{18}H_{18}F_3N_4O_3$) requires *m/z* 395.1, found *m/z* 395.2. HPLC purity: 97.9%. Anal. Calcd for $C_{18}H_{17}F_3N_4O_3$: C, 54.82; H, 4.35; N, 14.21. Found: C, 55.01; H, 4.59; N, 14.12.

2-Oxo-N-((1S or 1R)-1-(4-(trifluoromethoxy)phenyl)propyl)-2,3-dihydropyrido[2,3-b]pyrazine-4(1H)-carboxamide (6b). Resolution of the enantiomers of **6** was carried out chromatographically using a Chiralpak IC 50 mm ID × 500 mm L column (hexane/ethanol, 400:600) at 60 mL/min. Resolution of **6** (907 mg, 2.30 mmol) provided 429 mg of **6b** as the first eluting enantiomer, which was triturated with hexane/ethyl acetate (5:1) to afford **6b** (399 mg, 1.01 mmol, 44%, 88% theoretical) as a pale yellow solid. Analytical HPLC analysis carried out on a 4.6 mm ID × 250 mm L Chiralpak IC column with the same eluent as above at a flow rate of 0.5 mL/min indicated that **6b** was of >99.9% ee. ^{1}H NMR (300 MHz, DMSO-d_6) δ 0.88 (3H, t, *J* = 7.3 Hz), 1.70–1.90 (2H, m), 4.41 (2H, s), 4.81 (1H, q, *J* = 7.0 Hz), 7.11 (1H, dd, *J* = 7.7, 5.1 Hz), 7.26–7.38 (3H, m), 7.38–7.51 (2H, m), 8.02 (1H, dd, *J* = 4.9, 1.5 Hz), 10.35 (1H, d, *J* = 7.2 Hz), 10.83 (1H, brs). MS (ESI/APCI) mass calculated for $[M + H]^+$ ($C_{18}H_{18}F_3N_4O_3$) requires *m/z* 395.1, found *m/z* 395.1. HPLC purity: 100%. Anal. Calcd for $C_{18}H_{17}F_3N_4O_3$: C, 54.82; H, 4.35; N, 14.21. Found: C, 54.90; H, 4.50; N, 14.15.

2-Oxo-N-(1-(4-(trifluoromethoxy)phenyl)propyl)-1,2-dihydro-1,5-naphthyridine-4-carboxamide (7). To a mixture of **44** (372 mg, 1.96 mmol), **45** (650 mg, 2.54 mmol) and DIEA (1.03 mL, 5.87 mmol) in DMF (15 mL) was added HATU (1.12 g, 2.94 mmol). The mixture was stirred at rt for 2.5 h and then poured into water. The mixture was extracted with EtOAc, washed with water and saturated aqueous NaCl, dried over anhydrous Na_2SO_4 and concentrated in vacuo. The residue was purified by column chromatography (silica gel, hexane/ethyl acetate, 4:1 to

0:100), followed by a second column purification (silica gel, hexane/ethyl acetate, 4:1 to 0:100)) to afford **7** (341 mg, 0.871 mmol, 45%) as a white solid after recrystallization from ethyl acetate. ^{1}H NMR (300 MHz, DMSO-d_6) δ 0.95 (3H, t, J = 7.4 Hz), 1.78–1.92 (2H, m), 5.03 (1H, q, J = 6.9 Hz), 7.08 (1H, s), 7.30–7.40 (2H, m), 7.50–7.58 (2H, m), 7.63 (1H, dd, J = 8.5, 4.4 Hz), 7.79 (1H, dd, J = 8.3, 1.5 Hz), 8.58 (1H, dd, J = 4.5, 1.5 Hz), 10.47 (1H, d, J = 8.0 Hz), 12.17 (1H, brs). MS (ESI/APCI) mass calculated for $[M + H]^+$ ($C_{19}H_{17}F_3N_3O_3$) requires *m/z* 392.1, found *m/z* 392.2. HPLC purity: 95.7%.

3-Methyl-N-(1-(4-(trifluoromethoxy)phenyl)propyl)pyrazolo[1,5-b][1,2,4]triazine-8-carboxamide (8). A mixture of compound **51** (30 mg, containing 50% of **49**), **45** (46 mg, 0.18 mmol), HOBt (24 mg, 0.18 mmol), EDCI (34 mg, 0.18 mmol), and Et_3N (20 mg, 0.20 mmol) in DMF (3 mL) was stirred at 10–15 °C for 16 h. The mixture was diluted with water (15 mL), extracted with EtOAc (10 mL × 3). The combined organic layer was washed with saturated aqueous NaCl (10 mL), dried over anhydrous Na_2SO_4 and concentrated in vacuo. The residue was purified by preparative HPLC (column: Fuji C18 (25 mm ID × 300 mm L), YMC (20 mm ID × 250 mm L); mobile phase A: 0.05% HCl in water; mobile phase B: 0.05% HCl in acetonitrile; flow rate: 25 mL/min), and most of CH_3CN was removed under reduced pressure. The remaining solvent was removed by lyophilization to give **8** (4 mg, 3% in 2 steps) as a yellow solid. ^{1}H NMR (400 MHz, DMSO-d_6) δ 0.93 (3H, t, J = 7.2 Hz), 1.81–1.92 (2H, m), 2.63 (3H, s), 4.97–5.06 (1H, m), 7.32 (2H, d, J = 8.0 Hz), 7.52 (2H, d, J = 8.8 Hz), 8.14 (1H, d, J = 8.4 Hz), 8.56 (1H, s), 8.81 (1H, s). MS (ESI/APCI) mass calculated for $[M + H]^+$ ($C_{17}H_{17}F_3N_5O_2$) requires *m/z* 380.1, found *m/z* 380.2. HPLC purity: 100%.

3-Oxo-N-(1-(4-(trifluoromethoxy)phenyl)propyl)-3,4-dihydroquinoxaline-1(2H)-carboxamide (10). To a solution of **55h** (313 mg, 1.00 mmol) and **45** (307 mg, 1.20 mmol) in DMF (10 mL)

was added Et_3N (418 μL, 3.00 mmol) at rt. After being stirred at 80 °C for 24 h, the mixture was quenched with water and extracted with EtOAc. The organic layer was separated, washed with water and saturated aqueous NaCl, dried over anhydrous $MgSO_4$ and concentrated in vacuo. The residue was purified by column chromatography (silica gel, hexane/ethyl acetate, 9:1 to 1:1) to give **10** (281 mg, 0.714 mmol, 72%) as a white solid. ^{1}H NMR (300 MHz, $CDCl_3$) δ 0.88 (3H, t, *J* = 7.3 Hz), 1.69–1.86 (2H, m), 4.30–4.52 (2H, m), 4.81 (1H, q, *J* = 7.2 Hz), 5.39 (1H, d, *J* = 7.2 Hz), 6.91–6.97 (1H, m), 7.07–7.37 (7H, m), 8.02 (1H, brs). MS (ESI/APCI) mass calculated for $[M + H]^+$ ($C_{19}H_{19}F_3N_3O_3$) requires *m/z* 394.1, found *m/z* 394.1. HPLC purity: 96.9%. mp 198 °C. Anal. Calcd for $C_{19}H_{18}F_3N_3O_3$: C, 58.01; H, 4.61; N, 10.68. Found: C, 58.17; H, 4.70; N, 10.59.

N-(1-(4-Methoxyphenyl)propyl)-2-oxo-2,3-dihydropyrido[2,3-b]pyrazine-4(1H)-carboxamide (11). To a solution of 3,4-dihydropyrido[2,3-b]pyrazin-2(1H)-one (23.5 mg, 0.160 mmol) and Et_3N (65.9 μL, 0.470 mmol) in THF (5.0 mL) and DMA (1.0 mL) was added triphosgene (46.8 mg, 0.160 mmol) at 0 °C. After stirring at 0 °C for 2 h, Et_3N (65.9 μL, 0.470 mmol) and 1-(4-methoxyphenyl)propan-1-amine hydrochloride (159 mg, 0.790 mmol) was added at 0 °C. The mixture was stirred at rt for 2 h and then quenched with water. The mixture was extracted with EtOAc, washed with saturated aqueous NaCl, dried over anhydrous Na_2SO_4 and concentrated in vacuo. The residue was purified by column chromatography (basic silica gel, hexane/ethyl acetate, 1:1 to 0:100) to give **11** (6.33 mg, 0.019 mmol, 12%) as a white solid after trituration with hexane/diisopropyl ether. ^{1}H NMR (300 MHz, $CDCl_3$) δ 0.79–1.00 (3H, m), 1.76–1.97 (2H, m), 3.78 (3H, s), 4.68 (2H, s), 4.83 (1H, q, *J* = 7.2 Hz), 6.86 (2H, d, *J* = 8.7 Hz), 6.96 (1H, dd, *J* = 7.7, 5.1 Hz), 7.08–7.37 (3H, m), 7.97 (1H, dd, *J* = 5.1, 1.3 Hz), 9.69 (1H, brs), 10.35 (1H, d, *J* = 7.6 Hz). MS (ESI/APCI) mass calculated for $[M - H]^-$ ($C_{18}H_{19}N_4O_3$) requires *m/z* 339.2, found *m/z* 339.1. HPLC purity: 99.8%.

2-Oxo-N-(1-(4-(trifluoromethyl)phenyl)propyl)-2,3-dihydropyrido[2,3-b]pyrazine-4(1H)-carboxamide (12). To a solution of **55a** (314 mg, 1.00 mmol) in DMF (10 mL) were added 1-(4-(trifluoromethyl)phenyl)propan-1-amine (**S23g**) (223 mg, 1.10 mmol) and Et_3N (0.418 mL, 3.00 mmol). The mixture was stirred at rt for 16 h and then concentrated in vacuo. The residue was diluted with water and extracted with EtOAc. The organic layer was separated, washed with saturated aqueous $NaHCO_3$, water and saturated aqueous NaCl, dried over anhydrous $MgSO_4$ and concentrated in vacuo. The residue was purified by column chromatography (silica gel, hexane/ethyl acetate, 9:1 to 3:2) to give **12** (314 mg, 0.830 mmol, 83%) as a colorless prisms after recrystallized from hexane/ethyl acetate. ^{1}H NMR (300 MHz, $CDCl_3$) δ 0.97 (3H, t, *J* = 7.3 Hz), 1.89 (2H, quin, *J* = 7.3 Hz), 4.67 (2H, s), 4.93 (1H, q, *J* = 6.8 Hz), 7.01 (1H, dd, *J* = 7.7, 5.1 Hz), 7.19 (1H, dd, *J* = 7.5, 1.5 Hz), 7.44 (2H, d, *J* = 8.3 Hz), 7.58 (2H, d, *J* = 8.3 Hz), 8.01 (1H, dd, *J* = 4.9, 1.5 Hz), 9.16 (1H, brs), 10.48 (1H, d, *J* = 7.2 Hz). MS (ESI/APCI) mass calculated for $[M + H]^+$ ($C_{18}H_{18}F_3N_4O_2$) requires *m/z* 379.1, found *m/z* 379.2. HPLC purity: 100%. mp 105 °C. Anal. Calcd for $C_{18}H_{17}F_3N_4O_2$: C, 57.14; H, 4.53; N, 14.81. Found: C, 56.89; H, 4.55; N, 14.74.

N-(1-(4-Cyclopropylphenyl)propyl)-2-oxo-2,3-dihydropyrido[2,3-b]pyrazine-4(1H)-carboxamide (13). The title compound was prepared as a pale yellow solid after recrystallization from hexane/ethyl acetate in 23% yield from **55a** and 1-(4-cyclopropylphenyl)propan-1-amine (**S23a**) using the procedure analogous to that described for the synthesis of **12**. ^{1}H NMR (300 MHz, $CDCl_3$) δ 0.61–0.70 (2H, m), 0.86–0.98 (5H, m), 1.79–1.95 (3H, m), 4.61–4.75 (2H, m), 4.79–4.90 (1H, m), 6.92–7.06 (3H, m), 7.10–7.24 (3H, m), 7.99 (1H, dd, *J* = 5.1, 1.7 Hz), 8.36–8.67 (1H, m), 10.33 (1H, d, *J* = 7.2 Hz). MS (ESI/APCI) mass calculated for $[M + H]^+$ ($C_{20}H_{23}N_4O_2$) requires *m/z* 351.2, found *m/z* 351.2. HPLC purity: 98.0%.

N-(1-(4-(Azetidin-1-yl)phenyl)propyl)-2-oxo-2,3-dihydropyrido[2,3-b]pyrazine-4(1H)-carboxamide (14). The title compound was prepared as a colorless prisms after recrystallization from hexane/ethyl acetate in 80% yield from **55a** and 1-(4-(azetidin-1-yl)phenyl)propan-1-amine (**S23b**) using the procedure analogous to that described for the synthesis of **12**. ^{1}H NMR (300 MHz, $CDCl_3$) δ 0.91 (3H, t, *J* = 7.3 Hz), 1.74–1.96 (2H, m), 2.27–2.39 (2H, m), 3.84 (4H, t, *J* = 7.2 Hz), 4.60–4.72 (2H, m), 4.74–4.85 (1H, m), 6.38–6.45 (2H, m), 6.90–6.99 (1H, m), 7.09–7.21 (3H, m), 7.97 (1H, dd, *J* = 5.1, 1.7 Hz), 8.53 (1H, s), 10.24 (1H, d, *J* = 7.9 Hz). MS (ESI/APCI) mass calculated for $[M + H]^+$ ($C_{20}H_{24}N_5O_2$) requires *m/z* 366.2, found *m/z* 366.2. HPLC purity: 100%. mp 176 °C. Anal. Calcd for $C_{20}H_{23}N_5O_2$: C, 65.73; H, 6.34; N, 19.16. Found: C, 65.73; H, 6.23; N, 18.93.

2-Oxo-N-(1-(3-(trifluoromethoxy)phenyl)propyl)-2,3-dihydropyrido[2,3-b]pyrazine-4(1H)-carboxamide (15). To a solution of **55a** (369 mg, 1.17 mmol) and 1-(3-(trifluoromethoxy)phenyl)propan-1-amine hydrochloride (**S24c**) (335 mg, 1.31 mmol) in DMF (10 mL) was added Et_3N (0.409 mL, 2.94 mmol) at rt. After being stirred for 16 h, the mixture was quenched with water and extracted with EtOAc. The organic layer was separated, washed with water and saturated aqueous NaCl, dried over anhydrous $MgSO_4$ and concentrated in vacuo. The residue was purified by column chromatography (silica gel, hexane/ethyl acetate, 9:1 to 33:67) to give **15** (202 mg, 0.512 mmol, 44%) as a white solid after recrystallization from hexane/ethyl acetate. ^{1}H NMR (300 MHz, $CDCl_3$) δ 0.96 (3H, t, *J* = 7.3 Hz), 1.82–1.93 (2H, m), 4.68 (2H, s), 4.92 (1H, q, *J* = 6.9 Hz), 7.00 (1H, dd, *J* = 7.5, 4.9 Hz), 7.09 (1H, dd, *J* = 7.9, 1.1 Hz), 7.14–7.20 (2H, m), 7.23–7.29 (1H, m), 7.31–7.39 (1H, m), 8.00 (1H, dd, *J* = 4.9, 1.5 Hz), 8.57–8.77 (1H, m), 10.44 (1H, d, *J* = 7.2 Hz). MS (ESI/APCI) mass calculated for $[M + H]^+$

($C_{18}H_{18}F_3N_4O_2$) requires *m/z* 395.1, found *m/z* 395.2. HPLC purity: 99.7%. mp 110 °C. Anal. Calcd for $C_{18}H_{17}F_3N_4O_3$: C, 54.82; H, 4.35; N, 14.21. Found: C, 54.69; H, 4.37; N, 14.16.

2-Oxo-N-(1-(2-(trifluoromethoxy)phenyl)propyl)-2,3-dihydropyrido[2,3-b]pyrazine-4(1H)-carboxamide (16). The title compound was prepared as a white solid in 78% yield from **55a** and 1-(2-(trifluoromethoxy)phenyl)propan-1-amine hydrochloride (**S24d**) using the procedure analogous to that described for the synthesis of **15**. ^{1}H NMR (300 MHz, DMSO-d_6) δ 0.89 (3H, t, *J* = 7.4 Hz), 1.66–1.91 (2H, m), 4.40 (2H, s), 4.97–5.15 (1H, m), 7.11 (1H, dd, *J* = 7.7, 4.9 Hz), 7.26–7.42 (4H, m), 7.44–7.53 (1H, m), 8.00 (1H, dd, *J* = 5.0, 1.6 Hz), 10.41 (1H, d, *J* = 7.7 Hz), 10.80 (1H, s). MS (ESI/APCI) mass calculated for $[M + H]^+$ ($C_{18}H_{18}F_3N_4O_2$) requires *m/z* 395.1, found *m/z* 395.2. HPLC purity: 99.4%. mp 178 °C. Anal. Calcd for $C_{18}H_{17}F_3N_4O_3$: C, 54.82; H, 4.35; N, 14.21; F,14.45. Found: C, 55.00; H, 4.49; N, 14.20; F, 14.21.

N-(1-(3-fluoro-4-(trifluoromethoxy)phenyl)propyl)-2-oxo-2,3-dihydropyrido[2,3-b]pyrazine-4(1H)-carboxamide (17). The title compound was prepared as a white solid after crystallization from hexane/ethyl acetate in 63% yield from **55a** and 1-(3-fluoro-4-(trifluoromethoxy)phenyl)propan-1-amine hydrochloride (**S24e**) using the procedure analogous to that described for the synthesis of **15**. ^{1}H NMR (300 MHz, DMSO-d_6) δ 0.77–0.95 (3H, m), 1.81 (2H, quin, *J* = 7.3 Hz), 4.35–4.47 (2H, m), 4.81 (1H, q, *J* = 7.2 Hz), 7.11 (1H, dd, *J* = 7.7, 5.1 Hz), 7.27 (1H, d, *J* = 8.3 Hz), 7.32 (1H, dd, *J* = 7.9, 1.5 Hz), 7.44–7.58 (2H, m), 8.02 (1H, dd, *J* = 4.9, 1.5 Hz), 10.30 (1H, d, *J* = 7.2 Hz), 10.81 (1H, s). MS (ESI/APCI) mass calculated for $[M + H]^+$ ($C_{18}H_{17}F_4N_4O_3$) requires *m/z* 413.1, found *m/z* 413.1. HPLC purity: 100%. mp 154 °C. Anal. Calcd for $C_{18}H_{16}F_4N_4O_3$: C, 52.43; H, 3.91; N, 13.59. Found: C, 52.48; H, 3.89; N, 13.30.

N-(1-(2-Fluoro-4-(trifluoromethoxy)phenyl)propyl)-2-oxo-2,3-dihydropyrido[2,3-b]pyrazine-4(1H)-carboxamide (18). The title compound was prepared as a white solid after

recrystallization from hexane/ethyl acetate in 87% yield from **55a** and 1-(2-fluoro-4-(trifluoromethoxy)phenyl)propan-1-amine hydrochloride (**S24f**) using the procedure analogous to that described for the synthesis of **15**. ^{1}H NMR (300 MHz, DMSO-d_6) δ 0.89 (3H, t, J = 7.2 Hz), 1.70–1.88 (2H, m), 4.40 (2H, s), 5.00 (1H, q, J = 7.4 Hz), 7.11 (1H, dd, J = 7.9, 4.9 Hz), 7.22 (1H, d, J = 8.7 Hz), 7.27–7.42 (2H, m), 7.49 (1H, t, J = 8.5 Hz), 8.02 (1H, dd, J = 4.9, 1.9 Hz), 10.43 (1H, d, J = 7.5 Hz), 10.81 (1H, s). MS (ESI/APCI) mass calculated for $[M + H]^+$ ($C_{18}H_{17}F_4N_4O_3$) requires *m/z* 413.1, found *m/z* 413.2. HPLC purity: 97.2%. mp 173.9–176.3 °C.

N-(2-Methoxy-1-(4-(trifluoromethoxy)phenyl)ethyl)-2-oxo-2,3-dihydropyrido[2,3-b]pyrazine-4(1H)-carboxamide (19). The title compound was prepared as a white solid after trituration with hexane in 55% yield from **55a** and 2-methoxy-1-(4-(trifluoromethoxy)phenyl)ethanamine using the procedure analogous to that described for the synthesis of **6**. ^{1}H NMR (300 MHz, DMSO-d_6) δ 3.28 (3H, s), 3.55–3.71 (2H, m), 4.33–4.50 (2H, m), 4.99–5.13 (1H, m), 7.11 (1H, dd, J = 7.9, 4.9 Hz), 7.27–7.39 (3H, m), 7.42–7.53 (2H, m), 8.00 (1H, dd, J = 4.9, 1.7 Hz), 10.51 (1H, d, J = 7.4 Hz), 10.83 (1H, brs). MS (ESI/APCI) mass calculated for $[M + H]^+$ ($C_{18}H_{18}F_3N_4O_4$) requires *m/z* 411.1, found *m/z* 411.1. HPLC purity: 99.8%. mp 163 °C. Anal. Calcd for $C_{18}H_{17}F_3N_4O_4$: C, 52.69; H, 4.18; N, 13.65. Found: C, 52.83; H, 4.33; N, 13.55.

N-(3-Methoxy-1-(4-(trifluoromethoxy)phenyl)propyl)-2-oxo-2,3-dihydropyrido[2,3-b]pyrazine-4(1H)-carboxamide (20). The title compound was prepared as a white solid in 25% yield from **55a** and 3-methoxy-1-(4-(trifluoromethoxy)phenyl)propan-1-amine hydrochloride (**S24h**) using the procedure analogous to that described for the synthesis of **15**. ^{1}H NMR (300 MHz, DMSO-d_6) δ 2.01 (2H, q, J = 6.0 Hz), 3.21 (3H, s), 3.25–3.33 (2H, m), 4.29–4.51 (2H, m), 5.01 (1H, q, J = 6.8 Hz), 7.11 (1H, dd, J = 7.9, 4.9 Hz), 7.26–7.37 (3H, m), 7.39–7.50 (2H, m), 8.02 (1H, dd, J = 4.9, 1.5 Hz), 10.31 (1H, d, J = 7.5 Hz), 10.81 (1H, brs). MS (ESI/APCI) mass calculated for

$[M + H]^+$ ($C_{18}H_{18}F_3N_4O_4$) requires *m/z* 424.1, found *m/z* 425.2. HPLC purity: 99.8%. mp 132 °C. Anal. Calcd for $C_{19}H_{19}F_3N_4O_4$: C, 53.77; H, 4.51; N, 13.20; F,13.43. Found: C, 53.50; H, 4.52; N, 13.02; F, 13.37.

2-Oxo-N-(1-(4-(trifluoromethoxy)phenyl)butyl)-2,3-dihydropyrido[2,3-b]pyrazine-4(1H)-carboxamide (21). The title compound was prepared as a white solid after crystallization from hexane/ethyl acetate in 73% yield from **55a** and 1-(4-(trifluoromethoxy)phenyl)butan-1-amine hydrochloride using the procedure analogous to that described for the synthesis of **15**. ^{1}H NMR (300 MHz, $CDCl_3$) δ 0.86–1.01 (3H, m), 1.23–1.51 (2H, m), 1.68–1.94 (2H, m), 4.58–4.75 (2H, m), 4.96 (1H, q, *J* = 7.5 Hz), 7.00 (1H, dd, *J* = 7.7, 5.1 Hz), 7.10–7.22 (3H, m), 7.31–7.38 (2H, m), 8.00 (1H, dd, *J* = 4.9, 1.5 Hz), 8.99 (1H, s), 10.40 (1H, d, *J* = 7.5 Hz). MS (ESI/APCI) mass calculated for $[M + H]^+$ ($C_{19}H_{20}F_3N_4O_3$) requires *m/z* 424.1, found *m/z* 409.2. HPLC purity: 99.7%. mp 171.7–173.7 °C. Anal. Calcd for $C_{19}H_{19}F_3N_4O_3$: C, 55.88; H, 4.69; N, 13.72. Found: C, 55.94; H, 4.78; N, 13.54.

N-(2-Hydroxy-1-(4-(trifluoromethoxy)phenyl)ethyl)-2-oxo-2,3-dihydropyrido[2,3-b]pyrazine-4(1H)-carboxamide (22). A mixture of *tert*-butyl (2-hydroxy-1-(4-(trifluoromethoxy)phenyl)ethyl)carbamate (**S30**) (52 mg, 0.16 mmol) and 2 M HCl solution in EtOH (2 mL, 4.00 mmol) was stirred at 60 °C for 2 min and then concentrated in vacuo. To the residue were added DMF (2 mL), Et_3N (0.045 mL, 0.32 mmol), and **55a** (50.9 mg, 0.16 mmol) at rt. The mixture was stirred at rt overnight and then poured into saturated aqueous NaCl. The mixture was extracted with EtOAc, washed with saturated aqueous NaCl, dried over anhydrous $MgSO_4$, and concentrated in vacuo. The residue was purified by column chromatography (silica gel, hexane/ethyl acetate, 1:1 to 0:100), followed by a preparative HPLC purification (column: L-Column2 ODS 20 mm ID × 150 mm L; mobile phase A: 0.1% TFA in water; mobile phase B:

0.1% TFA in acetonitrile; flow rate: 20 mL/min). The desired fraction was neutralized with saturated aqueous $NaHCO_3$, concentrated in vacuo to remove most of acetonitrile, and extracted with EtOAc. The organic layer was separated, dried over anhydrous $MgSO_4$, and concentrated in vacuo to give **22** (32.2 mg, 0.081 mmol, 50%) as a white solid. ^{1}H NMR (300 MHz, DMSO-d_6) δ 3.51–3.80 (2H, m), 4.29–4.53 (2H, m), 5.09 (1H, t, J = 5.1 Hz), 7.11 (1H, dd, J = 7.7, 5.1 Hz), 7.28–7.35 (4H, m), 7.40–7.51 (2H, m), 8.01 (1H, dd, J = 4.9, 1.5 Hz), 10.39 (1H, d, J = 7.2 Hz), 10.79 (1H, brs). MS (ESI/APCI) mass calculated for $[M + H]^+$ ($C_{17}H_{16}F_3N_4O_4$) requires *m/z* 397.1, found *m*/*z* 397.1. HPLC purity: 98.8%. mp 190 °C.

N-(2-Hydroxy-2-methyl-1-(4-(trifluoromethoxy)phenyl)propyl)-2-oxo-2,3-dihydropyrido[2,3-b]pyrazine-4(1H)-carboxamide (23). The title compound was prepared as a white solid after trituration with hexane/ethyl acetate in 82% yield from **55a** and 1-amino-2-methyl-1-(4-(trifluoromethoxy)phenyl)propan-2-ol hydrochloride (**S32**) using the procedure analogous to that described for the synthesis of **15**. ^{1}H NMR (300 MHz, $CDCl_3$) δ 1.16 (3H, s), 1.37 (3H, s), 1.70 (1H, s), 4.55–4.76 (2H, m), 4.91 (1H, d, J = 8.3 Hz), 7.02 (1H, dd, J = 7.9, 4.9 Hz), 7.13–7.22 (3H, m), 7.37–7.46 (2H, m), 8.07 (1H, dd, J = 4.9, 1.5 Hz), 8.51 (1H, s), 10.93 (1H, d, J = 8.3 Hz). MS (ESI/APCI) mass calculated for $[M + H]^+$ ($C_{19}H_{20}F_3N_4O_4$) requires *m/z* 425.1, found *m*/*z* 425.1. HPLC purity: 99.5%. mp 164.7–168.5 °C. Anal. Calcd for $C_{19}H_{19}F_3N_4O_4$: C, 53.77; H, 4.51; N, 13.20. Found: C, 53.91; H, 4.66; N, 13.22.

N-(2-(Methylsulfonyl)-1-(4-(trifluoromethoxy)phenyl)ethyl)-2-oxo-2,3-dihydropyrido[2,3-b]pyrazine-4(1H)-carboxamide (24). A mixture of *m*-CPBA (68.7 mg, 0.28 mmol) and **56** (54 mg, 0.13 mmol) in EtOAc (10 mL) was stirred at rt overnight. Then saturated aqueous $Na_2S_2O_3$ was added at rt and the mixture was stirred for 5 min at the same temperature. The mixture was poured into saturated aqueous $NaHCO_3$ and extracted with EtOAc. The organic layer was

separated, washed with saturated aqueous $NaHCO_3$ and saturated aqueous NaCl, dried over anhydrous $MgSO_4$ and concentrated in vacuo. The resulting solid was triturated from hexane/ethyl acetate to give **24** (38.2 mg, 0.083 mmol, 66%) as a white solid. ^{1}H NMR (300 MHz, DMSO-d_6) δ 2.91 (3H, s), 3.63 (1H, dd, J = 14.7, 4.5 Hz), 4.00 (1H, dd, J = 14.5, 9.2 Hz), 4.26–4.56 (2H, m), 5.46 (1H, td, J = 8.5, 3.8 Hz), 7.11 (1H, dd, J = 7.9, 4.9 Hz), 7.30 (1H, dd, J = 7.9, 1.5 Hz), 7.33–7.41 (2H, m), 7.53–7.61 (2H, m), 7.98 (1H, dd, J = 4.9, 1.5 Hz), 10.62 (1H, d, J = 7.9 Hz), 10.82 (1H, s). MS (ESI/APCI) mass calculated for $[M + H]^+$ ($C_{18}H_{18}F_3N_4O_5S$) requires *m/z* 459.1, found *m/z* 459.2. HPLC purity: 99.7%. mp 147.2–150.8 °C. Anal. Calcd for $C_{18}H_{17}F_3N_4O_5S$: C, 47.16; H, 3.74; N, 12.22. Found: C, 46.92; H, 3.80; N, 12.00.

N-(2-Methoxy-1-(4-(trifluoromethoxy)phenyl)ethyl)-6-methyl-2-oxo-2,3-dihydropyrido[2,3-b]pyrazine-4(1H)-carboxamide (25). To a suspension of **54c** (118 mg, 0.72 mmol) in THF (20 mL) was added triphosgene (171 mg, 0.58 mmol) at rt. The mixture was stirred at 40 °C under Ar for 1 h. After cooling to rt, the mixture was concentrated in vacuo. The residue was diluted with THF and concentrated in vacuo (this procedure was repeated three times). To a solution of the residue in THF (20 mL) were added 2-methoxy-1-(4-(trifluoromethoxy)phenyl)ethanamine hydrochloride (**S24i**) (235 mg, 0.87 mmol) and Et_3N (0.302 mL, 2.16 mmol) at rt. The mixture was stirred at rt for 16 h and then poured into water. The mixture was extracted with EtOAc, dried over anhydrous Na_2SO_4 and concentrated in vacuo. The residue was purified by column chromatography (silica gel, hexane/ethyl acetate, 4:1 to 0:100) to give **25** (58.3 mg, 0.137 mmol, 19%) as a white solid after crystallization from hexane/ethyl acetate (2:1). ^{1}H NMR (300 MHz, DMSO-d_6) δ 2.42 (3H, s), 3.29 (3H, s), 3.56–3.70 (2H, m), 4.39 (2H, s), 4.97–5.09 (1H, m), 6.96 (1H, d, J = 8.3 Hz), 7.22 (1H, d, J = 8.0 Hz), 7.27–7.37 (2H, m), 7.42–7.53 (2H, m), 10.72 (1H, s), 10.80 (1H, d, J = 7.2 Hz). MS (ESI/APCI) mass calculated for $[M + H]^+$ ($C_{19}H_{20}F_3N_4O_4$)

requires *m/z* 425.1, found *m/z* 425.2. HPLC purity: 95.1%. mp 175 °C.

N-(2-Methoxy-1-(4-(trifluoromethoxy)phenyl)ethyl)-7-methyl-2-oxo-2,3-dihydropyrido[2,3-b]pyrazine-4(1H)-carboxamide (26). The title compound was prepared as a pale yellow solid in 96% yield following the general procedure described for preparation of compound **15**, by using 4-nitrophenyl 7-methyl-2-oxo-2,3-dihydropyrido[2,3-*b*]pyrazine-4(1*H*)-carboxylate and 2-methoxy-1-(4-(trifluoromethoxy)phenyl)ethanamine hydrochloride. ^{1}H NMR (300 MHz, DMSO-d_6) δ 2.26 (3H, s), 3.28 (3H, s), 3.56–3.68 (2H, m), 4.32–4.48 (2H, m), 4.99–5.11 (1H, m), 7.14 (1H, d, *J* = 1.5 Hz), 7.27–7.37 (2H, m), 7.41–7.51 (2H, m), 7.85 (1H, d, *J* = 1.3 Hz), 10.38 (1H, d, *J* = 7.4 Hz), 10.78 (1H, brs). MS (ESI/APCI) mass calculated for $[M + H]^+$ ($C_{19}H_{20}F_3N_4O_4$) requires *m/z* 425.1, found *m/z* 425.2. HPLC purity: 99.1%. mp 149 °C.

N-(2-Methoxy-1-(4-(trifluoromethoxy)phenyl)ethyl)-8-methyl-2-oxo-2,3-dihydropyrido[2,3-b]pyrazine-4(1H)-carboxamide (27). To a solution of **55a** (82.5 mg, 0.251 mmol) in DMF (5 mL) were added 2-methoxy-1-(4-(trifluoromethoxy)phenyl)ethanamine hydrochloride (68.3 mg, 0.251 mmol) and Et_3N (0.096 mL, 0.689 mmol). The mixture was stirred at rt for 16 h and then poured into $NaHCO_3$ aqueous solution. The mixture was extracted with EtOAc, washed with 1 M HCl aqueous solution and saturated aqueous NaCl, dried over anhydrous Na_2SO_4 and concentrated in vacuo. The residue was purified by column chromatography (silica gel, hexane/ethyl acetate, 9:1 to 0:100), followed by a preparative HPLC purification (column: L-Column2 ODS 20 mm ID × 150 mm L; mobile phase A: 0.1% TFA in water; mobile phase B: 0.1% TFA in acetonitrile; flow rate: 20 mL/min). The desired fraction was neutralized with saturated aqueous $NaHCO_3$, concentrated in vacuo to remove most of acetonitrile, and extracted with EtOAc. The organic layer was separated, dried over anhydrous Na_2SO_4, and concentrated in vacuo to afford **27** (73.1 mg, 0.172 mmol, 69%) as a white solid. ^{1}H NMR (300 MHz, DMSO-

d_6) δ 2.30 (3H, s), 3.27 (3H, s), 3.56–3.68 (2H, m), 4.33–4.49 (2H, m), 5.00–5.10 (1H, m), 7.03 (1H, d, *J* = 5.7 Hz), 7.27–7.36 (2H, m), 7.41–7.51 (2H, m), 7.93 (1H, d, *J* = 5.3 Hz), 10.28 (1H, d, *J* = 7.6 Hz), 10.35 (1H, s). MS (ESI/APCI) mass calculated for $[M + H]^+$ ($C_{19}H_{20}F_3N_4O_4$) requires *m/z* 425.1, found *m/z* 425.1. HPLC purity: 99.9%. mp 128 °C.

7-Cyclopropyl-N-(2-methoxy-1-(4-(trifluoromethoxy)phenyl)ethyl)-2-oxo-2,3-dihydropyrido[2,3-b]pyrazine-4(1H)-carboxamide (28). A mixture of **61** (432 mg, 0.740 mmol) in TFA (2.1 mL) and H_2O (0.236 mL) was stirred at rt for 3.5 h and then concentrated in vacuo. The residue was dissolved in DMF (10 mL) and 8 M NH_3 solution in MeOH (2.0 mL, 16.0 mmol) was added. The mixture was stirred at rt for 1 h and then concentrated in vacuo. The residue was diluted with EtOAc. The solution was washed with water and saturated aqueous NaCl, dried over anhydrous Na_2SO_4 and concentrated in vacuo to give **28** (279 mg, 0.590 mmol, 80%) as a white solid after trituration with hexane/ethyl acetate (10:1). ^{1}H NMR (300 MHz, DMSO-d_6) δ 0.61–0.71 (2H, m), 0.93–1.05 (2H, m), 1.90–2.03 (1H, m), 3.28 (3H, s), 3.55–3.71 (2H, m),4.30–4.49 (2H, m), 5.00–5.12 (1H, m), 6.96 (1H, d, *J* = 2.3 Hz), 7.32 (2H, d, *J* = 7.9 Hz), 7.46 (2H, d, *J* = 8.7 Hz), 7.85 (1H, d,*J* = 1.9 Hz), 10.34 (1H, d, *J* = 7.5 Hz), 10.69 (1H, s). MS (ESI/APCI) mass calculated for $[M + H]^+$ ($C_{21}H_{22}F_3N_4O_4$) requires *m/z* 425.2, found *m/z* 451.1. HPLC purity: 98.8%. mp 149 °C.

7-Chloro-N-(2-methoxy-1-(4-(trifluoromethoxy)phenyl)ethyl)-2-oxo-2,3-dihydropyrido[2,3-b]pyrazine-4(1H)-carboxamide (29). To a solution of **54g** (132.4 mg, 0.72 mmol) and Et_3N (305 μL, 2.16 mmol) in THF (6 mL) and DMA (6 mL) was slowly added a solution of triphosgene (214 mg, 0.72 mmol) in THF (3.0 mL) at 0 °C. After stirring at 0 °C for 2 h, a mixture of Et_3N (508 μL, 3.61 mmol) and 2-methoxy-1-(4-(trifluoromethoxy)phenyl)ethanamine hydrochloride (980 mg, 3.61 mmol) in THF (3.0 mL) and DMA (6.0 mL) was added at the same temperature.

The mixture was stirred at rt for 3 h and then quenched with water. The phases were separated and the aqueous phase was extracted with EtOAc. The combined organic phases were washed with water and saturated aqueous NaCl, dried over anhydrous Na_2SO_4 and concentrated in vacuo. The residue was purified by column chromatography (silica gel, hexane/ethyl acetate, 99:1 to 3:2) to give **29** (10.4 mg, 0.023 mmol, 3.2%) as a pale yellow solid after trituration with hexane/ethyl acetate (10:1). ^{1}H NMR (300 MHz, DMSO-d_6) δ 3.29 (3H, s), 3.53–3.71 (2H, m), 4.32–4.52 (2H, m), 4.99–5.12 (1H, m), 7.27–7.38 (3H, m),7.48 (2H, d, J = 8.7 Hz), 8.06 (1H, d, J = 2.3 Hz), 10.13 (1H, d, J = 7.2 Hz), 10.93 (1H, brs). MS (ESI/APCI) mass calculated for $[M + H]^+$ ($C_{18}H_{17}ClF_3N_4O_4$) requires *m/z* 445.1, found *m/z* 445.1. HPLC purity: 96.5%.

7-Methoxy-N-(2-methoxy-1-(4-(trifluoromethoxy)phenyl)ethyl)-2-oxo-2,3-dihydropyrido[2,3-b]pyrazine-4(1H)-carboxamide (30). A mixture of **62** (395 mg, 0.69 mmol) in TFA (10 mL) and water (1.1 mL) was stirred at rt for 3 h and then concentrated in vacuo. The residue was dissolved in DMF (19 mL) and 8 M NH_3 solution in MeOH (3.73 mL, 29.8 mmol) was added. The mixture was stirred at rt for 2 h and then concentrated in vacuo. The residue was diluted with EtOAc. The solution was washed with water and saturated aqueous NaCl, dried over anhydrous Na_2SO_4 and concentrated in vacuo. The residue was purified by column chromatography (silica gel, hexane/ethyl acetate, 99:1 to 0:100) to give **30** (203 mg, 0.461 mmol, 67%) as a white solid after trituration with hexane/ethyl acetate (10:1). ^{1}H NMR (300 MHz, DMSO-d_6) δ 3.28 (3H, s), 3.54–3.68 (2H, m), 3.83 (3H, s), 4.30–4.51 (2H, m), 4.98–5.12 (1H, m), 6.96 (1H, d, J = 2.6 Hz), 7.27–7.37 (2H, m), 7.46 (2H, d, J = 8.7 Hz), 7.76 (1H, d, J = 2.6 Hz), 10.02 (1H, d, J = 7.5 Hz), 10.76 (1H, brs). MS (ESI/APCI) mass calculated for $[M + H]^+$ ($C_{19}H_{20}F_3N_4O_5$) requires *m/z* 441.1, found *m/z* 441.2. HPLC purity: 98.7%.

7-Isopropoxy-N-(2-methoxy-1-(4-(trifluoromethoxy)phenyl)ethyl)-2-oxo-2,3-dihydropyrido[2,3-b]pyrazine-4(1H)-carboxamide (31). A mixture of **63** (90 mg, 0.15 mmol) in TFA (2.13 mL) and water (0.239 mL) was stirred at rt for 3 h. The mixture was concentrated in vacuo. The residue was dissolved in DMF (4 mL) and 8 M NH_3 solution in MeOH (0.808 mL, 6.46 mmol) was added. The mixture was stirred at rt for 2 h and concentrated in vacuo. The residue was diluted with EtOAc. The solution was washed with water and saturated aqueous NaCl, dried over anhydrous Na_2SO_4 and concentrated in vacuo. The residue was purified by column chromatography (silica gel, hexane/ethyl acetate, 99:1 to 0:100) to give **31** (67.2 mg, 0.143 mmol, 95%) as a white amorphous solid. ^{1}H NMR (300 MHz, DMSO-d_6) δ 1.29 (6H, d, J = 6.0 Hz), 3.28 (3H, s), 3.52–3.69 (2H, m), 4.28–4.49 (2H, m), 4.60 (1H, dt, J = 12.1, 6.0 Hz), 5.04 (1H, d, J = 7.2 Hz), 6.94 (1H, d, J = 2.6 Hz), 7.27–7.37 (2H, m), 7.46 (2H, d, J = 8.7 Hz), 7.73 (1H, d, J = 2.6 Hz), 10.01 (1H, d, J = 7.2 Hz), 10.72 (1H, s). MS (ESI/APCI) mass calculated for $[M + H]^+$ ($C_{21}H_{24}F_3N_4O_5$) requires *m/z* 469.2, found *m/z* 469.2. HPLC purity: 99.1%.

7-Methoxy-N-((1S)-2-methoxy-1-(4-(trifluoromethoxy)phenyl)ethyl)-2-oxo-2,3-dihydropyrido[2,3-b]pyrazine-4(1H)-carboxamide (32). Resolution of the enantiomers of **30** was carried out chromatographically using a Chiralpak IA 20 mm ID × 250 mm L column (CO_2/methanol, 860:140) at 50 mL/min. Resolution of **30** (200 mg, 0.454 mmol) provided 90.0 mg of **32** as the first eluting enantiomer, which was crystallized from hexane/ethyl acetate to afford **32** (78.3 mg, 0.178 mmol, 39%, 78% theoretical) as a white solid. Analytical HPLC analysis carried out on a 4.6 mm ID × 150 mm L Chiralpak IA column (CO_2/methanol, 820:180) at a flow rate of 4.0 mL/min indicated that **32** was of 99% ee. ^{1}H NMR (300 MHz, DMSO-d_6) δ 3.28 (3H, s), 3.52–3.70 (2H, m), 3.83 (3H, s), 4.26–4.52 (2H, m), 4.97–5.13 (1H, m), 6.96 (1H, d,

J = 2.6 Hz), 7.32 (2H, d, *J* = 8.3 Hz), 7.46 (2H, d, *J* = 8.7 Hz), 7.76 (1H, d, *J* = 2.6 Hz), 10.02 (1H, d, *J* = 7.5 Hz), 10.77 (1H, brs). MS (ESI/APCI) mass calculated for $[M + H]^+$ ($C_{19}H_{20}F_3N_4O_5$) requires *m/z* 441.1, found *m/z* 411.1. HPLC purity: 100%. mp 77.6–78.6 °C. Anal. Calcd for $C_{19}H_{19}N_4O_5F_3 \cdot 0.25H_2O$: C, 51.30; H, 4.42; F, 12.81; N, 12.59. Found: C, 51.58; H, 4.71; F, 12.52; N, 12.41.

7-Methoxy-N-((1R)-2-methoxy-1-(4-(trifluoromethoxy)phenyl)ethyl)-2-oxo-2,3-dihydropyrido[2,3-b]pyrazine-4(1H)-carboxamide (33). Resolution of the enantiomers of **30** was carried out chromatographically using a Chiralpak IA 20 mm ID × 250 mm L column (CO_2/methanol, 860:140) at 50 mL/min. Resolution of **30** (200 mg, 0.454 mmol) provided 94.0 mg of **33** as the second eluting enantiomer, which was crystallized from hexane/ethyl acetate to afford **33** (60.0 mg, 0.136 mmol, 30%, 60% theoretical) as a white solid. Analytical HPLC analysis carried out on a 4.6 mm ID × 150 mm L Chiralpak IA column (CO_2/methanol, 820:180) at a flow rate of 4.0 mL/min indicated that **33** was of >99.9% ee. ^{1}H NMR (300 MHz, DMSO-d_6) δ 3.28 (3H, s), 3.53–3.67 (2H, m), 3.83 (3H, s), 4.27–4.51 (2H, m), 4.96–5.16 (1H, m), 6.96 (1H, d, *J* = 3.0 Hz), 7.32 (2H, d, *J* = 8.3 Hz), 7.41–7.54 (2H, m), 7.76 (1H, d, *J* = 2.6 Hz), 10.02 (1H, d, *J* = 7.2 Hz), 10.76 (1H, brs). MS (ESI/APCI) mass calculated for $[M + H]^+$ ($C_{19}H_{20}F_3N_4O_5$) requires *m/z* 441.1, found *m/z* 411.1. HPLC purity: 100%.

7-Methoxy-N-((1S or 1R)-2-methoxy-1-(4-(trifluoromethyl)phenyl)ethyl)-2-oxo-2,3-dihydropyrido[2,3-b]pyrazine-4(1H)-carboxamide (34). Resolution of the enantiomers of **67** was carried out chromatographically using a Chiralpak AD 50 mm ID × 500 mm L column (hexane/ethanol, 600:400) at 80 mL/min. Resolution of **67** (444 mg, 1.05 mmol) provided 210 mg of **34** as the first eluting enantiomer, which was crystallized from hexane/ethyl acetate to afford **34** (197 mg, 0.464 mmol, 44%, 88% theoretical) as a white solid. Analytical HPLC

analysis carried out on a 4.6 mm ID × 250 mm L Chiralpak AD column (hexane/ethanol, 700:300) at a flow rate of 1.0 mL/min indicated that **34** was of >99.9% ee. ^{1}H NMR (300 MHz, DMSO-d_6) δ 3.28 (3H, s), 3.61–3.68 (2H, m), 3.83 (3H, s), 4.29–4.50 (2H, m), 5.03–5.16 (1H, m), 6.97 (1H, d, J = 2.6 Hz), 7.56 (2H, d, J = 8.3 Hz), 7.69 (2H, d, J = 8.3 Hz), 7.77 (1H, d, J = 2.6 Hz), 10.07 (1H, d, J = 7.2 Hz),10.77 (1H, brs). MS (ESI/APCI) mass calculated for $[M + H]^+$ ($C_{19}H_{20}F_3N_4O_4$) requires *m/z* 425.1, found *m/z* 425.1. HPLC purity: 100%. mp 144 °C.

7-Methoxy-N-((1R or 1S)-2-methoxy-1-(4-(trifluoromethyl)phenyl)ethyl)-2-oxo-2,3-dihydropyrido[2,3-b]pyrazine-4(1H)-carboxamide (35). Resolution of the enantiomers of **67** was carried out chromatographically using a Chiralpak AD 50 mm ID × 500 mm L column (hexane/ethanol, 600:400) at 80 mL/min. Resolution of **67** (444 mg, 1.05 mmol) provided 210 mg of **35** as the second eluting enantiomer, which was crystallized from hexane/ethyl acetate to afford **35** (189 mg, 0.444 mmol, 43%, 85% theoretical) as a white solid. Analytical HPLC analysis carried out on a 4.6 mm ID × 250 mm L Chiralpak AD column (hexane/ethanol, 700:300) at a flow rate of 1.0 mL/min indicated that **35** was of >99.9% ee. ^{1}H NMR (300 MHz, DMSO-d_6) δ 3.28 (3H, s), 3.61–3.67 (2H, m), 3.83 (3H, s), 4.30–4.50 (2H, m), 5.04–5.16 (1H, m), 6.97 (1H, d, J = 2.6 Hz), 7.56 (2H, d, J = 8.3 Hz), 7.69 (2H, d, J = 8.3 Hz), 7.77 (1H, d, J = 2.6 Hz), 10.07 (1H, d, J = 7.5 Hz),10.77 (1H, s). MS (ESI/APCI) mass calculated for $[M + H]^+$ ($C_{19}H_{20}F_3N_4O_4$) requires *m/z* 425.1, found *m/z* 425.1. HPLC purity: 100%. mp 142 °C.

N-((1S)-1-(3-Fluoro-4-(trifluoromethoxy)phenyl)-2-methoxyethyl)-7-methoxy-2-oxo-2,3-dihydropyrido[2,3-b]pyrazine-4(1H)-carboxamide (36). Resolution of the enantiomers of **68** was carried out chromatographically using a Chiralpak AD 50 mm ID × 500 mm L column (hexane/ethanol, 860:140) at 80 mL/min. Resolution of **68** (1.34 g, 2.93 mmol) provided 652 mg of **36** as the first eluting enantiomer, which was crystallized from hexane/ethyl acetate to afford

36 (578 mg, 1.26 mmol, 43%, 86% theoretical) as a white solid. Analytical HPLC analysis carried out on a 4.6 mm ID × 250 mm L Chiralpak AD column (hexane/ethanol, 650:350) at a flow rate of 1.0 mL/min indicated that **36** was of 99.8% ee. ^{1}H NMR (300 MHz, DMSO-d_6) δ 3.29 (3H, s), 3.53–3.72 (2H, m), 3.83 (3H, s), 4.24–4.54 (2H, m), 4.95–5.16 (1H, m), 6.96 (1H, d, J = 2.6 Hz), 7.29 (1H, d, J = 8.3 Hz), 7.39–7.61 (2H, m), 7.75 (1H, d, J = 2.6 Hz), 10.02 (1H, d, J = 7.5 Hz), 10.78 (1H, brs). MS (ESI/APCI) mass calculated for $[M + H]^+$ ($C_{19}H_{20}F_3N_4O_4$) requires *m/z* 459.1, found *m/z* 459.2. HPLC purity: 100%. mp 151.2–152.2 °C. Anal. Calcd for $C_{19}H_{18}F_4N_4O_5$: C, 49.79; H, 3.96; F, 16.58; N, 12.22. Found: C, 49.84; H, 4.14; F, 16.38; N, 12.12.

N-((1R)-1-(3-Fluoro-4-(trifluoromethoxy)phenyl)-2-methoxyethyl)-7-methoxy-2-oxo-2,3-dihydropyrido[2,3-b]pyrazine-4(1H)-carboxamide (37). Resolution of the enantiomers of **68** was carried out chromatographically using a Chiralpak AD 50 mm ID × 500 mm L column (hexane/ethanol, 860:140) at 80 mL/min. Resolution of **68** (1.34 g, 2.93 mmol) provided 680 mg of **37** as the second eluting enantiomer, which was crystallized from hexane/ethyl acetate to afford **37** (563 mg, 1.22 mmol, 41%, 83% theoretical) as a white solid. Analytical HPLC analysis carried out on a 4.6 mm ID × 250 mm L Chiralpak AD column (hexane/ethanol, 650:350) at a flow rate of 1.0 mL/min indicated that **36** was of 99.6% ee. ^{1}H NMR (300 MHz, DMSO-d_6) δ 3.29 (3H, s), 3.53–3.70 (2H, m), 3.83 (3H, s), 4.29–4.51 (2H, m), 4.98–5.12 (1H, m), 6.97 (1H, d, J = 3.0 Hz), 7.29 (1H, d, J = 8.3 Hz), 7.39–7.59 (2H, m), 7.75 (1H, d, J = 2.6 Hz), 10.02 (1H, d, J = 7.2 Hz), 10.78 (1H, brs). MS (ESI/APCI) mass calculated for $[M + H]^+$ ($C_{19}H_{20}F_3N_4O_4$) requires *m/z* 459.1, found *m/z* 459.1. HPLC purity: 98.2%. mp 151.2–152.2 °C. Anal. Calcd for $C_{19}H_{18}N_4O_5F_4 \cdot 0.3H_2O$: C, 49.21; H, 4.04; F, 16.39; N, 12.08. Found: C, 49.17; H, 4.05; F, 16.20; N, 12.04.

tert-Butyl Ethyl (3-Nitropyridin-2-yl)malonate (39). To a suspension of potassium *tert*-butoxide (26.6 g, 237 mmol) in THF (500 mL) at 60 °C was added dropwise *tert*-butyl ethyl malonate (45 mL, 237 mmol), followed by **38** (25.0 g, 158 mmol) in THF (50 mL). The mixture was refluxed for 3 h. The mixture was concentrated in vacuo and the residue was diluted with 1 M HCl aqueous solution (100 mL). The aqueous solution was extracted with EtOAc and the combined organic phase was washed with saturated aqueous NaCl, dried over anhydrous Na_2SO_4 and concentrated in vacuo to give crude **39** (66.7 g). This was used in the next reaction without further purification. ^{1}H NMR (400 MHz, $CDCl_3$) δ 1.30 (3H, t, *J* = 7.2 Hz), 1.49 (9H, s), 4.29–4.33 (2H, m), 5.43 (1H, s), 7.51 (1H, dd, *J* = 8.4, 4.2 Hz), 8.46 (1H, d, *J* = 8.4 Hz), 8.82 (1H, d, *J* = 5.2 Hz).

Ethyl (3-Nitropyridin-2-yl)acetate (40). To a solution of crude **39** (66.7 g) in CH_2Cl_2 (300 mL) was added TFA (100 mL). The mixture was stirred at rt overnight. The mixture was concentrated in vacuo and the residue was diluted with $NaHCO_3$ aqueous solution (100 mL). The mixture was extracted with EtOAc, washed with saturated aqueous NaCl, dried over anhydrous Na_2SO_4 and concentrated in vacuo to give crude **40** (29.0 g). This was used in the next reaction without further purification. ^{1}H NMR (400 MHz, $CDCl_3$) δ 1.26 (3H, t, *J* = 7.2 Hz), 4.20 (2H, q, *J* = 7.2 Hz), 4.33 (2H, s), 7.48 (1H, dd, *J* = 8.0, 1.2 Hz), 8.43 (1H, dd, *J* = 8.4, 1.2 Hz), 8.80 (1H, dd, *J* = 8.4, 1.2 Hz).

Ethyl (3-Aminopyridin-2-yl)acetate (41). A mixture of crude **40** (29.0 g) and 10% Pd/C (containing 50% water, 2.90 g) in EtOH (400 mL) was stirred under 50 psi of H_2 at rt for 3 h. The mixture was filtered through celite and the filtrate was concentrated in vacuo to give crude **40** (25.5 g). This was used in the next reaction without further purification. ^{1}H NMR (400 MHz,

$CDCl_3$) δ 1.26 (3H, t, *J* = 7.2 Hz), 3.85 (2H, s), 4.17 (2H, q, *J* = 7.2 Hz), 4.32 (2H, br s), 6.99–7.06 (2H, m), 7.99–8.01 (1H, m).

Ethyl (3-((Diethoxyacetyl)amino)pyridin-2-yl)acetate (42). To a mixture of crude **41** (25.5 g, 142 mmol) and 2,2-diethoxylacetic acid (23.0 g, 156 mmol) in DMF (300 mL) was added DIEA (70.3 mL, 425 mmol), followed by HATU (80.7 g, 212 mmol). The mixture was stirred at rt overnight. The mixture was diluted with water and extracted with EtOAc (300 mL × 2). The combined organic phase was washed with $NaHCO_3$ aqueous solution and then saturated aqueous NaCl, dried over anhydrous Na_2SO_4 and concentrated in vacuo. The residue was purified by column chromatography (silica gel, petroleum/ethyl acetate, 3:1) to give **42** (26.0 g, 53% in 4 steps from **38**). ^{1}H NMR (400 MHz, $CDCl_3$) δ 1.27–1.33 (9H, m), 3.69–3.83 (4H, m), 3.90 (2H, s), 4.20 (2H, q, *J* = 7.2 Hz), 4.97 (1H, s), 7.25–7.28 (1H, m), 8.29–8.35 (2H, m), 9.53 (1H, br s). 2,2-Diethoxylacetic acid was prepared in the following method. To a solution of ethyl 2,2-diethoxyacetate (17.8 g, 101 mmol)in EtOH (50 mL) was added 2 M NaOH aqueous solution (101 mL, 202 mmol). The mixture was stirred at rt for 16 h and then EtOH was removed under reduced pressure. The aqueous phase was extracted with Et_2O. The aqueous phase was acidified with 2 M HCl aqueous solution to pH 3~4, saturated with solid NaCl and extracted with EtOAc. The combined organic phases were dried over anhydrous Na_2SO_4 and concentrated in vacuo to afford 2,2-diethoxyacetic acid (3.37 g, 22.7 mmol, 23%) as a colorless oil. ^{1}H NMR (300 MHz, DMSO-d_6) δ 1.13 (6H, t, *J* = 7.2 Hz), 3.46–3.67 (4H, m), 4.80 (1H, s), 12.92 (1H, brs).

Ethyl 2-Oxo-1,2-dihydro-1,5-naphthyridine-4-carboxylate (43). To a solution of **42** (3.00 g, 9.67 mmol) in TFA (50 mL) was added H_2O (2 mL), followed by 2 drops of I_2 fresh solution (30 mg of I_2 was suspended in TFA (10 mL)). The mixture was heated to 50 °C overnight and then concentrated in vacuo. The residue was dissolved in toluene (50 mL) and piperidine (3 mL). The

resulting mixture was refluxed for 6 h, and then concentrated in vacuo. The residue was purified by column chromatography (silica gel, petroleum ether/ethyl acetate, 1:1) to give **43** (550 mg, 26%). ^{1}H NMR (400 MHz, $CDCl_3$) δ 1.44 (3H, t, J = 7.2 Hz), 4.53 (2H, q, J = 7.2 Hz), 7.07 (1H, s), 7.48–7.51 (1H, m), 7.74–7.77 (1H, m), 8.66–8.68 (1H, m), 12.38 (1H, br s).

2-Oxo-1,2-dihydro-1,5-naphthyridine-4-carboxylic Acid (44). To a solution of **43** (70 mg, 0.32 mmol) in EtOH (5 mL) was added 2 M NaOH aqueous solution (4 mL). The mixture was stirred at rt for 2 h. EtOH was removed under reduced pressure and the aqueous phase was acidified to pH ~5 with 1 M HCl aqueous solution. The precipitate was collected by filtration and dried to give **44** (53 mg, 87%) as a beige solid. ^{1}H NMR (400 MHz, DMSO-d_6) δ 7.02 (1H, s), 7.64–7.67 (1H, m), 7.80 (1H, d, J = 8.8 Hz), 8.55 (1H, d, J = 4.0 Hz), 12.26 (1H, d, J = 10.4 Hz), 14.86 (1H, br s).

1H-Pyrazole-1,5-diamine (47). To a vigorously stirred solution of 2*H*-pyrazol-3-ylamine (**46**) (4.00 g, 48.2 mmol) in DMF (50 mL) cooled in an ice-salt bath was added KOH (20.0 g, 357 mmol). The mixture was stirred at 0 °C for 20 min. Then, hydroxylamine-*O*-sulfonic acid (5.45 g, 48.2 mmol) was added in portions. The mixture was stirred vigorously at 10–15 °C for 2 h. The mixture was filtered by a cake of celite and the celite was washed with CH_2Cl_2 (50 mL × 2). The combined filtrate was concentrated in vacuo. The residue was purified by column chromatography (silica gel, CH_2Cl_2/methanol, 100:0 to 60:1) to afford **47** (less polar, 810 mg, 17% yield) as a yellow solid and **48** (more polar, 520 mg, 11% yield) as a yellow solid. The structures were confirmed by nuclear overhauser effect (NOE) experiments (See the Supporting Information). ^{1}H NMR for **47** (400 MHz, DMSO-d_6) δ 4.91 (2H, brs), 5.14 (1H, d, J = 2.0 Hz), 5.66 (2H, brs), 6.86 (1H, d, J = 1.6 Hz). ^{1}H NMR for **48** (400 MHz, DMSO-d_6) δ 4.41 (2H, brs), 5.22 (1H, d, J = 2.4 Hz), 5.85 (2H, brs), 7.08 (1H, d, J = 2.0 Hz).

3-Methylpyrazolo[1,5-b][1,2,4]triazine (49). To a solution of 2-oxo-propionaldehyde (40% aqueous solution, 689 mg, 3.83 mmol) in H_2O (4 mL) and concd HCl (0.2 mL) was added **47** (300 mg, 3.06 mmol) in small portions at 60 °C. The mixture was heated to reflux for 1 h. After cooling to 15 °C, the mixture was basified to pH ~8 with saturated aqueous $NaHCO_3$ and extracted with CH_2Cl_2 (10 mL × 3). The combined organic layer was dried over anhydrous Na_2SO_4 and concentrated in vacuo. The residue was purified by preparative TLC (CH_2Cl_2/methanol, 10:1) to give **49** (150 mg, 37% yield) as a yellow solid. The structure was confirmed by heteronuclear multiple bond correlation (HMBC) experiments (See the Supporting Information). ^{1}H NMR (400 MHz, $CDCl_3$) δ 2.65 (3H, s), 6.79 (1H, d, J = 2.4 Hz), 8.12 (1H, d, J = 2.8 Hz), 8.30 (1H, s).

3-Methylpyrazolo[1,5-b][1,2,4]triazine-8-carbaldehyde (50). $POCl_3$ (800 mg, 5.26 mmol) was added dropwise to DMF (5 mL) at 0 °C under N_2. After 30 min of stirring at 0 °C, a solution of **49** (150 mg, 1.12 mmol) in DMF (3 mL) was added dropwise at the same temperature. The mixture was warmed to 40 °C and stirred for 16 h. After cooling to 10 °C, the mixture was diluted with water (20 mL) and basified to pH ~9 with 1 M NaOH aqueous solution. The mixture was extracted with EtOAc (15mL × 3). The combined organic layer was washed with saturated aqueous NaCl (15 mL), dried over anhydrous Na_2SO_4, and concentrated in vacuo. The residue was purified by column chromatography (silica gel, petroleum ether/ethyl acetate, 5:1) to give **50** (50 mg, 28% yield) as a yellow solid. ^{1}H NMR (400 MHz, $CDCl_3$) δ 2.75 (3H, s), 8.59–8.63 (2H, m), 10.29 (1H, s).

3-Methylpyrazolo[1,5-b][1,2,4]triazine-8-carboxylic acid (51). A mixture of **50** (50 mg, 0.31 mmol), $NaClO_2$ (140 mg, 1.55 mmol), NaH_2PO_4 (94 mg, 0.78 mmol), and 2-methyl-2-butene (55 mg, 0.78 mmol) in *t*-BuOH (5 mL) and H_2O (2 mL) was stirred at 30 °C for 16 h. The solvent

was removed under reduced pressure and the residue was diluted with water (10 mL). The mixture was extracted with CH_2Cl_2 (10 mL × 5). The combined organic layer was washed with saturated aqueous NaCl (10 mL), dried over anhydrous Na_2SO_4, and concentrated in vacuo to give **51** (30 mg, containing 50% of **49**) as a yellow solid. ^{1}H NMR (400 MHz, DMSO-d_6) δ 2.57 (3H, s), 8.57 (1H, s), 8.78 (1H, s), 12.73 (1H, brs).

Methyl N-(3-Nitropyridin-2-yl)glycinate (53a). The mixture of **52a** (36.6 g, 231 mmol), methyl glycinate hydrochloride (29 g, 231 mmol), and Et_3N (80 mL, 577 mmol) in DMF (231 mL) was stirred at 90 °C for 3 h. After cooling to rt, the mixture was poured into water. The resulting solid was collected by filtration, washed with water, and dried to give **53a** (49.8 g, 236 mmol, quantitative yield) as a yellow solid. This was used in the next reaction without further purification. ^{1}H NMR (300 MHz, $CDCl_3$) δ 3.80 (3H, s), 4.40 (2H, d, J = 5.7 Hz), 6.74 (1H, dd, J = 8.3, 4.5 Hz), 8.36–8.55 (3H, m). MS (ESI/APCI) mass calculated for $[M + H]^+$ ($C_8H_{10}N_3O_4$) requires *m/z* 212.1, found *m/z* 212.1.

Methyl N-(4-Methyl-3-nitropyridin-2-yl)glycinate (53b). To a mixture of **52b** (1.51 g, 8.77 mmol) and methyl glycinate hydrochloride (1.16 g, 9.21 mmol) in DMF (12 mL) was added Et_3N (3.06 mL, 21.9 mmol). The mixture was stirred at 80 °C for 16 h. The solvent was evaporated and the residue was diluted with EtOAc. The organic layer was washed with water and saturated aqueous NaCl, dried over anhydrous Na_2SO_4. The solvent was evaporated. The residue was purified by column chromatography (silica gel, hexane/ethyl acetate, 19:1 to 4:1) to give **53b** (0.614 g, 2.73 mmol, 31%) as a yellow solid. ^{1}H NMR (300 MHz, DMSO-d_6) δ 2.39 (3H, s), 3.63 (3H, s), 4.14 (2H, d, J = 5.7 Hz), 6.69 (1H, dd, J = 4.9, 0.8 Hz), 7.83 (1H, t, J = 5.9 Hz), 8.13 (1H, d, J = 4.9 Hz). MS (ESI/APCI) mass calculated for $[M + H]^+$ ($C_9H_{12}N_3O_4$) requires *m/z* 226.1, found *m/z* 226.3.

Methyl N-(6-Methyl-3-nitropyridin-2-yl)glycinate (53c). The title compound was prepared in 94% yield as a yellow solid from **52c** and methyl glycinate hydrochloride using the procedure analogous to that described for the synthesis of **53b**. ^{1}H NMR (300 MHz, DMSO-d_6) δ 2.38 (3H, s), 3.66 (3H, s), 4.29 (2H, d, J = 6.1 Hz), 6.70 (1H, d, J = 8.3 Hz), 8.34 (1H, d, J = 8.3 Hz), 8.76 (1H, t, J = 5.5 Hz). MS (ESI/APCI) mass calculated for $[M + H]^+$ ($C_9H_{12}N_3O_4$) requires *m/z* 226.1, found *m/z* 226.1.

Methyl N-(5-Methyl-3-nitropyridin-2-yl)glycinate (53d). The title compound was prepared as a yellow solid in 70% yield from **52d** and methyl glycinate hydrochloride using the procedure analogous to that described for the synthesis of **53b**. ^{1}H NMR (300 MHz, DMSO-d_6) δ 2.24 (3H, s), 3.64 (3H, s), 4.28 (2H, d, J = 5.7 Hz), 8.27–8.37 (2H, m), 8.60 (1H, t, J = 5.7 Hz).

Methyl N-(5-Iodo-3-nitropyridin-2-yl)glycinate (53e). To a solution of **52e** (11.1 g, 39.0 mmol) in EtOH (350 mL) were added methyl glycinate hydrochloride (9.80 g, 78.1 mmol) and Et_3N (13.6 mL, 97.6 mmol) at rt. After being refluxed for 16 h, the reaction mixture was concentrated, and the residue was quenched with water and extracted with EtOAc. The organic layer was separated, washed with water and saturated aqueous NaCl, dried over anhydrous $MgSO_4$ and concentrated in vacuo. The residue was crystallized from hexane/ethyl acetate to give **53e** (9.79 g, 29.0 mmol, 74%) as (a) yellow solid. ^{1}H NMR (300 MHz, $CDCl_3$) δ 3.79 (3H, s), 4.36 (2H, d, J = 5.5 Hz), 8.43 (1H, brs), 8.53 (1H, d, J = 2.1 Hz), 8.70 (1H, d, J = 2.1 Hz). MS (ESI/APCI) mass calculated for $[M + H]^+$ ($C_8H_9IN_3O_4$) requires *m/z* 338.0, found *m/z* 337.9.

Methyl N-(5-Bromo-3-nitropyridin-2-yl)glycinate (53f). The title compound was prepared as a dark yellow solid in 82% yield from **52f** and methyl glycinate hydrochloride using the procedure analogous to that described for the synthesis of **53e**. ^{1}H NMR (300 MHz, $CDCl_3$) δ 3.80 (3H, s),

4.37 (2H, d, J = 5.7 Hz), 8.37–8.51 (2H, m), 8.57 (1H, d, J = 2.3 Hz). MS (ESI/APCI) mass calculated for $[M + H]^+$ ($C_8H_9BrN_3O_4$) requires *m/z* 290.0, found *m/z* 290.0.

Methyl 2-((5-Chloro-3-nitropyridin-2-yl)amino)acetate (53g). To a stirred solution of **53f** (400 mg, 1.38 mmol) in NMP (13.8 mL) was added copper(I) chloride (410 mg, 4.14 mmol). The mixture was stirred at 150 °C for 2.5 h under microwave irradiation. The mixture was partitioned between EtOAc and water, and the gray solid was filtered off. The phases of the filtrate were separated and the aqueous phase was extracted with EtOAc. The combined organic phases were washed with water and then saturated aqueous NaCl, dried over anhydrous Na_2SO_4 and concentrated in vacuo. The residue was purified by column chromatography (silica gel, hexane/ethyl acetate, 99:1 to 4:1) to give **53g** (181 mg, 0.737 mmol, 53%) as a yellow solid after trituration with diisopropyl ether. The filtrate was concentrated to give the residue. The residue was triturated with hexane/diisopropyl ether (5:1) to give **53g** (36.1 mg, 0.147 mmol, 11%) as a yellow solid. ^{1}H NMR (300 MHz, DMSO-d_6) δ 3.65 (3H, s), 4.29 (2H, d, J = 5.7 Hz), 8.54 (2H, s), 8.81 (1H, t, J = 5.5 Hz). MS (ESI/APCI) mass calculated for $[M + H]^+$ ($C_8H_9ClN_3O_4$) requires *m/z* 246.0, found *m/z* 246.0.

3,4-Dihydropyrido[2,3-b]pyrazin-2(1H)-one (54a). A mixture of **53a** (24.1 g, 114 mmol) and 10% Pd/C (containing 50% water, 3.0 g) in EtOH (381 mL) was stirred at rt overnight under H_2. The catalyst was filtered off and evaporated. A suspension of the residue in EtOH (500 mL) was refluxed for 16 h. After cooling to rt, the solid was collected by filtration, washed with EtOH, and dried to give **54a** (16.8 g, 113 mmol, 99%) as a gray solid. ^{1}H NMR (300 MHz, DMSO-d_6) δ 3.89 (2H, d, J = 1.5 Hz), 6.54 (1H, dd, J = 7.5, 4.9 Hz), 6.67 (1H, s), 6.91 (1H, dd, J = 7.5, 0.8 Hz), 7.59 (1H, dd, J = 4.9, 1.5 Hz), 10.34 (1H, brs).

8-Methyl-3,4-dihydropyrido[2,3-b]pyrazin-2(1H)-one (54b). A mixture of **53b** (610 mg, 2.71 mmol) and 10% Pd/C (containing 50% water, 500 mg) in EtOH (60 mL) was hydrogenated under balloon pressure at rt for 16 h. The catalyst was removed by filtration and the filtrate was stirred at 80 °C for 8 h. The solvent was removed under reduced pressure. The resulting solid was triturated with hexane/ethyl acetate (1:2) to afford **54b** (258 mg, 1.58 mmol, 58%) as a dark purple solid. ^{1}H NMR (300 MHz, DMSO-d_6) δ 2.14 (3H, s), 3.83 (2H, d, J = 1.9 Hz), 6.45 (1H, d, J = 5.3 Hz), 6.58 (1H, s), 7.51 (1H, d, J = 4.9 Hz), 9.91 (1H, s). MS (ESI/APCI) mass calculated for $[M + H]^+$ ($C_8H_{10}N_3O$) requires *m/z* 164.1, found *m/z* 164.2.

6-Methyl-3,4-dihydropyrido[2,3-b]pyrazin-2(1H)-one (54c). A mixture of **53c** (3.08 g, 13.7 mmol) and 10% Pd/C (containing 50% water, 1.5 g) in EtOH (200 mL) was hydrogenated under balloon pressure at rt for 1.5 h. The catalyst was filtered off and the filtrate was stirred at 80 °C for 8 h. EtOH was removed to ~50 mL, to which ethyl acetate/hexane (30 mL/15 mL) were added. The resulting solid was collected by filtration, rinsed with hexane/ethyl acetate (2:1) and dried to afford **54c** (1.911 g, 11.71 mmol, 86%) as a gray solid. ^{1}H NMR (300 MHz, DMSO-d_6) δ 2.20 (3H, s), 3.86 (2H, d, J = 1.9 Hz), 6.39 (1H, d, J = 7.6 Hz), 6.60 (1H, s), 6.82 (1H, d, J = 7.6 Hz), 10.25 (1H, s). MS (ESI/APCI) mass calculated for $[M + H]^+$ ($C_8H_{10}N_3O$) requires *m/z* 164.1, found *m/z* 164.2.

7-Methyl-3,4-dihydropyrido[2,3-b]pyrazin-2(1H)-one (54d). A mixture of **53d** (6.99 g, 31.0 mmol) and 10% Pd/C (containing 50% water, 2.0 g) in EtOH (100 mL) was stirred at rt overnight under H_2. The catalyst was filtered off and evaporated. A suspension of the residue in EtOH (100 mL) was refluxed for 5 h and then concentrated to ~1/3 volume in vacuo. To the residue was added *i*-Pr_2O (30 mL) and the precipitate was collected by filtration, rinsed with *i*-Pr_2O and dried to give **54d** (4.56 g, 27.9 mmol, 90%) as a gray solid. ^{1}H NMR (300 MHz,

DMSO-d_6) δ 2.09 (3H, s), 3.85 (2H, d, J = 1.5 Hz), 6.45 (1H, s), 6.72–6.80 (1H, m), 7.39–7.48 (1H, m), 10.31 (1H, s).

7-Iodo-3,4-dihydropyrido[2,3-b]pyrazin-2(1H)-one (54e). A mixture of **53e** (6.0 g, 17.8 mmol) and 5% Pt/C (500 mg) in THF (300 mL) was hydrogenated under balloon pressure at rt overnight. The catalyst was removed by filtration and the filtrate was concentrated in vacuo to give methyl 2-((3-amino-5-iodopyridin-2-yl)amino)acetate as brown oil. This product was subjected to the next reaction without further purification. MS (ESI/APCI) *m/z* 308.0 $[M + H]^+$. A solution of methyl 2-((3-amino-5-iodopyridin-2-yl)amino)acetate (5.47 g, 17.8 mmol) in EtOH (200 mL) was refluxed for 16 h. The reaction mixture was concentrated, and the residue was triturated with *i*-Pr_2O to give **54e** (4.48 g, 16.3 mmol, 91%) as a gray solid. ^{1}H NMR (300 MHz, DMSO-d_6) δ 3.93 (2H, d, J = 1.5 Hz), 6.96 (1H, br. s), 7.12 (1H, d, J = 1.1 Hz), 7.74 (1H, d, J = 1.9 Hz), 10.42 (1H, br. s). MS (ESI/APCI) mass calculated for $[M + H]^+$ ($C_7H_7IN_3O$) requires *m/z* 276.0, found *m/z* 276.0.

7-Chloro-3,4-dihydropyrido[2,3-b]pyrazin-2(1H)-one (54g). A solution of **53g** (181 mg, 0.74 mmol) in THF (12.5 mL) was hydrogenated over 5% Pt/C (20 mg) at rt for 2 h. The catalyst was filtered off and washed with EtOH, and the filtrate was concentrated in vacuo. The residue was dissolved in EtOH (10 mL), and the mixture was stirred at reflux overnight. Since the starting material remained, 2 M HCl solution in MeOH (1 mL) was added to the mixture, which was stirred at reflux for further 10 min. After the solvent was removed under reduced pressure, the residue was diluted with EtOAc and neutralized with saturated aqueous $NaHCO_3$. The phases were separated and the aqueous phase was extracted with EtOAc. The combined organic phases were washed with saturated aqueous NaCl, dried over anhydrous Na_2SO_4 and concentrated in vacuo to give **54g** (132 mg, 0.721 mmol, 98%) as a brown solid. This was used in the next

reaction without further purification. ^{1}H NMR (300 MHz, DMSO-d_6) δ 3.93 (2H, d, J = 1.5 Hz), 6.92 (1H, d, J = 2.3 Hz), 6.98 (1H, s), 7.59 (1H, d, J = 2.3 Hz),10.48 (1H, s). MS (ESI/APCI) mass calculated for $[M + H]^+$ ($C_7H_7ClN_3O$) requires *m/z* 184.0, found *m/z* 184.0.

4-Nitrophenyl 2-Oxo-2,3-dihydropyrido[2,3-b]pyrazine-4(1H)-carboxylate (55a). To a solution of **54a** (3.0 g, 20.1 mmol) in DMA (170 mL) and pyridine (30 mL) was added 4-nitrophenyl chloroformate (4.87 g, 24.1 mmol) at rt. After being stirred for 20 h, the mixture was quenched with water and extracted with EtOAc. The organic layer was separated, washed with 1 M HCl aqueous solution, water and saturated aqueous NaCl, dried over anhydrous $MgSO_4$ and concentrated in vacuo. The residue was crystallized from hexane/ethyl acetate to give **55a** (4.83 g, 15.4 mmol, 76%) as a colorless needle. ^{1}H NMR (300 MHz, DMSO-d_6) δ 4.51 (2H, s), 7.26 (1H, dd, J = 7.9, 4.5 Hz), 7.40 (1H, dd, J = 7.9, 1.5 Hz), 7.48–7.58 (2H, m), 8.11 (1H, dd, J = 4.7, 1.7 Hz), 8.26–8.35 (2H, m). MS (ESI/APCI) mass calculated for $[M + H]^+$ ($C_{14}H_{11}N_4O_5$) requires *m/z* 315.1, found *m/z* 315.1.

4-Nitrophenyl 8-Methyl-2-oxo-2,3-dihydropyrido[2,3-b]pyrazine-4(1H)-carboxylate (55b). To a solution of **54b** (50.5 mg, 0.31 mmol) and DIEA (0.162 mL, 0.93 mmol) in THF (4 mL) was added 4-nitrophenyl chloroformate (81 mg, 0.40 mmol) at 0 °C. After being stirred at rt for 1 h, the mixture was poured into water, extracted with EtOAc, dried over anhydrous Na_2SO_4 and concentrated in vacuo. The resulting solid was triturated with hexane/ethyl acetate (2:1), collected by filtration, rinsed with hexane/ethyl acetate (2:1) and dried to afford **55b** (51.9 mg, 0.158 mmol, 51%) as a tan solid. ^{1}H NMR (300 MHz, DMSO-d_6) δ 2.32 (3H, s), 4.47 (2H, s), 7.15 (1H, d, J = 4.9 Hz), 7.48–7.57 (2H, m), 8.01 (1H, d, J = 4.9 Hz), 8.26–8.36 (2H, m), 10.52 (1H, s). MS (ESI/APCI) mass calculated for $[M + H]^+$ ($C_{15}H_{13}N_4O_5$) requires *m/z* 329.1, found *m/z* 329.2.

4-Nitrophenyl 7-Methyl-2-oxo-2,3-dihydropyrido[2,3-b]pyrazine-4(1H)-carboxylate (55d). To a solution of **54d** (1 g, 6.13 mmol) in DMA (40 mL) were added 4-nitrophenyl chloroformate (1.48 g, 7.35 mmol) and pyridine (15 mL) at rt. The mixture was stirred at rt for 16 h and then water (ca. 100 mL) was added. The resulting precipitate was collected by filtration, rinsed with water and dried to afford **55d** (1.63 g, 4.97 mmol, 81%) as a beige solid. ^{1}H NMR (300 MHz, DMSO-d_6) δ 2.29 (3H, s), 4.48 (2H, s), 7.20 (1H, d, J = 1.3 Hz), 7.45–7.58 (2H, m), 7.95 (1H, d, J = 1.3 Hz), 8.21–8.38 (2H, m), 10.85 (1H, s).

4-Nitrophenyl 3-Oxo-3,4-dihydroquinoxaline-1(2H)-carboxylate (55h). To a solution of **54h** (447 mg, 3.02 mmol) in DMA (18 mL) and pyridine (4 mL) was added 4-nitrophenyl chloroformate (730 mg, 3.62 mmol) at rt. After being stirred at 80 °C for 24 h, the mixture was quenched with water at rt and extracted with EtOAc. The organic layer was separated, washed with 1 M HCl aqueous solution, water and saturated aqueous NaCl, dried over anhydrous $MgSO_4$ and concentrated in vacuo. The residue was crystallized from hexane/ethyl acetate to give **55h** (657 mg, 2.10 mmol, 70%) as a yellow solid. ^{1}H NMR (300 MHz, DMSO-d_6) δ 4.44 (2H, brs), 7.00–7.10 (2H, m), 7.14–7.23 (1H, m), 7.56–7.65 (2H, m), 7.68–7.75 (1H, m), 8.25–8.36 (2H, m), 10.80 (1H, s). MS (ESI/APCI) mass calculated for $[M - H]^-$ ($C_{15}H_{10}N_3O_5$) requires *m/z* 312.1, found *m*/*z* 312.1.

N-(2-(Methylsulfanyl)-1-(4-(trifluoromethoxy)phenyl)ethyl)-2-oxo-2,3-dihydropyrido[2,3-b]pyrazine-4(1H)-carboxamide (56). The title compound was prepared as a white solid after crystallization from hexane/ethyl acetate in 46% yield from **55a** and 2-(methylsulfanyl)-1-(4-(trifluoromethoxy)phenyl)ethanamine (**S23j**) using the procedure analogous to that described for the synthesis of **12**. ^{1}H NMR (300 MHz, $CDCl_3$) δ 2.05 (3H, s), 2.97 (2H, d, J = 6.0 Hz), 4.69 (2H, s), 5.24 (1H, q, J = 6.4 Hz), 7.01 (1H, dd, J = 7.7, 5.1 Hz), 7.12–7.25 (3H, m), 7.34–7.46

(2H, m), 8.03 (1H, dd, J = 4.9, 1.5 Hz), 9.55 (1H, brs), 10.76 (1H, d, J = 7.2 Hz). MS (ESI/APCI) mass calculated for $[M + H]^+$ ($C_{18}H_{18}F_3N_4O_3S$) requires *m/z* 427.1, found *m/z* 427.1. HPLC purity: 100%. mp 114.5–117.1 °C. Anal. Calcd for $C_{18}H_{17}F_3N_4O_3S$: C, 50.70; H, 4.02; N, 13.14. Found: C, 50.78; H, 4.18; N, 12.97.

7-Iodo-1-((2-(trimethylsilyl)ethoxy)methyl)-3,4-dihydropyrido[2,3-b]pyrazin-2(1H)-one (57). To a stirred solution of **54e** (6.05 g, 22.0 mmol) in DMF (100 mL) and DMSO (150 mL) was added KHMDS (26.4 mL, 26.4 mmol) dropwise at 0 °C under N_2. The mixture was stirred at 0 °C for 20 min and SEMCl (5.74 mL, 30.8 mmol) was added at 0 °C. The mixture was stirred at rt for 3 h and then poured into water. The mixture was extracted with EtOAc, washed with water and saturated aqueous NaCl, dried over anhydrous Na_2SO_4 and concentrated in vacuo. The residue was purified by column chromatography (silica gel, hexane/ethyl acetate, 100:0 to 4:1), followed by a second column purification (basic silica gel, hexane/ethyl acetate, 100:0 to 4:1) to afford **57** (3.41 g, 8.41 mmol, 38%) as a tan solid. ^{1}H NMR (300 MHz, DMSO-d_6) δ −0.04 (9H, s), 0.86 (2H, t, J = 7.7 Hz), 3.55 (2H, t, J = 7.7 Hz), 4.02 (2H, d, J = 1.5 Hz), 5.26 (2H, s), 7.08 (1H, s), 7.50 (1H, d, J = 1.5 Hz), 7.88 (1H, d, J = 1.9 Hz). MS (ESI/APCI) mass calculated for $[M + H]^+$ ($C_{13}H_{21}IN_3O_2Si$) requires *m/z* 406.0, found *m/z* 406.1.

7-Iodo-N-(2-methoxy-1-(4-(trifluoromethoxy)phenyl)ethyl)-2-oxo-1-((2-(trimethylsilyl)ethoxy)methyl)-2,3-dihydropyrido[2,3-b]pyrazine-4(1H)-carboxamide (58). To a stirred solution of **57** (1.11 g, 2.73 mmol) in THF (42 mL) was added a solution of triphosgene (647 mg, 2.18 mmol) in THF (6.3 mL) dropwise at rt under N_2. The mixture was stirred at 40 °C for 1 h under N_2 and then concentrated in vacuo. The residue was diluted with THF and concentrated in vacuo (this procedure was repeated three times), and suspended in THF (21 mL). The mixture was added dropwise to a mixture of 2-methoxy-1-(4-

(trifluoromethoxy)phenyl)ethanamine hydrochloride (889 mg, 3.27 mmol) and Et_3N (1.15 mL, 8.18 mmol) in THF (14mL) with stirring at rt. The mixture was stirred at 60 °C overnight. The mixture was concentrated in vacuo and the residue was diluted with EtOAc. This solution was washed with water and saturated aqueous NaCl, dried over anhydrous Na_2SO_4 and concentrated in vacuo. The residue was purified by column chromatography (silica gel, hexane/ethyl acetate, 99:1 to 7:3) to give **58** (1.17 g, 1.76 mmol, 64%) as a pale orange solid. ^{1}H NMR (300 MHz, DMSO-d_6) δ 0.00 (9H, s), 0.91 (2H, t, J = 7.7 Hz), 3.34 (3H, s), 3.52–3.76 (4H, m), 4.60 (2H, s),5.03–5.17 (1H, m), 5.36 (2H, s), 7.37 (2H, d, J = 8.3 Hz), 7.52 (2H, d, J = 8.7 Hz), 8.01 (1H, d, J = 1.9 Hz), 8.39 (1H, d, J =1.9 Hz), 9.96 (1H, d, J = 7.2 Hz). MS (ESI/APCI) mass calculated for $[M + H]^+$ ($C_{24}H_{31}F_3IN_4O_5Si$) requires *m/z* 667.1, found *m/z* 667.1.

7-Iodo-N-(2-methoxy-1-(4-(trifluoromethyl)phenyl)ethyl)-2-oxo-1-((2-(trimethylsilyl)ethoxy)methyl)-2,3-dihydropyrido[2,3-b]pyrazine-4(1H)-carboxamide (59). To a solution of **57** (1.53 g, 3.77 mmol) in THF (60 mL) was added a solution of triphosgene (0.896 g, 3.02 mmol) in THF (8 mL) at rt. After being stirred at 40 °C for 5 h, the mixture was concentrated in vacuo. To a mixture of 2-methoxy-1-(4-(trifluoromethyl)phenyl)ethanamine hydrochloride (**S24l**) (1.16 g, 4.53 mmol) and Et_3N (1.58 mL, 11.3 mmol) in THF (60 mL) was added a solution of the residue obtained above in THF (10 mL) at rt. The mixture was stirred at 60 °C for 16 h, and then quenched with water and extracted with EtOAc. The organic layer was separated, washed with water and saturated aqueous NaCl, dried over anhydrous $MgSO_4$ and concentrated in vacuo. The residue was purified by column chromatography (basic silica gel, hexane/ethyl acetate, 19:1 to 7:3) to give **59** (2.18 g, 3.35 mmol, 89%) as a pale orange solid. ^{1}H NMR (300 MHz, $CDCl_3$) δ 0.00 (9H, s), 0.90–0.99 (2H, m), 3.38 (3H, s), 3.59–3.73 (4H, m), 4.65 (2H, d, J = 1.1 Hz), 5.12–5.20 (1H, m), 5.27 (2H, s), 7.42–7.51 (2H, m), 7.53–7.62 (2H, m),

7.95 (1H, d, J = 1.9 Hz), 8.25 (1H, d, J = 1.9 Hz), 10.15 (1H, d, J = 6.8 Hz). MS (ESI/APCI) mass calculated for $[M + H]^+$ ($C_{24}H_{31}F_3IN_4O_4Si$) requires *m/z* 651.1, found *m/z* 651.1.

N-(1-(3-Fluoro-4-(trifluoromethoxy)phenyl)-2-methoxyethyl)-7-iodo-2-oxo-1-((2-(trimethylsilyl)ethoxy)methyl)-2,3-dihydropyrido[2,3-b]pyrazine-4(1H)-carboxamide (60). To a stirred solution of **57** (3.83 g, 9.45 mmol) in THF (144 mL) was added a solution of triphosgene (2.24 g, 7.56 mmol) in THF (22 mL) dropwise at rt under N_2. The mixture was stirred at 40 °C for 3 h under N_2 and concentrated in vacuo. The residue was diluted with THF and concentrated in vacuo (this procedure was repeated three times), and suspended in THF (72 mL). The mixture was added dropwise to a mixture of 1-(3-fluoro-4-(trifluoromethoxy)phenyl)-2-methoxyethanamine (**S23k**) (2.87 g, 11.3 mmol) and Et_3N (2.66 mL, 18.9 mmol) in THF (48 mL) with stirring at rt. The mixture was stirred at 60 °C overnight. The mixture was concentrated in vacuo and the residue was partitioned between EtOAc and water. The phases were separated and the aqueous phase was extracted with EtOAc. The combined organic phases were washed with saturated aqueous NaCl, dried over anhydrous Na_2SO_4 and concentrated in vacuo. The residue was purified by column chromatography (silica gel, hexane/ethyl acetate, 99:1 to 7:3) to give **60** (6.15 g, 8.98 mmol, 95%) as a pale yellow amorphous solid. ^{1}H NMR (300 MHz, DMSO-d_6) δ 0.00 (9H, s), 0.85–0.97 (2H, m), 3.35 (3H, s), 3.59–3.77 (4H, m), 4.60 (2H, s), 5.03–5.18 (1H, m), 5.37 (2H, s), 7.36 (1H, d, J = 8.7 Hz), 7.46–7.64 (2H, m), 8.02 (1H, d, J = 1.9 Hz), 8.38 (1H, d, J = 1.9 Hz), 9.96 (1H, d, J = 7.2 Hz).

7-Cyclopropyl-N-(2-methoxy-1-(4-(trifluoromethoxy)phenyl)ethyl)-2-oxo-1-((2-(trimethylsilyl)ethoxy)methyl)-2,3-dihydropyrido[2,3-b]pyrazine-4(1H)-carboxamide (61). A mixture of **58** (683 mg, 1.03 mmol), cyclopropylboronic acid (176 mg, 2.05 mmol), K_3PO_4 (802 mg, 3.59 mmol), Cy_3P (117 mg, 0.410 mmol), and $Pd(OAc)_2$ (46.0 mg, 0.210 mmol) was stirred

at 100 °C overnight under Ar. The mixture was filtered and the filtrate was washed with water and saturated aqueous NaCl, dried over anhydrous Na_2SO_4 and concentrated in vacuo. The residue was purified by column chromatography (silica gel, hexane/ethyl acetate, 99:1 to 7:3) to give **61** (432 mg, 0.743 mmol, 73%) as a pale yellow solid. ^{1}H NMR (300 MHz, $CDCl_3$) δ 0.00 (9H, s), 0.64–0.78 (2H, m), 0.90–0.99 (2H, m), 1.00–1.13 (2H, m), 1.83–1.99 (1H, m), 3.39 (3H, s), 3.59–3.73 (4H, m), 4.65 (2H, d, *J* = 1.1 Hz), 5.17 (1H, d, *J* = 7.5 Hz), 5.29 (2H, s), 7.17 (2H, d, *J* = 7.9 Hz), 7.34–7.45 (3H, m), 7.86 (1H, d, *J* = 1.9 Hz), 10.29 (1H, d, *J* = 7.5 Hz). MS (ESI/APCI) mass calculated for $[M + H]^+$ ($C_{27}H_{36}F_3IN_4O_5Si$) requires *m/z* 581.2, found *m/z* 581.2.

7-Methoxy-N-(2-methoxy-1-(4-(trifluoromethoxy)phenyl)ethyl)-2-oxo-1-((2-(trimethylsilyl)ethoxy)methyl)-2,3-dihydropyrido[2,3-b]pyrazine-4(1H)-carboxamide (62). A mixture of **58** (900 mg, 1.35 mmol), bis(pinacolato)diboron (707 mg, 2.70 mmol), KOAc (546 mg, 5.40 mmol), and $PdCl_2$(dppf) (99 mg, 0.14 mmol) in DMF (13.5 mL) was stirred at 80 °C overnight under Ar. The mixture was quenched with water and extracted with EtOAc. The combined organic layer was washed with saturated aqueous NaCl, dried over anhydrous Na_2SO_4 and concentrated in vacuo to afford crude *N*-(2-methoxy-1-(4-(trifluoromethoxy)phenyl)ethyl)-2-oxo-7-(4,4,5,5-tetramethyl-1,3,2-dioxaborolan-2-yl)-1-((2-(trimethylsilyl)ethoxy)methyl)-2,3-dihydropyrido[2,3-*b*]pyrazine-4(1*H*)-carboxamide (1.55 g). This was used in the next reaction without further purification. MS (ESI/APCI) *m/z* 667.4 $[M + H]^+$. To a stirred solution of the crude product obtained above (1.55 g) in THF (23 mL) was added 2 M NaOH aqueous solution (4.64 mL, 9.28 mmol) at 0 °C. After 30 min of stirring at 0 °C, hydrogen peroxide (0.813 mL, 9.28 mmol) was added to the mixture. The mixture was stirred at rt for 1.5 h and then quenched with ice-water at rt and extracted with EtOAc. The combined organic layer was washed with

saturated aqueous NaCl and dried over anhydrous Na_2SO_4 and concentrated in vacuo. The residue was purified by column chromatography (silica gel, hexane/ethyl acetate, 99:1 to 1:1) to give 7-hydroxy-*N*-(2-methoxy-1-(4-(trifluoromethoxy)phenyl)ethyl)-2-oxo-1-((2-(trimethylsilyl)ethoxy)methyl)-2,3-dihydropyrido[2,3-*b*]pyrazine-4(1*H*)-carboxamide (0.678 g, 1.22 mmol, 90% in 2 steps from **58**) as a pale yellow oil. ^{1}H NMR (300 MHz, $CDCl_3$) δ 0.00 (9H, s), 0.89–1.01 (2H, m), 3.39 (3H, s), 3.60–3.74 (4H, m), 4.65 (2H, s), 5.10–5.20 (1H,m), 5.27 (2H, s), 6.28 (1H, brs), 7.17 (2H, d, *J* = 7.9 Hz), 7.33 (1H, d, *J* = 2.6 Hz), 7.37–7.47 (2H, m), 7.72 (1H, d, *J* = 2.6Hz), 9.96 (1H, d, *J* = 7.2 Hz). MS (ESI/APCI) mass calculated for $[M + H]^+$ ($C_{24}H_{31}F_3N_4O_6Si$) requires *m/z* 557.2, found *m/z* 557.3. To a stirred solution of 7-hydroxy-*N*-(2-methoxy-1-(4-(trifluoromethoxy)phenyl)ethyl)-2-oxo-1-((2-(trimethylsilyl)ethoxy)methyl)-2,3-dihydropyrido[2,3-*b*]pyrazine-4(1*H*)-carboxamide (560 mg, 1.01 mmol) in DMF (13 mL) was added K_2CO_3 (140 mg, 1.01 mmol) and methyl iodide (95 μL, 1.51 mmol). The mixture was stirred at rt overnight. The mixture was quenched with water and extracted with EtOAc. The combined organic layer was washed with saturated aqueous NaCl, dried over anhydrous Na_2SO_4 and concentrated in vacuo. The residue was purified by column chromatography (silica gel, hexane/ethyl acetate, 99:1 to 3:2) to give **62** (395 mg, 0.692 mmol, 69%) as a white amorphous solid. ^{1}H NMR (300 MHz, $CDCl_3$) δ 0.00 (9H, s), 0.86–1.01 (2H, m), 3.39 (3H, s), 3.58–3.73 (4H, m), 3.90 (3H, s), 4.65 (2H, s),5.10–5.22 (1H, m), 5.29 (2H, s), 7.17 (2H, d, *J* = 8.3 Hz), 7.31–7.47 (3H, m), 7.75 (1H, d, *J* = 2.6 Hz), 9.98 (1H, d, *J* = 7.2Hz). MS (ESI/APCI) mass calculated for $[M + H]^+$ ($C_{25}H_{34}F_3N_4O_6Si$) requires *m/z* 571.2, found *m/z* 571.3.

7-Isopropoxy-N-(2-methoxy-1-(4-(trifluoromethoxy)phenyl)ethyl)-2-oxo-1-((2-(trimethylsilyl)ethoxy)methyl)-2,3-dihydropyrido[2,3-b]pyrazine-4(1H)-carboxamide (63). To a stirred solution of 7-hydroxy-*N*-(2-methoxy-1-(4-(trifluoromethoxy)phenyl)ethyl)-2-oxo-1-((2-

(trimethylsilyl)ethoxy)methyl)-2,3-dihydropyrido[2,3-*b*]pyrazine-4(1*H*)-carboxamide (102 mg, 0.180 mmol) in DMF (2.4 mL) were added K_2CO_3 (25.6 mg, 0.180 mmol) and 2-iodopropane (28.0 μL, 0.280 mmol). The mixture was stirred at 70 °C overnight. The mixture was quenched with water and extracted with EtOAc. The combined organic layer was washed with saturated aqueous NaCl, dried over anhydrous Na_2SO_4 and concentrated in vacuo. The residue was purified by column chromatography (silica gel, hexane/ethyl acetate, 99:1 to 7:3) to give **63** (90 mg, 0.150 mmol, 82%) as a colorless oil. ^{1}H NMR (300 MHz, $CDCl_3$) δ 0.00 (9H, s), 0.90–1.00 (2H, m), 1.38 (6H, d, *J* = 6.0 Hz), 3.39 (3H, s), 3.61–3.72 (4H, m), 4.56 (1H, dt, *J* = 12.2, 6.2 Hz), 4.65 (2H, s), 5.11–5.21 (1H, m), 5.28 (2H, s), 7.17 (2H, d, *J* = 7.9 Hz), 7.34 (1H, d, *J* = 2.6 Hz), 7.38–7.44 (2H, m), 7.73 (1H, d, *J* = 2.6 Hz), 9.99 (1H, d, *J* = 7.5 Hz). MS (ESI/APCI) mass calculated for $[M + H]^+$ ($C_{27}H_{38}F_3N_4O_6Si$) requires *m/z* 599.2, found *m/z* 599.3.

7-Methoxy-N-(2-methoxy-1-(4-(trifluoromethyl)phenyl)ethyl)-2-oxo-1-((2-(trimethylsilyl)ethoxy)methyl)-2,3-dihydropyrido[2,3-b]pyrazine-4(1H)-carboxamide (64). A mixture of **59** (1.19 g, 1.83 mmol), bis(pinacolato)diboron (0.941 g, 3.67 mmol), KOAc (0.742 g, 7.34 mmol), and $PdCl_2$(dppf) (0.137 g, 0.18 mmol) in DMF (18 mL) was stirred at 80 °C overnight under Ar. The mixture was quenched with water and extracted with EtOAc. The combined organic layer was washed with water and saturated aqueous NaCl, dried over anhydrous Na_2SO_4 and concentrated in vacuo to give crude *N*-(2-methoxy-1-(4-(trifluoromethyl)phenyl)ethyl)-2-oxo-7-(4,4,5,5-tetramethyl-1,3,2-dioxaborolan-2-yl)-1-((2-(trimethylsilyl)ethoxy)methyl)-2,3-dihydropyrido[2,3-*b*]pyrazine-4(1*H*)-carboxamide (1.19 g). This was used in the next reaction without further purification. MS (ESI/APCI) mass calculated for $[M + H]^+$ ($C_{30}H_{43}BF_3N_4O_6Si$) requires *m/z* 651.3, found *m/z* 651.3. To a stirred solution of the crude product obtained above (1.19 g) in THF (18 mL) was added 2 M NaOH aqueous solution

(3.67 mL, 7.34 mmol) at 0 °C. After 30 min of stirring at 0 °C, hydrogen peroxide (0.642 mL, 7.34 mmol) was added to the mixture. The mixture was stirred at rt for 2 h. The mixture was quenched with ice-water and acidified with 1 M HCl aqueous solution, and extracted with EtOAc. The combined organic layer was washed with water and saturated aqueous NaCl, dried over anhydrous Na_2SO_4 and concentrated in vacuo. The residue was purified by column chromatography (silica gel, hexane/ethyl acetate, 99:1 to 1:1) to give 7-hydroxy-*N*-(2-methoxy-1-(4-(trifluoromethyl)phenyl)ethyl)-2-oxo-1-((2-(trimethylsilyl)ethoxy)methyl)-2,3-dihydropyrido[2,3-*b*]pyrazine-4(1*H*)-carboxamide (0.796 g, 1.47 mmol, 80% in 2 steps from **59**) as a pink oil. ^{1}H NMR (300 MHz, $CDCl_3$) δ 0.00 (9H, s), 0.87–1.03 (2H, m), 3.39 (3H, s), 3.58–3.75 (4H, m), 4.54–4.76 (2H, m), 5.13–5.23 (1H, m), 5.24–5.34 (2H, m), 7.33 (1H, d, J = 2.3 Hz), 7.45–7.54 (2H, m), 7.54–7.63 (2H, m), 7.72 (1H, d, J = 2.6 Hz), 10.09 (1H, d, J = 7.2 Hz). MS (ESI/APCI) mass calculated for $[M + H]^+$ ($C_{24}H_{32}F_3N_4O_5Si$) requires *m/z* 541.2, found *m/z* 541.2. To a stirred solution of 7-hydroxy-*N*-(2-methoxy-1-(4-(trifluoromethyl)phenyl)ethyl)-2-oxo-1-((2-(trimethylsilyl)ethoxy)methyl)-2,3-dihydropyrido[2,3-*b*]pyrazine-4(1*H*)-carboxamide (796 mg, 1.47 mmol) in DMF (19 mL) was added K_2CO_3 (205 mg, 1.47 mmol) and methyl iodide (139 μL, 2.21 mmol). The mixture was stirred at rt overnight. The mixture was quenched with water and extracted with EtOAc. The combined organic layer was washed with saturated aqueous NaCl, dried over anhydrous Na_2SO_4 and concentrated in vacuo. The residue was purified by column chromatography (silica gel, hexane/ethyl acetate, 99:1 to 11:9) to give **64** (665 mg, 1.20 mmol, 81%) as a white solid. ^{1}H NMR (300 MHz, $CDCl_3$) δ 0.00 (9H, s), 0.84–1.01 (2H, m), 3.39 (3H, s), 3.57–3.75 (4H, m), 3.90 (3H, s), 4.65 (2H, s),5.14–5.24 (1H, m), 5.29 (2H, s), 7.37 (1H, d, J = 2.6 Hz), 7.44–7.53 (2H, m), 7.56–7.65 (2H, m), 7.76 (1H, d, J = 2.6

Hz),10.03 (1H, d, J = 7.2 Hz). MS (ESI/APCI) mass calculated for $[M + H]^+$ ($C_{25}H_{34}F_3N_4O_5Si$) requires *m/z* 555.2, found *m/z* 555.2.

N-(1-(3-Fluoro-4-(trifluoromethoxy)phenyl)-2-methoxyethyl)-7-methoxy-2-oxo-1-((2-(trimethylsilyl)ethoxy)methyl)-2,3-dihydropyrido[2,3-b]pyrazine-4(1H)-carboxamide (65). A mixture of **60** (6.15 g, 8.98 mmol), bis(pinacolato)diboron (4.61 g, 18.0 mmol), KOAc (3.64 g, 36.0 mmol), and $PdCl_2$(dppf) (0.657 g, 0.90 mmol) in DMF (90 mL) was stirred at 80 °C overnight under Ar. The mixture was quenched with water and extracted with EtOAc. The combined organic layer was washed with water and saturated aqueous NaCl, dried over anhydrous Na_2SO_4 and concentrated in vacuo to give crude *N*-(1-(3-fluoro-4-(trifluoromethoxy)phenyl)-2-methoxyethyl)-2-oxo-7-(4,4,5,5-tetramethyl-1,3,2-dioxaborolan-2-yl)-1-((2-(trimethylsilyl)ethoxy)methyl)-2,3-dihydropyrido[2,3-*b*]pyrazine-4(1*H*)-carboxamide. This was used in the next reaction without further purification. MS (ESI/APCI) mass calculated for $[M + H]^+$ ($C_{30}H_{42}BF_4N_4O_7Si$) requires *m/z* 685.3, found *m/z* 685.3. To a stirred solution of the crude product obtained above (theoretical amount: 6.15 g, 8.98 mmol) in THF (90 mL) was added 2 M NaOH aqueous solution (18.0 mL, 35.9 mmol) at 0 °C. After 30 min of stirring at 0 °C, hydrogen peroxide (3.15 mL, 35.9 mmol) was added to the mixture. The mixture was stirred at rt for 2 h. The mixture was quenched with ice-water and acidified with 1 M HCl aqueous solution, and extracted with EtOAc. The combined organic layer was washed with water and saturated aqueous NaCl, dried over anhydrous Na_2SO_4 and concentrated in vacuo. The residue was purified by column chromatography (silica gel, hexane/ethyl acetate, 99:1 to 1:1) to give *N*-(1-(3-fluoro-4-(trifluoromethoxy)phenyl)-2-methoxyethyl)-7-hydroxy-2-oxo-1-((2-(trimethylsilyl)ethoxy)methyl)-2,3-dihydropyrido[2,3-*b*]pyrazine-4(1*H*)-carboxamide (4.99 g, 8.69 mmol, 97% in 2 steps from **60**) as a brown oil. ^{1}H NMR (300 MHz, $CDCl_3$) δ 0.00 (9H, s),

0.86–1.02 (2H, m), 3.39 (3H, s), 3.60–3.72 (4H, m), 4.65 (2H, d, *J* = 1.1 Hz), 5.12 (1H, dt, *J* = 7.1, 4.7 Hz), 5.28 (2H, s), 7.08–7.27 (3H, m), 7.35 (1H, d, *J* = 2.5 Hz), 7.72 (1H, d, *J* = 2.6 Hz), 10.03 (1H, d, *J* =7.4 Hz). MS (ESI/APCI) mass calculated for $[M + H]^+$ ($C_{24}H_{31}F_4N_4O_6Si$) requires *m/z* 575.2, found *m/z* 575.2. To a stirred solution of *N*-(1-(3-fluoro-4-(trifluoromethoxy)phenyl)-2-methoxyethyl)-7-hydroxy-2-oxo-1-((2-(trimethylsilyl)ethoxy)methyl)-2,3-dihydropyrido[2,3-*b*]pyrazine-4(1*H*)-carboxamide (8.47 g, 14.7 mmol) in DMF (189 mL) was added K_2CO_3 (2.05 g, 14.7 mmol) and methyl iodide (1.39 mL, 22.1 mmol). The mixture was stirred at rt overnight and then concentrated in vacuo. The residue was partitioned between EtOAc and water. The phases were separated, and the aqueous phase was extracted with EtOAc. The combined organic phases were washed with saturated aqueous NaCl, dried over anhydrous Na_2SO_4 and concentrated in vacuo. The residue was purified by column chromatography (silica gel, hexane/ethyl acetate, 99:1 to 3:2) to give **65** (5.22 g, 8.87 mmol, 60%) as a pale yellow amorphous solid. ^{1}H NMR (300 MHz, $CDCl_3$) δ 0.00 (9H, s), 0.88–1.01 (2H, m), 3.40 (3H, s), 3.58–3.74 (4H, m), 3.90 (3H, s), 4.65 (2H, s),5.13 (1H, dt, *J* = 7.2, 4.7 Hz), 5.30 (2H, s), 7.11–7.31 (3H, m), 7.33–7.42 (1H, m), 7.76 (1H, d, *J* = 2.6 Hz), 10.01 (1H, d, *J* =7.5 Hz). MS (ESI/APCI) mass calculated for $[M + H]^+$ ($C_{25}H_{32}F_4N_4O_6Si$) requires *m/z* 589.2, found *m/z* 589.2.

7-Methoxy-N-(2-methoxy-1-(4-(trifluoromethyl)phenyl)ethyl)-2-oxo-2,3-dihydropyrido[2,3-b]pyrazine-4(1H)-carboxamide (67). A mixture of **64** (665 mg, 1.20 mmol) in TFA (17.3 mL) and water (1.93 mL) was stirred at rt for 1 h and then concentrated in vacuo. The residue was dissolved in DMF (33 mL) and 8 M NH_3 solution in MeOH (6.46 mL, 51.7 mmol) was added. The mixture was stirred at rt for 10 min and concentrated in vacuo. The residue was diluted with EtOAc. The solution was washed with water and saturated aqueous NaCl, dried over anhydrous

Na_2SO_4 and concentrated in vacuo to give **67** (474 mg, 1.12 mmol, 93%) as a white solid after trituration with hexane/ethyl acetate (10:1). ^{1}H NMR (300 MHz, DMSO-d_6) δ 3.28 (3H, s), 3.59–3.68 (2H, m), 3.83 (3H, s), 4.25–4.55 (2H, m), 5.00–5.17 (1H, m), 6.97 (1H, d, J = 3.0 Hz), 7.56 (2H, d, J = 8.3 Hz), 7.64–7.73 (2H, m), 7.77 (1H, d, J = 2.6 Hz), 10.07 (1H, d, J = 7.5 Hz), 10.77 (1H, s). MS (ESI/APCI) mass calculated for $[M + H]^+$ ($C_{19}H_{20}F_3N_4O_4$) requires *m/z* 425.1, found *m/z* 425.1.

N-(1-(3-Fluoro-4-(trifluoromethoxy)phenyl)-2-methoxyethyl)-7-methoxy-2-oxo-2,3-dihydropyrido[2,3-b]pyrazine-4(1H)-carboxamide (68). A mixture of **65** (5.22 g, 8.87 mmol) in TFA (128 mL) and water (14.3 mL) was stirred at rt for 1.5 h and then concentrated in vacuo. The residue was dissolved in DMF (243 mL) and 8 M NH_3 solution in MeOH (47.8 mL, 382 mmol) was added. The mixture was stirred at rt for 2 h and concentrated in vacuo. The residue was diluted with EtOAc. The solution was washed with water and saturated aqueous NaCl, dried over anhydrous Na_2SO_4 and concentrated in vacuo to give **68** (3.37 g, 7.36 mmol, 83%) as pale yellow solid after trituration with hexane/ethyl acetate (10:1). ^{1}H NMR (300 MHz, DMSO-d_6) δ 3.29 (3H, s), 3.63 (2H, tt, J = 9.6, 4.9 Hz), 3.83 (3H, s), 4.26–4.52 (2H, m), 4.95–5.15 (1H,m), 6.97 (1H, d, J = 2.6 Hz), 7.29 (1H, d, J = 8.3 Hz), 7.41–7.60 (2H, m), 7.75 (1H, d, J = 3.0 Hz), 10.02 (1H, d, J = 7.5 Hz),10.77 (1H, s). MS (ESI/APCI) mass calculated for $[M + H]^+$ ($C_{19}H_{19}F_4N_4O_5$) requires *m/z* 459.1, found *m/z* 459.1.

Enzyme Assay Protocol. *Preparation of human PDE.* Human PDE1A, 3A, 4D2, 5A1, 7B, 8A1, 9A2, and 11A4 enzymes were purchased from BPS Bioscience. Human PDE6AB enzyme was purchased from SB Drug Discovery. Human PDE2A3 full-length gene was transduced into Sf9, and human PDE2A3 enzyme was purified by His-tag affinity column and gel filtration. Human

PDE10A2 was generated from COS-7 cells transfected with the full-length gene. The enzymes were stored at −70 °C until use.

PDE2A3 enzyme inhibitory assay. PDE activity was measured using a SPA (Scintillation Proximity Assay) (GE Healthcare). To evaluate the inhibitory activity of the compound, 10 μL of serially diluted compounds were reacted with 20 μL of PDE enzyme (final concentration 0.023 nM) in assay buffer (50 mM HEPES-NaOH, 8.3 mM $MgCl_2$, 1.7 mM EGTA, and 0.1% bovine serum albumin (BSA) (pH 7.4)) for 30 min at rt. The final concentration of DMSO in the reaction solution was 1%. Compounds were tested in duplicate in 96-well half-area plates (Corning) or a 384-well OptiPlate (PerkinElmer). We used an 8 concentration serial dilution dose response ranging from 100 μM to 10 pM compound concentrations. To start the reaction, 10 μL of substrate [^{3}H] cGMP (final concentration 77 nM, PerkinElmer) was added to a total volume of 40 μL. After reaction for 60 min at rt, 20 μL of 20 mg/mL yttrium SPA beads containing zinc sulfate was added to terminate the PDE reaction. After allowing to settle for an additional 60 min, the assay plates were counted in a scintillation counter (PerkinElmer) to allow calculation of the inhibition rate. The inhibition rate was calculated on the basis of the 0% control wells with enzyme and DMSO, and the 100% control wells without enzyme. All IC_{50} values were obtained by fitting the results to the following 4 Parameter Logistic Equation:

$$y = A + (B - A)/(1 + (10^{((C - x)*D)}))$$

where A is the minimum y value, B is the maximum y value, C is $Log(EC_{50})$ value, and D is the slope factor.

Human PDE enzyme assay. PDE activities were measured using a SPA (GE Healthcare). To evaluate the inhibitory activity, 10 μL of serially diluted compounds were incubated with 20 μL of PDE enzymes, except for PDE1A, in the following assay buffer: 50 mM HEPES-NaOH, 8.3

mM $MgCl_2$, 1.7 mM EGTA, and 0.1% BSA (pH 7.4) for 30 min at rt. The PDE1A enzyme assay was performed in the following assay buffer: 50 mM Tris-HCl, 8.3 mM $MgCl_2$, 0.2 mM $CaCl_2$, 0.1% BSA, and 30 nM Calmodulin (pH 7.5). The final concentration of DMSO in the assay was 1%, and compounds were tested in duplicate in 96-well half-area plates (Corning). We used an 4 concentration serial dilution dose response ranging from 10 μM to 10 nM compound concentrations. To start the reaction, 10 μL of substrate ([^{3}H] cGMP (final concentration 77 nM, PerkinElmer) for PDE1A, 5A1, 6AB, 9A2, 10A2, and 11A4 or [^{3}H] cAMP (final concentration 14.7 nM, PerkinElmer) for PDE3A, 4D2, 7B, and 8A1) was added for a final assay volume of 40 μL. After 60 min incubation at rt, 20 μL of 20 mg/mL yttrium SPA beads containing zinc sulfate was added to terminate the PDE reaction. After allowing to settle for more than 120 min, the assay plates were counted in a scintillation counter (PerkinElmer) to allow calculation of the inhibition rate.

Estimation of LogD at pH 7.4. $LogD_{7.4}$, which is the partition coefficient of the compounds between 1-octanol and aqueous buffer at pH 7.4, was measured using a chromatographic procedure based on a published method.[57] The instruments utilized were a Waters Alliance 2795 HPLC system and a 2996 UV–vis detector (Milford, MA, USA).

Transcellular Transport Study Using a Transporter-Expression System. Human MDR1-expressing LLC-PK1 cells were cultured as reported previously with minor modifications.[58] The transcellular transport study was performed as reported previously.[59] In brief, the cells were grown for 7 days in an HTS Transwell 96-well permeable support (pore size: 0.4 μm, surface area: 0.143 cm^2) with a polyethylene terephthalate membrane (Corning Life Sciences, Lowell, MA, USA) at a density of 1.125×10^5 cells/well. The cells were preincubated with M199 at 37 °C for 30 min. Subsequently, transcellular transport was initiated by the addition of M199 either

to apical compartments (75 μL) or to the basolateral compartments (250 μL) containing 10 μM digoxin, 200 μM lucifer yellow as a marker for the monolayer tightness, and 10 μM test compounds, and then terminated by the removal of each assay plate after 2 h. The aliquots (25 μL) in the opposite compartments were mixed with acetonitrile containing alprenolol and diclofenac as an internal standard and then centrifuged. The compound concentrations in the supernatant were measured by LC–MS/MS. The apparent permeability (P_{app}) of test compounds in the receiver wells was determined and the efflux ratio (ER) for the MDR1 membrane permeability test was calculated using the following equation: ER = $P_{app,BtoA}/P_{app,AtoB}$

where $P_{app,AtoB}$ is the apical-to-basal passive permeability–surface area product and $P_{app,BtoA}$ is the basal-to-apical passive permeability–surface area product.

In Vitro Metabolic Clearance Assay. In vitro oxidative metabolic studies of the test compounds were carried out using hepatic microsomes obtained from humans, rats, or mice. The reaction mixture with a final volume of 0.05 mL consisted of 0.2 mg/mL hepatic microsomes in 50 mM KH_2PO_4–K_2HPO_4 phosphate buffer (pH 7.4) and 1 μM test compound. The reaction was initiated by the addition of an NADPH-generating system containing 25 mM $MgCl_2$, 25 mM glucose 6-phosphate, 2.5 mM β-$NADP^+$, and 7.5 units/mL glucose 6-phosphate dehydrogenase at 20 vol% of the reaction mixture. After addition of the NADPH-generating system, the mixture was incubated at 37 °C for 0, 15, and 30 min. The reaction was terminated by addition of an equivalent volume of acetonitrile. After the samples were mixed and centrifuged, the supernatant fractions were analyzed using LC–MS/MS. For metabolic clearance determinations, chromatograms were analyzed to determine the disappearance of the parent compound from the reaction mixtures. All incubations were carried out in duplicate.

Protein Expression and Purification. The PDE2A catalytic domain (578–919) was cloned into a pFastBac vector, for expression in Sf9 cells, utilizing an N-terminal 6× poly-histidine tag containing a TEV cleavage site. Large-scale production of recombinant protein was carried out in Sf9 cells. The pellet from 10L of baculovirus-infected Sf9 cells was resuspended in 600 mL of lysis buffer containing 25 mM Tris (pH 7.6), 1 M NaCl, 20 mM imidazole, 5% glycerol, and 3 Roche cOmplete Protease Inhibitor tablets. The cell suspension was homogenized with the Polytron PT-3100, centrifuged for 1 h at 13,000 rpm (JA-14 rotor), and the clarified supernatant was brought to 800 mL with lysis buffer before batch binding with 10 mL of Probond Ni resin (Invitrogen) and rolling for 2 h at 4 °C. The beads were collected by low speed centrifugation (3,500 rpm, JS-4.2 rotor), loaded into a gravity column, and washed slowly overnight with 2 L of wash buffer containing 25 mM Tris (pH 7.6), 1 M NaCl, 20 mM imidazole, and 5% glycerol. The following day, the protein was eluted with buffer containing 25 mM Tris (pH 7.9), 50 mM NaCl, 250 mM imidazole, and 10% glycerol. The 1.5 mL sample eluted from the Nickel capture step was brought to 9 mL with Mono Q buffer A containing 25 mM Tris (pH 7.9), and 10% glycerol. After the full sample volume was bound to the Mono Q column, a salt gradient was applied from 0 to ~800 mM NaCl in 40 mL. Fractions corresponding to the unphosphorylated protein (identified by MS with MW = 40178 Da) were pooled for further purification by size-exclusion chromatography (SEC) on a Superdex 200 column equilibrated in 1XTBS pH 7.4, 0.5 mM DTT, 1 mM EDTA, and 10% glycerol. Peak SEC fractions were collected and concentrated to 12 mg/mL for crystallization.

Crystallization and Structure Determination. Crystals suitable for data collection were first grown in hanging drops using the vapor diffusion method at rt by adding 0.5 µL of protein solution with 1 mM of IBMX (1-methyl-3-(2-methylpropyl)-2,3,6,7-tetrahydro-1*H*-purine-2,6-

dione) and 0.5 μL of reservoir solution (30% PEG 3350, 0.1 M Tris pH 7.5, and 0.2 M $MgCl_2$). PDE2A IBMX crystals were soaked in a drop containing 5 mM of **36**, 31% PEG 3350, 0.1 M Tris (pH 7.5), and 0.2 M $MgCl_2$ for 6 days. Crystals were transferred through a fresh cryo-protected soak drop immediately before being harvested and flash frozen in liquid nitrogen. X-ray diffraction data were collected at ALS beamline 5.0.2 using a Pilatus3 6M (Dectris) detector from a single cryogenically protected crystal (100 K) at a wavelength of 1 Å. The crystals belong to space group C121 and contain three enzyme molecules per asymmetric unit. X-ray diffraction data were reduced using the HKL2000[60] software package. The structure was determined by molecular replacement with PHASER within the CCP4 program suite and refined with REFMAC.[61] Several cycles of model building using MIfit[62] and refinement using REFMAC were performed to improve the quality of the model. The coordinates and structure factors have been deposited in the Protein Data Bank (PDB) with accession code 5VP0.

Animal Experiments. The care and use of animals and the experimental protocols were approved by the Experimental Animal Care and Use Committee of Takeda Pharmaceutical Company Limited.

Pharmacokinetic Analysis in Rat or Mouse Cassette Dosing. Compound **36** was administered intravenously (0.1 mg/kg) or orally (1 mg/kg) by cassette dosing to nonfasted male Crl:CD(SD)(IGS) rats (8W, n = 3) or male ICR mice (8W, n = 3). The combination for a cassette dosing was determined to avoid combinations of compounds with the same molecular weight. The solution of compounds in dimethylacetamide containing 50% (v/v) 1,3 butanediol at 0.1 mg/mL/kg was administered intravenously to isoflurane-anesthetized mice via femoral vein. The suspension of compounds in 0.5% methyl cellulose with water was used for vehicle (1 mg/kg) and was administered orally by gavage. After administration, blood samples were collected via

tail vein by syringes with heparin at 5, 10, 15, 30 min, 1, 2, 4, and 8 h (iv) and 15, 30 min, 1, 2, 4, and 8 h (po), and centrifuged to obtain the plasma fraction. The plasma samples were deproteinized by mixing with acetonitrile followed by centrifugation. The compound concentrations in the supernatant were measured by LC–MS/MS with a standard curve. Pharmacokinetic parameters were calculated by the non-compartmental analysis. The area under the concentration-time curve (AUC) and the area under the first moment curve (AUMC) were calculated using the linear trapezoidal method. The mean residence time (MRT) was calculated as AUMC/AUC. The total clearance (CL_{total}) was calculated as doseiv/AUC_{iv}. The volume of distribution (Vd_{ss}) was calculated as $CL_{total} \times MRT_{iv}$. Oral bioavailability ($F$) was calculated as $(AUC_{po}/dose_{po})/(AUC_{iv}/dose_{iv}) \times 100$.

Brain and Plasma Concentration in Rats and Mice. Compound **36** was suspended in 0.5% (w/v) methylcellulose in distilled water, and was administered at a volume of 2 mL/kg body weight for rats and 10 mL/kg for mice. Seven-week-old male SD rats (Charles River Laboratories Japan, Inc., Yokohama, Japan) and seven-week-old male ICR mice (CLEA Japan Inc., Tokyo, Japan) were euthanized 2 h after oral administration of **36** (10 mg/kg). Blood was centrifuged and the supernatants were collected as plasma. Brain was homogenized in physiological saline. Concentrations of **36** were measured in aliquots of rat plasma and tissues, which were mixed well with acetonitrile containing internal standards and then centrifuged. The supernatants were diluted with solvents for LC–MS/MS analysis (mobile phase A: 10 mM ammonium formate/formic acid (100/0.2, v/v), mobile phase B: acetonitrile/formic acid (100/0.2, v/v)). The diluted solutions were injected into an LC–MS/MS (API5000, AB Sciex, Foster City, CA) equipped with a Shimadzu Shim-pack XR-ODS column (2.2 μm packing particle size, 2.0 mm ID × 30 mm L) maintained at 50 °C. The chromatographic separation was performed using

gradient elution at a flow rate of 0.7 mL/min. The LC time program was as follows: Mobile phase B was held at 5% for 0.2 min, and increased linearly to 99% in 1.1 min. After maintaining B at 99% for another 0.7 min, it was brought back to 5% in 0.01 min, followed by re-equilibration for 0.59 min. The total cycle time for one injection was 2.6 min. Compound **36** was detected using multiple reaction monitoring mode and the transition *m/z* 459.20 → 223.01. Analyst™ software (version 1.4.2) was used for data acquisition and processing.

Measurement of Cyclic Nucleotide Contents in Mouse Brains. *Animals*. Six-week-old male C57BL/6J mice were purchased from CLEA Japan, Inc**.** (Japan). After one week acclimation period, the eight-week-old mice were used for the experiment. The mice were housed in groups of 5/cage in a light-controlled room (12 h light/dark cycles with lights on at 07:00). Food and water were provided *ad libitum*. Thirty six mice were used in total (12 mice were used for each treatment group).

Measurements. Compound **36** was suspended in 0.5% (w/v) methylcellulose in distilled water and administered at a volume of 10 mL/kg body weight for mice. Either vehicle or compound **36** was administered orally to mice after a habituation period of more than 30 min. Compound **36** was administered at 3 and 10 mg/kg. A microwave fixation system (Muromachi Kikai, Tokyo, Japan) was used to sacrifice unanesthetized mice by exposure of the head to the microwave beam at 60 min after administration of **36**. Hippocampi were isolated and homogenized in 0.5 mol/L HCl, followed by centrifugation. The cGMP concentration in the supernatant was quantified using a cyclic GMP EIA kit (Cayman Chemical, USA) according to the manufacturer's instructions. Values were expressed as pmol/mg tissue weight.

Effects of 36 on the Novel Object Recognition (NOR) Task in Rats. *Animals*. Six-week-old male Long–Evans rats were purchased from Japan SLC Inc. Rats were acclimated for one week

prior to the experiment. The rats were housed in groups of 2 or 3/cage in a light-controlled room (12 h light/dark cycles with lights on at 07:00). Food and water were provided *ad libitum*.

Measurements. Compound **36** was suspended in 0.5% (w/v) methylcellulose in distilled water, and administered at a volume of 2 mL/kg body weight for rats. On day 1, rats were allowed to habituate to the behavioral test room for over 1 h, and then they were allowed to habituate individually to the empty test box (a gray-colored polyvinyl chloride box (40 × 40 × 50 cm)) for 10 min. The test was comprised of two, 3 min trials called the acquisition and retention trials, separated by a 48 h inter-trial interval (ITI). On day 2, in the acquisition trial, rats were allowed to explore two identical objects (A1 and A2) for 3 min. Object exploration was defined as rats' licking, sniffing, or touching the object with forelimbs while sniffing. Leaning against the object to look upward and standing or sitting on the object were excluded. The exploration time of rats for each object (A1 and A2) was scored manually. Rats that scored less than 10 s of total exploration time during the acquisition trials were excluded from further study. On day 4, in the retention trial, rats were again allowed to explore a familiar object (A3) and a novel object (B) for 3 min. Exploration times for the familiar and novel objects were manually scored in the same way as in the acquisition trial. Vehicle or **36** (0.01, 0.1, and 1 mg/kg) was administered orally 2 h prior to the acquisition trial. The novelty discrimination index (NDI) was calculated using the following equation: novel object interaction time/total interaction time × 100 (%).Forty rats were prepared in total, and then one rat treated with 1 mg/kg was excluded because its total exploration time in the acquisition trial was less than 10 s (6.95 s). Numbers of rats treated with vehicle and those treated with 0.01, 0.1, and 1 mg/kg of compound **36** were 10, 10, 10, and 9, respectively.

ASSOCIATED CONTENT

Supporting Information.

The Supporting Information is available free of charge on the ACS publications website at DOI: xxxxx.

Full synthetic procedures and characterization for all analogs (i.e. RHS benzylamine moieties **S23**, **S24**, and **S32**, pyrazolo[1,5-*a*]pyrimidine derivative **5**, and 5,6-dihydro-1,6-naphthyridine derivative **9**) whose procedures are not included in the main manuscript.

Alternative synthetic routes for **32** and **36**.

Synthesis of (+)-di-(*p*-toluoyl)-$_{D}$-tartaric acid salt of **S47** suitable for X-ray crystallography.

Full details of the X-ray structure analyses of **S41a** and **S46**.

Molecular formula strings.

Accession Codes

The coordinates of the crystal structure of PDE2A in complex with compound **36** (5VP0) have been deposited in the Protein Data Bank. Authors will release the atomic coordinates and experimental data upon article publication.

AUTHOR INFORMATION

Corresponding Author

*Phone: +81-466-32-1217. Fax: +81-466-29-4458. E-mail: satoshi.mikami@takeda.com.

Notes

The authors declare no competing financial interest.

ACKNOWLEDGMENTS

We acknowledge Stephanie Merison for helpful discussions and synthetic support, Naohiro Taya for preparing the crystalline acid salt (**S47**) of RHS benzylamine **S46** (see Supporting Information) suitable for single crystal X-ray analysis, Mitsuyoshi Nishitani for obtaining the single crystal X-ray structure of **S47**, and Gyorgy Snell and Scott Lane (Takeda California, Inc.) for crystallographic data collection and processing of **36**. We also thank Miki Hara, Natsumi Fujii, and Teppei Otsuda for chiral separations.

ABBREVIATIONS

HATU, 1-(bis(dimethylamino)methylene)-1*H*-1,2,3-triazolo[4,5-*b*]pyridinium 3-oxid hexafluorophosphate; dppf, 1,1'-bis(diphenylphosphino)ferrocene; B_2pin_2, bis(pinacolato)diboron; BSA, bovine serum albumin; CNS, central nervous system; cAMP, 3',5'-cyclic adenosine monophosphate; cGMP, 3',5'-cyclic guanosine monophosphate; DIEA, *N*,*N*-diisopropylethylamine; DMA, *N*,*N*-dimethylacetamide; DMF, *N*,*N*-dimethylformamide; EDCI, 1-ethyl-3-(3-dimethylaminopropyl)carbodiimide; HBA, hydrogen bond acceptor; HBD, hydrogen bond donor; HOBt, 1-hydroxybenzotriazole; HOSA, hydroxylamine-*O*-sulfonic acid; LE, ligand efficiency; LC–MS/MS, liquid chromatography tandem mass spectrometry; LTP, long-term potentiation; *m*-CPBA, *m*-chloroperoxybenzoic acid; MDR1, multidrug resistance protein 1; NOR, novel object recognition; NDI, novelty discrimination index; P-gp, P-glycoprotein; PK, pharmacokinetic; PDE, phosphodiesterase; KHMDS, potassium bis(trimethylsilyl)amide; PDB, Protein Data Bank; RHS, right-hand side; rt, room temperature; SAR, structure–activity relationship; SBDD, structure-based drug design; TPSA, topological polar surface area; SEM, (2-(trimethylsilyl)ethoxy)methyl; S.E.M., standard error of mean

REFERENCES

(1) Bender, A. T.; Beavo, J. A. Cyclic Nucleotide Phosphodiesterases: Molecular Regulation to Clinical Use. *Pharmacol. Rev.* **2006**, *58*, 488–520.

(2) Conti, M.; Beavo, J. Biochemistry and Physiology of Cyclic Nucleotide Phosphodiesterases: Essential Components in Cyclic Nucleotide Signaling. *Annu. Rev. Biochem.* **2007**, *76*, 481–511.

(3) Francis, S. H.; Blount, M. A.; Corbin, J. D. Mammalian Cyclic Nucleotide Phosphodiesterases: Molecular Mechanisms and Physiological Functions. *Physiol. Rev.* **2011**, *91*, 651–690.

(4) Keravis, T.; Lugnier, C. Cyclic Nucleotide Phosphodiesterase (PDE) Isozymes as Targets of the Intracellular Signalling Network: Benefits of PDE Inhibitors in Various Diseases and Perspectives for Future Therapeutic Developments. *Br. J. Pharmacol.* **2012**, *165*, 1288–1305.

(5) Beavo, J. A. Cyclic Nucleotide Phosphodiesterases: Functional Implications of Multiple Isoforms. *Physiol. Rev.* **1995**, *75*, 725–748.

(6) Bolger, G. B.; Rodgers, L.; Riggs, M. Differential CNS Expression of Alternative mRNA Isoforms of the Mammalian Genes Encoding cAMP-Specific Phosphodiesterases. *Gene* **1994**, *149*, 237–244.

(7) van Staveren, W. C.; Steinbusch, H. W.; Markerink-Van Ittersum, M.; Repaske, D. R.; Goy, M. F.; Kotera, J.; Omori, K.; Beavo, J. A.; De Vente, J. mRNA Expression Patterns of the cGMP-Hydrolyzing Phosphodiesterases Types 2, 5, and 9 during Development of the Rat Brain. *J. Comp. Neurol.* **2003**, *467*, 566–580.

(8) Reyes-Irisarri, E.; Markerink-Van Ittersum, M.; Mengod, G.; de Vente, J. Expression of the cGMP-Specific Phosphodiesterases 2 and 9 in Normal and Alzheimer's Disease Human Brains.

Eur. J. Neurosci. **2007**, *25*, 3332–3338.

(9) Stephenson, D. T.; Coskran, T. M.; Wilhelms, M. B.; Adamowicz, W. O.; O'Donnell, M. M.; Muravnick, K. B.; Menniti, F. S.; Kleiman, R. J.; Morton, D. Immunohistochemical Localization of Phosphodiesterase 2A in Multiple Mammalian Species. *J. Histochem. Cytochem.* **2009**, *57*, 933–949.

(10) Lakics, V.; Karran, E. H.; Boess, F. G. Quantitative Comparison of Phosphodiesterase mRNA Distribution in Human Brain and Peripheral Tissues. *Neuropharmacology* **2010**, *59*, 367–374.

(11) Stephenson, D. T.; Coskran, T. M.; Kelly, M. P.; Kleiman, R. J.; Morton, D.; O'Neill, S. M.; Schmidt, C. J.; Weinberg, R. J.; Menniti, F. S. The Distribution of Phosphodiesterase 2A in the Rat Brain. *Neuroscience* **2012**, *226*, 145–155.

(12) Frey, U.; Huang, Y. Y.; Kandel, E. R. Effects of cAMP Simulate a Late Stage of LTP in Hippocampal CA1 Neurons. *Science* **1993**, *260*, 1661–1664.

(13) Son, H.; Lu, Y. F.; Zhuo, M.; Arancio, O.; Kandel, E. R. The Specific Role of cGMP in Hippocampal LTP. *Learn. Mem.* **1998**, *5*, 231–245.

(14) Lu, Y.; Kandel, E., R.; Hawkins, R. D. Nitric Oxide Signaling Contributes to Late-Phase LTP and CREB Phosphorylation in the Hippocampus. *J. Neurosci.* **1999**, *19*, 10250–10261.

(15) Prickaerts, J.; de Vente, J.; Honig, W.; Steinbusch, H. W. M.; Blokland, A. cGMP, but Not cAMP, in Rat Hippocampus Is Involved in Early Stages of Object Memory Consolidation. *Eur. J. Pharmacol.* **2002**, *436*, 83–87.

(16) Sanderson, T. M.; Sher, E. The Role of Phosphodiesterases in Hippocampal Synaptic Plasticity. *Neuropharmacology* **2013**, *74*, 86–95.

(17) Bernabeau, R.; Schimitz, P.; Faillace, M. P.; Izquierdo, I.; Medina, J. H. Hippocampal cGMP and cAMP Are Differentially Involved in Memory Processing of Inhibitory Avoidance Learning. *NeuroReport* **1996**, *7*, 585–588.

(18) Niewoehner, U.; Schauss, D.; Hendrix, M.; Koenig, G.; Boess, F. G.; van der Staay, F. J.; Schreiber, R.; Schlemmer, K. H.; Grosser, R. Novel Substituted Imidazotriazinones as PDE II-Inhibitors. WO 2002050078, June 27, 2002.

(19) Abaarghaz, M.; Biondi, S.; Duranton, J.; Limanton, E.; Mondadori, C.; Wagner, P. Benzo[1,4]diazepin-2-one Derivatives as Phosphodiesterase PDE2 Inhibitors, Preparation and Therapeutic Use Thereof. WO 2005063723, July 14, 2005.

(20) Schmidt, B.; Weinbrenner, S.; Flockerzi, D.; Kuelzer, R.; Tenor, H.; Kley, H.-P. Triazolophthalazines. WO 2006024640, March 9, 2006.

(21) Schmidt, B.; Weinbrenner, S.; Flockerzi, D.; Külzer, R.; Tenor, H.; Kley, H.-P. Triazolophthalazines. WO 2006072612, July 13, 2006.

(22) Schmidt, B.; Weinbrenner, S.; Flockerzi, D.; Külzer, R.; Tenor, H.; Kley, H.-P. Triazolophthalazines. WO 2006072615, July 13, 2006.

(23) Buijnsters, P.; De Angelis, M.; Langlois, X.; Rombouts, F. J. R.; Sanderson, W.; Tresadern, G.; Ritchie, A.; Trabanco, A. A.; VanHoof, G.; Van Roosbroeck, Y.; Andrés, J.-I. Structure-Based Design of a Potent, Selective, and Brain Penetrating PDE2 Inhibitor with Demonstrated Target Engagement. *ACS Med. Chem. Lett.* **2014**, *5*, 1049–1053.

(24) Rombouts, F. J. R.; Tresadern, G.; Buijnsters, P.; Langlois, X.; Tovar, F.; Steinbrecher, T. B.; Vanhoof, G.; Somers, M.; Andrés, J.-I.; Trabanco, A. A. Pyrido[4,3-*e*][1,2,4]triazolo[4,3-*a*]pyrazines as Selective, Brain Penetrant Phosphodiesterase 2 (PDE2) Inhibitors. *ACS Med. Chem. Lett.* **2015**, *6*, 282–286.

(25) Redrobe, J. P.; Jørgensen, M.; Christoffersen, C. T.; Montezinho L. P.; Bastlund, J. F.; Carnerup, M.; Bundgaard, C.; Lerdrup, L.; Plath, N. In Vitro and In Vivo Characterisation of Lu AF64280, a Novel, Brain Penetrant Phosphodiesterase (PDE) 2A Inhibitor: Potential Relevance to Cognitive Deficits in Schizophrenia. *Psychopharmacology* (*Berlin*) **2014**, *231*, 3151–3167.

(26) Helal, C. J. Identification of a Brain Penetrant, Highly Selective Phosphodiesterase 2A Inhibitor for the Treatment of Cognitive Impairment Associated with Schizophrenia (CIAS). 244th ACS National Meeting & Exposition, Philadelphia, PA, USA, August 19–23, 2012.

(27) Chappie, T. A.; Humphrey, J. M.; Verhoest, P. R.; Yang, E.; Helal, C. J. Imidazo[5,1-*f*][1,2,4]triazines for the Treatment of Neurological Disorders. WO 2012114222, August 30, 2012.

(28) Helal, C. J.; Chappie, T. A.; Humphrey, J. M. Pyrazolo[3,4-*d*]pyrimidine Compounds and Their Use as PDE2 Inhibitors and/or CYP3A4 Inhibitors. WO 2012168817, December 13, 2012.

(29) Mikami, S.; Nakamura, S.; Ashizawa, T.; Sasaki, S.; Taniguchi, T.; Nomura, I.; Kawasaki, M. Nitrogenated Heterocyclic Compound. WO 2013161913, October 31, 2013.

(30) Nakamura, S.; Mikami, S.; Kawasaki, M.; Nomura, I.; Ashizawa, T.; Taniguchi, T. Heterocyclic Compound. WO 2014010732, January 16, 2014.

(31) Kawasaki, M; Mikami, S.; Nakamura, S.; Negoro, N.; Ikeda, S.; Nomura, I.; Ashizawa, T.; Imaeda, T.; Seto, M.; Sasaki, S.; Marui, S.; Taniguchi, T. Heterocyclic Compound. WO 2015012328, January 29, 2015.

(32) Seto, M.; Banno, Y.; Imaeda, T.; Kajita, Y.; Ashizawa, T.; Kawasaki, M.; Nakamura, S.; Mikami, S.; Nomura, I.; Taniguchi, T.; Marui, S. Heterocyclic Compound. WO 2015060368, April 30, 2015.

(33) Shen, D.-M.; Egbertson, M.; Berger, R.; Qian, X.; Qian, Y.; Harper, B.; Yang, M.; Zack, Z. Q.; Rada, V. L.; Wang, D.; Cernak, T. A.; Sinz, C. J.; Wang, M.; Wilson, J. E.; Xu, S. Pyrimidone Carboxamide Compounds as PDE2 Inhibitors. WO 2015096651, July 2, 2015.

(34) Trabanco, A. A.; Buijnsters, P.; Rombouts, F. J. R. Towards Selective Phosphodiesterase 2A (PDE2A) Inhibitors: A Patent Review (2010–Present). *Expert Opin. Ther. Pat.* **2016**, *26*, 933–946.

(35) Gomez, L.; Massari, M. E.; Vickers, T.; Freestone, G.; Vernier, W.; Ly, K.; Xu, R.; McCarrick, M.; Marrone, T.; Metz, M.; Yan, Y. G.; Yoder, Z. W.; Lemus, R.; Broadbent, N. J.; Barido, R.; Warren, N.; Schmelzer, K.; Neul, D.; Lee, D.; Andersen, C. B.; Sebring, K.; Aertgeerts, K.; Zhou, X.; Tabatabaei, A.; Peters, M.; Breitenbucher, J. G. Design and Synthesis of Novel and Selective Phosphodiesterase 2 (PDE2a) Inhibitors for the Treatment of Memory Disorders. *J. Med. Chem.* **2017**, *60*, 2037–2051.

(36) Helal, C. J.; Arnold, E. P.; Boyden, T. L.; Chang, C.; Chappie, T. A.; Fennell, K. F.; Forman, M. D.; Hajos, M.; Harms, J. F.; Hoffman, W. E.; Humphrey, J. M.; Kang, Z.; Kleiman, R. J.; Kormos, B. L.; Lee, C. W.; Lu, J.; Maklad, N.; McDowell, L.; Mente, S.; O'Connor, R. E.; Pandit, J.; Piotrowski, M.; Schmidt, A. W.; Schmidt, C. J.; Ueno, H.; Verhoest, P. R.; Yang, E. X. Application of Structure-Based Design and Parallel Chemistry to Identify a Potent, Selective, and Brain Penetrant Phosphodiesterase 2A Inhibitor. *J. Med. Chem.* **2017**, *60*, 5673–5698.

(37) Boess, F. G.; Hendrix, M.; van der Staay, F.-J.; Erb, C.; Schreiber, R.; van Staveren, W.; de Vente, J.; Prickaerts, J.; Blokland, A.; Koenig, G. Inhibition of Phosphodiesterase 2 Increases Neuronal cGMP, Synaptic Plasticity and Memory Performance. *Neuropharmacology* **2004**, *47*, 1081–1092.

(38) Rutten, K.; Van Donkelaar, E. L.; Ferrington, L.; Blokland, A.; Bollen, E.; Steinbusch, H.

W. M.; Kelly, P. A. T.; Prickaerts, J. H. H. J. Phosphodiesterase Inhibitors Enhance Object Memory Independent of Cerebral Blood Flow and Glucose Utilization in Rats. *Neuropsychopharmacology* **2009**, *34*, 1914–1925.

(39) Reneerkens, O. A. H.; Rutten, K.; Bollen, E.; Hage, T.; Blokland, A.; Steinbusch, H. W. M.; Prickaerts, J. Inhibition of Phoshodiesterase Type 2 or Type 10 Reverses Object Memory Deficits Induced by Scopolamine or MK-801. *Behav. Brain Res.* **2013**, *236*, 16–22.

(40) Mikami, S.; Sasaki, S.; Asano, Y.; Ujikawa, O.; Fukumoto, S.; Nakashima, K.; Oki, H.; Kamiguchi, N.; Imada, H.; Iwashita, H.; Taniguchi, T. Discovery of an Orally Bioavailable, Brain-Penetrating, In Vivo Active Phosphodiesterase 2A Inhibitor Lead Series for the Treatment of Schizophrenia. *J. Med. Chem.* [Online early access]. DOI: 10.1021/acs.jmedchem.7b00709. Published Online: July 31, 2017. http://pubs.acs.org/doi/pdf/10.1021/acs.jmedchem.7b00709 (accessed August 9, 2017).

(41) Bischoff, E. Potency, Selectivity, and Consequences of Nonselectivity of PDE Inhibition. *Int. J. Impotence Res.* **2004**, *16*, S11–S14.

(42) Young, R. A.; Ward, A. Milrinone. A Preliminary Review of Its Pharmacological Properties and Therapeutic Use. *Drugs* **1988**, *36*, 158–192.

(43) Cote, R. H.; Feng, Q.; Valeriani, B. A. Relative Potency of Various Classes of Phosphodiesterase (PDE) Inhibitors for Rod and Cone Photoreceptor PDE. *Invest. Ophthalmol.* **2003**, *44*, 1524–1527.

(44) Zhang, X; Feng, Q.; Cote, R. H. Efficacy and Selectivity of Phosphodiesterase-Targeted Drugs in Inhibiting Photoreceptor Phosphodiesterase (PDE6) in Retinal Photoreceptors. *Invest. Ophthalmol. Visual Sci.* **2005**, *46*, 3060–3066.

(45) Pissarnitski, D. Phosphodiesterase 5 (PDE5) Inhibitors for the Treatment of Male Erectile Disorder: Attaining Selectivity Versus PDE6. *Med. Res. Rev.* **2006**, *26*, 369–395.

(46) Pierce, A. C.; Sandretto, K. L.; Bemis, G. W. Kinase Inhibitors and the Case for CH···O Hydrogen Bonds in Protein–Ligand Binding. *Proteins: Struct., Funct., Genet.* **2002**, *49*, 567–576.

(47) Zhang, K. Y.; Card, G. L.; Suzuki, Y.; Artis, D. R.; Fong, D.; Gillette, S.; Hsieh, D.; Neiman, J.; West, B. L.; Zhang, C.; Milburn, M. V.; Kim, S. H.; Schlessinger, J.; Bollag, G. A Glutamine Switch Mechanism for Nucleotide Selectivity by Phosphodiesterases. *Mol. Cell* **2004**, *15*, 279–286.

(48) Zhu, J.; Yang, Q.; Dai, D.; Huang, Q. X□ray Crystal Structure of Phosphodiesterase 2 in Complex with a Highly Selective, Nanomolar Inhibitor Reveals a Binding-Induced Pocket Important for Selectivity. *J. Am. Chem. Soc.* **2013**, *135*, 11708–11711.

(49) Hitchcock, S. A.; Pennington, L. D. Structure–Brain Exposure Relationships. *J. Med. Chem.* **2006**, *49*, 7559–7583.

(50) Hitchcock, S. A. Structural Modifications that Alter the P-Glycoprotein Efflux Properties of Compounds. *J. Med. Chem.* **2012**, *55*, 4877–4895.

(51) Compound **4c** was considered as a hypothetical form of **4b**, in which HBA (N4 nitrogen atom of the core) and HBD (NH of the amide) were completely neutralized via the intramolecular hydrogen bond.

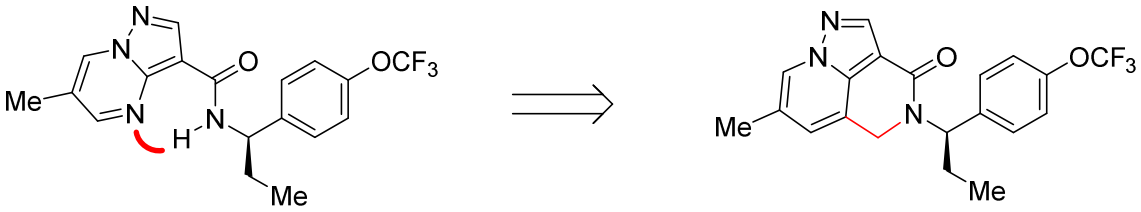

4b, TPSA: 69 **4c**, TPSA: 47

(52) Müller, K.; Faeh, C.; Diederich, F. Fluorine in Pharmaceuticals: Looking beyond Intuition. *Science* **2007**, *317*, 1881–1886.

(53) Wang, H.; Liu, Y.; Hou, J.; Zheng, M.; Robinson, H.; Ke, H. Structural Insight into Substrate Specificity of Phosphodiesterase 10. *Proc. Natl. Acad. Sci. U.S.A.* **2007**, *104*, 5782–5787.

(54) Iffland, A.; Kohls, D.; Low, S.; Luan, J.; Zhang, Y.; Kothe, M.; Cao, Q.; Kamath, A. V.; Ding, Y. H.; Ellenberger, T. Structural Determinants for Inhibitor Specificity and Selectivity in PDE2A Using the Wheat Germ In Vitro Translation System. *Biochemistry* **2005**, *44*, 8312–8325.

(55) Podzuweit, T.; Nennstiel, P.; Müller A. Isozyme Selective Inhibition of cGMP-Stimulated Cyclic Nucleotide Phosphodiesterases by Erythro-9-(2-hydroxy-3-nonyl) Adenine. *Cell. Signalling* **1995**, *7*, 733–738.

(56) Mathiasen, J. R.; DiCamillo, A. Novel Object Recognition in the Rat: A Facile Assay for Cognitive Function. *Curr. Protoc. Pharmacol.* **2010**, 5.59.1–5.59.15.

(57) Yamamoto, K.; Ikeda, Y. Kinetic Solubility and Lipophilicity Evaluation Connecting Formulation Technology Strategy Perspective. *J. Drug Delivery Sci. Technol.* **2016**, *33*, 13–18.

(58) Sugimoto, H.; Hirabayashi, H.; Kimura, Y.; Furuta, A.; Amano, N.; Moriwaki, T. Quantitative Investigation of the Impact of P-Glycoprotein Inhibition on Drug Transport across Blood-Brain Barrier in Rats. *Drug Metab. Dispos.* **2011**, *39*, 8–14.

(59) Takeuchi, T.; Yoshitomi, S.; Higuchi, T.; Ikemoto, K.; Niwa, S.; Ebihara, T.; Katoh, M.; Yokoi, T.; Asahi, S. Establishment and Characterization of the Transformants Stably-Expressing MDR1 Derived from Various Animal Species in LLC-PK1. *Pharm. Res.* **2006**, *23*, 1460–1472.

(60) Otwinowski, Z.; Minor, W. Processing of X-ray Diffraction Data Collected in Oscillation Mode. *Methods Enzymol.* **1997**, *276*, 307–326.

(61) Collaborative Computational Project, Number 4. The CCP4 Suite: Programs for Protein Crystallography. *Acta Crystallogr*., *Select. D: Biol*. *Crystallogr*. **1994**, *50*, 760–763.

(62) Smith, B.; Badger, J. *MIFit*, 2010. 10; https://github.com/mifit/mifit, June 12, 2010.

Table of Contents Graphic

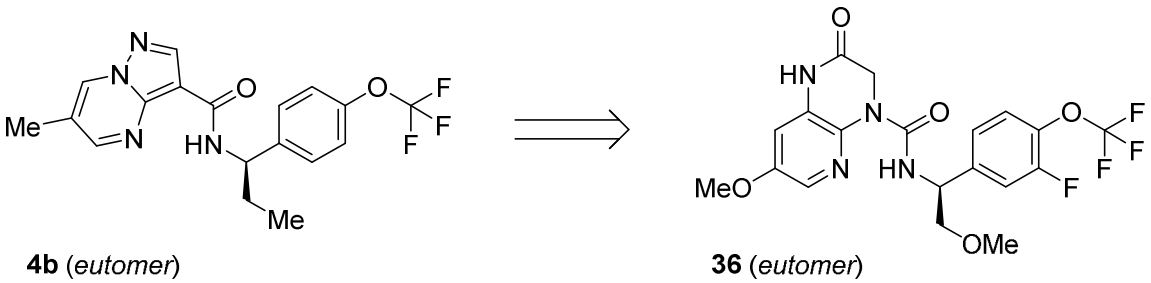

4b (*eutomer*)
PDE2A IC_{50} = 24 nM
PDE selectivity: 180x (vs. PDE3A)
TPSA: 69
MDR1 ratio: 0.40

36 (*eutomer*)
PDE2A IC_{50} = 0.61 nM
PDE selectivity: 4100x (vs. PDE1A)
TPSA: 102
MDR1 ratio: 0.87